Gradient Injection in Preparative Chromatography –
Exploitation of Sample Solvents Different than the Mobile Phase

Dissertation

zur Erlangung des akademischen Grades

Doktoringenieur

(Dr.-Ing.)

von: Diplom-Ingenieur Knut Gedicke

geboren am: 25. Feb. 1975

in: Magdeburg

genehmigt durch die Fakultät für Verfahrens- und Systemtechnik
der Otto-von-Guericke-Universität Magdeburg

Gutachter:

                       Prof. Dr.-Ing Andreas Seidel-Morgenstern

                       Prof. Dr.-Ing. Dorota Antos

eingereicht am: 7. Januar 2010

Promotionskolloquium am: 22. Juli 2010

Abstrakt

Die vorliegende Arbeit soll einen Beitrag zum besseren Verständnis der präparativen Batch-Flüssigkeits-Chromatographie leisten. Es wird die Verwendung eines anderen Lösungsmittels für die Injektion als für die Elution in dieser Arbeit untersucht – die Gradienteninjektion. Besonderes Augenmerk gilt dabei einer in der pharmazeutischen Industrie weit verbreiteten Methode, der Nutzung eines stärkeren Lösungsmittels für die Injektionen.

In einer theoretischen Untersuchung der Gradienteninjektion wurden Lösungen der Gleichgewichtstheorie für die Gradienteninjektion angewandt und erweitert. Dadurch konnten prinzipielle Effekte einer solchen Verfahrensführung abgeleitet werden. Die theoretisch ermittelten Resultate wurden in zwei experimentellen Studien bestätigt. Anhand einer experimentellen Fallstudie wurde eine einfache und effiziente Methode vorgeschlagen, anhand derer das Potential einer Prozessintensivierung durch den Einsatz der Gradienteninjektion überprüft werden kann. Es konnte gezeigt werden, dass die Gradienteninjektion Potential zur Verbesserung der Batch-Chromatographie besitzt. Randbedingen, lohnende Einsatzgebiete und Grenzen der Gradienteninjektion wurden identifiziert

Abstract

This work is meant as a contribution to increase the understanding of preparative batch liquid chromatography. It investigates on the use of a different sample solvent for injection than for the elution – the gradient injection. The use of a stronger sample solvent for injection, as often used in pharmaceutical industry, has been given special consideration.

For theoretical investigation of the gradient injection, solutions of the equilibrium theory have been applied and extended. This led to identification and derivation of general elution effects of such an injection method. The theoretical results have been verified in two experimental studies. Based on a experimental case study a rather simple and effective methodology has been suggested, suitable for process design and evaluation. It has been shown, that gradient injections have potential for process intensification. Suitable application areas and limits of the gradient injection have been identified.

Acknowledgement

Table of Contents

It is very instructive to observe the adsorption during filtration through a powder. First a colourless, then a yellow (carotene) liquid flows out from the bottom of the funnel, while a bright green ring forms at the top of the inulin column, below which a yellow ring soon appears. On subsequent washing of the inulin column with pure ligroin, both rings, the green and the yellow, are considerably widened and move down the column.

M.S. Tswett, *Tr. Varshav. Obshch. Estestvoispyt., Otd. Biol.* 14 (1903) 20

1. Introduction

Separation technology plays a crucial role in drug manufacture and life science industry, where the product specifications involve a high purity. Among several techniques, preparative chromatography – production scale chromatography – has evolved as a versatile yet expensive method. In the last years, chromatographic methods have been increasingly applied for the preparative separation of isomers, enantiomers, oligosaccharides and proteins. Efforts have been made to increase the productivity of such separation processes. These involve process intensification, as it is the case for sophisticated continuous simulated moving bed arrangements, e.g. [14, 22, 108, 119, 125, 155, 156], or the less complicated but still efficient steady state recycling with periodic injections to internal concentration profiles [56-58, 99, 138, 195]. Other works of process intensification concentrated on the coupling of the rather cost intensive chromatographic separation with a less costly crystallization step in order to yield an overall more efficient separation scheme, especially for the separation of stereoisomers [12, 39, 40, 43, 87, 93-96, 106, 107, 124, 162, 178]. However, batch elution chromatography is still a major method of choice to produce the first grams to kilograms of a new pharmaceutical product.

The application of chromatography in a large scale requires optimization of operating conditions, which should assure minimal cost of the separation. Columns are usually overloaded in preparative batch chromatography to achieve that goal. It is well

known that concentration overloading is superior to volume overloading [64, 98]. Hereby a typical restriction is given by limited solubility of the samples in the mobile phase applied to achieve good separations. A possibility to increase the column load is to use for the injection a solvent in which the sample has a higher solubility. The elution strength of such solvents is usually larger than that of the mobile phases. The use of an extra-solvent to dissolve the feed components is common in industrial practice for systems with low solubility of the samples in the mobile phase [114]. Jandera and Guiochon [80] reported resulting deformations and splitting of elution profiles at the column outlet for the example of non-aqueous reversed-phase chromatography. Feng *et al.* [33] observed similar phenomena for hydrophobic interaction chromatography of proteins. An additional obstacle of this technique is that the injection of very concentrated samples brings the risk of triggering undesired crystallization effects, which may reduce the permeability of the chromatographic system due to blocking phenomena.

The aim of this work was to bring further insight in the application of a stronger solvent for injection than that for the elution. This injection method is referred to as gradient injection throughout this work – since it represents in essence a solvent step gradient, which is immediately applied after the injection.

Fundamental background on preparative chromatography is summarized in Chapter 2. Thereby a focus is set on the so-called equilibrium theory.

A theoretical backbone for the application of the injection in a different solvent is derived in Chapter 3 by the consequent application of the equilibrium theory. Here typical phenomena, purely based on thermodynamic adsorption equilibria, are studied and explained for several isotherm combinations.

Some of the phenomena described theoretically are experimentally studied in Chapter 4. The experimental research has been performed in the following stages: a) chromatographic experiments under strongly overloaded conditions, b) analysis the influence of the mobile phase composition on the adsorption equilibrium of the component studied and c) development and validation of a simplified mathematical model. Another goal of Chapter 4 was to check if there exist extreme conditions, where precipitation within the chromatographic system occurs. In order to study sys-

tematically the overloading effect, a chromatographic system was chosen, which consisted of just one solute with reasonable retention in the mobile phase.

Finally in Chapter 5, the application of the injection in a strong solvent for separation is discussed for a specific example. For this a chromatographic system was chosen, which consisted of two solutes to be separated. The experimental strategy for determination of the necessary physical interactions (developed and tested in chapter 4) was extended further for the use of a two solute system. With a simplified, yet efficient, mathematical description, accounting for the retention of the strong solvent and the dependence of the adsorption isotherms of the solutes on the modifier concentration, process optimization was performed by numerical simulation. The obtained optimized results were verified experimentally.

The results of this work are summarized in chapter 6.

The fundamental problems of nonlinear chromatography and the theory of preparative chromatography have been the topic of intense activity by chromatographers and chemical engineers. Each community has largely overlooked the activities, as well as the preoccupations and viewpoints, of the other one. Theoretical problems in nonlinear chromatography have been discussed in the literature for more than 50 years and some are still today. Some of these works have been quite influential in some circles, while others were completely ignored in others.

G. Guiochon, A. Fellinger, D.G. Shirazi, A.M. Katti, Fundamentals of Preparative and Nonlinear Chromatography, 2.nd edition

2. Background

2.1. Literature Survey

Chromatography is a thermal separation technique, where the samples to be separated are transported in with a carrier fluid (gas/liquid) parallel to a stationary phase (solid). The separation is achieved by the different strength of interactions of the samples with the stationary phase. Giddings showed clearly that these interactions (i.e. chemical potential discontinuities) are perpendicular to the flow direction, magnifying the result (a good separation) even for small degrees of separation [45, 65].

The history of liquid chromatography is summarized extensively in the works of George Guiochon [64-66]. The author strongly recommends the interested newcomer to preparative chromatography and its mathematical modelling to start its literature survey with the comprehensive review from 2002 [65].

The first reported use of chromatography has been in 1903 for preparative purposes by Tswett for the separation of extracted plant pigments [74]. Being more or less ignored for about 30 years the high selectivity of chromatography was utilized for the isolation of oxides of rare earth elements by ion exchange displacement chromatography in the frame work of the Manhattan Project mainly by Spedding *et al*. [168-

176]. In the early fifties the American Petroleum Institute used displacement chromatography to fractionate samples of crude oil and distillates to determine the content of paraffin's, naphthenes, olefins and aromatics [17, 110-113]. Another mile stone of the development of chromatography was in the early 1960's the patent by Union Oil based on the principle of a simulated moving bed (SMB) [14, 15]. This process was developed for the continuous large-scale separation of various petroleum distillates, e.g. p-xylene, o-xylene and ethyl-benzene. Today also a number of large scale separations in the food industry (e.g. fructose-glucose-sucrose [101], betaine separation from beet molasses [67], sucrose from molasses [189]) with more than 500.000 tons/anno are performed by SMB and SMB like processes. Ruthven and Ching wrote an excellent review [147] about the development of continuous counter current separation processes. Another, though less successful development of continuous chromatography has been the annular chromatography [77] in which the column is rotating around a fixed axis and the inlets and outlets are at fixed column positions. While a continuous chromatographic process sounds intriguing, such an arrangement represents NOT a process intensification (contrary to simulated moving bed arrangements). Kniep and Heuer [75, 102] showed mathematically that such an arrangement is in principle the same as a conventional batch system (though much more complicated to realize), only that the time coordinate is exchanged by an annular coordinate. Even Guiochon and Co-Workers did not buy into that idea, as the following suggests *'It seems that this solution is still looking for the problems it can solve'* [66].

Over the last 20 years, the use of semi preparative and preparative chromatography has been significantly increased. This is mainly due to the pharmaceutical industry, where chromatography is now an important general-purpose separation method [66]. The main reason is that the amounts of products required here are relatively easy to achieve with columns of only a few centimeters in inner diameter. The purification of enantiomers, peptides and proteins are the main focus of published applications, though many others have been reported also [66]. There are a number of reviews dealing with the application of chromatography for fine chemicals and pharmaceuticals for both analytical and preparative applications [36-38, 158, 184].

Besides the technical development of stationary phases and equipment, also the achieved theoretical understanding of the phenomena tremendously pushed the acceptance of chromatography. Especially the pioneering works on solutions of the

ideal model of chromatography (referred to as equilibrium theory) must be mentioned. Glueckauf [19, 48, 49] was the first who solved the ideal model of chromatography with competitive Langmuir isotherms. However, this solution remained rather unnoticed [63]. The development of solutions of the ideal model was driven in the late 1960s by the work of Helfferich (concept of coherence and h-transform) [69] and the works of Rhee, Aris and Amundson (entropy condition, ω-transform and method of characteristics) [142, 143], that led to a better understanding of the role of thermodynamics (i.e. the shape of the adsorption isotherm) on the peak profiles and the achievable separation. Guiochon and Co-workers made these solutions so popular and applicable for the interested user, that they where even credited for the solution of the ideal model for binary competitive Langmuir isotherms [53, 54]. This led to their interesting review on the history of the ideal model and its solutions [63]. The main results of the equilibrium theory for elution chromatography, such as self sharpening effects, band broadening and displacement are comprehensively reviewed in [70-73] and explained in detail in the books by Rhee *et al*. [142, 143] and Guiochon *et al*. [64, 66].

The methods of solving the ideal model were also applied to continuous countercurrent adsorption processes. The combined work of Morbidelli, Storti, Mazzotti and their co-workers was of the uttermost importance for the speed with which in the past 20 years simulated moving bed has been accepted as a separation technique. They provided easy to use design criteria for this complicated process, just based on adsorption isotherms. The rigorous derivation of these criteria for nonlinear isotherms is explained in [115, 116, 118, 123, 177], while user-friendly descriptions are given here [117, 122].

Another important aspect for the success of chromatography is the still increasing computing power, which makes it in our days rather easy to solve numerically more realistic models of chromatography. Among the most successfully applied models, I want to highlight the equilibrium dispersive model, which was initially derived by Wicke [192, 193]. It represents a trade off between the more realistic models including mass transfer between the fluid and the solid phase and the ideal model in which all mass transfer effects are neglected. The modeling of chromatography is treated in a number of reviews e.g. [55, 65] and books e.g. [64, 66, 159]. Again, I recommend

for a start the wonderful review by Guiochon summarizing 60 years of experience in chromatography [65].

With the previously mentioned works on the modeling and experimental verification it turns out that the most crucial information needed for quantitative descriptions are the adsorption equilibria – usually described by the adsorption isotherms. These functions are relationships between the concentrations of each compound in the two-phase system at constant temperature. Gas-solid equilibria have been studied over 200 years. Fontana showed that activated charcoal adsorbs gases and vapors [66]. The Gibbs isotherm [44] and the multilayer adsorption theory of Brunnauer, Emmet and Teller [16] provide valuable theoretical understanding for gas-solid equilibria. However, for liquid-solid equilibria, the situation is more complex. As a consequence, the understanding of liquid-solid equilibria remains more empirical [66]. In their excellent books Oscik [129] and Ruthven [146] provide comprehensive summary on adsorption and adsorption isotherms for both liquid-solid and gas-solid equilibria.

Besides the recent success of SMB and SMB like processes, elution chromatography is still the main method of chromatography used in practice. It is in our days more or less realized, that (among elution chromatography) isocratic elution (constant elution strength throughout the process)– whenever possible – leads to similar [167] or even larger production rates, higher recovery yields and easier operation compared to displacement and gradient chromatography [66]. Biochemicals on the other hand, cannot be extracted and purified by isocratic elution. Here, gradient elution, that is the progressive or step wise change of the elution strength of the carrier fluid throughout the elution, has to be applied [66].

Efficient preparative batch chromatography requires working under close to optimal conditions in terms of flow rate, column length and amount injected. It is well known that concentration overloading typically performs better than volume overloading for one to one mixtures of the solutes to be separated [55], i.e. where the tag along effect is not dominating. For such mixtures it has been shown that both injection concentration and injection volume need to be optimized. However, the optimal injection concentrations tend to be the maximal applicable. Often the problem is met that the solutes to be separated exhibit a limited solubility in the mobile phase suitable for separation. In order to introduce concentrated samples a stronger solvent could be used

for the sample injection. However, this methodology may cause undesired effects, such as band splitting [9, 33, 41, 76, 80, 100, 180-182, 186, 187, 191] or crystallisation in the capillaries [41] or the column [183], albeit the latter phenomena is less frequently reported. If crystallisation problems can be ruled out, the injection in a stronger solvent is an often-used method in industrial chromatography [114].

Ströhlein *et al.* [179, 181, 182] studied single solute-solvent interactions in bio-chromatography based on the equilibrium theory. This analysis included linear and Langmuir isotherms for the solvent (modifier) and linear isotherms of the solute (as a function of the modifier concentration). The authors have shown, that, depending on the migration velocities of the modifier and the solute, several phenomena can be observed, such as on-column concentration or dilution of the sample in case of injecting the sample in a weaker or a stronger solvent (compared to the elution strength of the mobile phase), respectively. Conditions where peak splitting can be observed were also shown. These effects could be described and experimentally verified with models just based on adsorption isotherms, in contrast to the qualitative descriptions of band splitting, done in [80, 183], where crystallisation and dissolution processes were included in the mathematical model.

Jandera *et al.* [85] performed an optimization of gradient-elution for reversed-phase liquid chromatography (RPLC). For a certain case study (separation of phenol and *o*-cresol on a C_{18} material) the injection of long pulses in a weak solvent was found to be beneficial due to on-column concentration. Virtually the same result was reported in [104]. However, for both examples studied the possibility of injecting very concentrated samples was apparently not considered thoroughly. The injection of wide pulses of diluted samples dissolved in a weak solvent represents the opposite of the practice applied in industry, were often the solutes to be separated are injected in a narrow pulse of high concentration.

2.2. Definitions

In the following section, basic definitions and assumptions for liquid chromatography are listed. Lets start with a sketch of a chromatographic column.
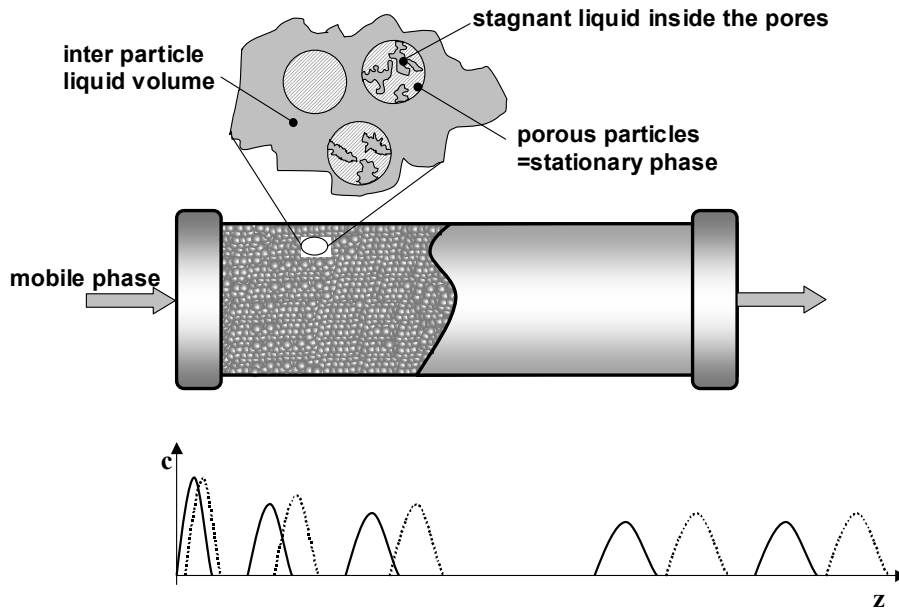
Figure 2.1: Scheme of a chromatographic column

A chromatographic column consists of the solid stationary and the fluid mobile phase. The fluid volume consists of the fluid around the particles (extra or inter particle liquid) and the (stagnant) fluid inside the pores of the particles. However, for most models, except the general rate model [11, 66, 121, 131, 146] the use of a total fluid volume V_0 is sufficient. The total porosity ε is thus defined as:

$$\varepsilon = \frac{V_0}{V_c} \tag{2-1}$$

Note that the volume of the liquid phase is often called dead volume of the chromatographic column (thus the subscript $\boldsymbol{0}$). Where V_c is total volume of the empty column, which can be calculated from its dimensions, e.g. for a cylindrical column of diameter d and length L (or cross sectional area of the column A_c)

$$V_c = \frac{\pi}{4} d^2 L = A_c L \tag{2-2}$$

The total volume of the fluid phase in the column can be determined from the retention time of an unretained tracer, which enters also the stagnant pore space. The tracer is injected at the beginning of the column and the mean retention time is meas-

ured with a suitable detector at the column outlet. The retention time of such an unretained tracer is called dead time of the chromatographic column t_0. The relation between the dead time, the porosity and the dead volume is:

$$V_0 = \varepsilon V_c = t_0 Q \qquad\qquad (2\text{-}3)$$

Q is the volumetric flow rate of the mobile phase. It is often difficult to find a tracer that is completely unretained and at the same time enters the pore space. Usually, a substance is used which retention time is sufficiently small. The porosity obtained from these experiments is used a reference value. Fornstedt and Co-Workers have shown that even though deviations in the real porosity yield erroneous adsorption isotherm models [149] it is still possible to correctly predict experimental band profiles [150], sufficient for engineering purposes.

Besides the porosity, also the phase ratio F of the solid phase volume V_S and the liquid phase volume V_0 is used.

$$F = \frac{V_S}{V_0} = \frac{1-\varepsilon}{\varepsilon} \qquad\qquad (2\text{-}4)$$

Also of importance is the linear mobile phase velocity u, the velocity, with which the mobile phase is traveling through the column. This velocity is defined as:

$$u = \frac{Q}{\varepsilon A_c} \qquad\qquad (2\text{-}5)$$

A measure for band-broadening effects such as axial diffusion and mass transfer resistances is the number of theoretical plates of a column, NTP, which can be obtained from the mean retention time (μ, the first absolute moment) and the variance (σ, the second relative moment) of a chromatographic peak:

$$NTP = \frac{\mu^2}{\sigma^2} \qquad\qquad (2\text{-}6)$$

Ideally, if adsorption occurs in the linear range of the adsorption isotherm and if band-broadening effects are symmetrical, peaks are characterized by a Gaussian distribution and NTP can be calculated with [188]

$$NTP = 5.54 \left(\frac{t_R}{w_{1/2}} \right)^2 \tag{2-7}$$

Where $w_{1/2}$ is the peak width at half the peak height and t_R $(=\mu)$ is the retention time of the peak maximum.

2.3. Modelling Batch Chromatography

Chromatography is a complex process where the components involved are subject to various physical phenomena. The mobile phase is percolating through the packed bed. It carries components that interact in different strength with the stationary phase. The components diffuse through the stagnant layer around the particles to the particle surface. Here, they are transported by diffusion into the pore space of the particles and from there to the particle surface. There, the components are subject to molecular interactions with the surface. Eventually, the reverse steps are happening and the components are swept out of the column [66]. Provided the components are not subject to chemical reaction, the mass balance for each component is conserved for any injected amount into the column. This should be the prerequisite for any preparative separation [66].

The outcome of the separation depends on the fluid dynamics, the mass transfer phenomena and to a large extend on the thermodynamic equilibrium. For liquid phase preparative chromatography without chemical reaction isothermal mass balance models (without the energy balance) have been found to sufficiently describe the phenomena involved [66]. This is due to the relatively small heat of adsorption and the large heat capacity of the liquid and the solid phases. In liquid chromatography the following assumptions can be used:

- negligible compression of the liquid phase, i.e. density and flow rate are constant along the column and independent of pressure and degree of adsorption,

- partial volumes of the samples are the same in both phases,

- radially homogeneous,

- no thermal effects, i.e. heats of adsorption, friction and mixing are negligible→isothermal,

- thermodynamic equilibria are not influenced by pressure,

- viscosity is constant and not affected by the feed.

These assumptions (plus a few more specific ones) lead to the development of several models of different accuracy for preparative chromatography (or better, for the description of the transport through a packed bed). In the following, I will introduce selected models and their assumptions, relevant to this work.

2.3.1.   Equilibrium Loadings – Adsorption Isotherms

In the previous sections we have - and the following sections we will see - that adsorption equilibria are of the uttermost importance for the success of a separation and the elution profiles (in the case of large sample amounts). In principle for chromatographic processes, where the mass transfer is not very slow (due to small particle sizes), thermodynamics control the shape of the band profiles, thus separation, recovery yield and productivity. The equilibrium concentration q_i on the solid surface of component i depends on the concentrations of all components in the fluid phase, $\mathbf{c}$, and the temperature. These equilibria are typically measured at constant temperature and are referred as *adsorption isotherms*.

Here, a short introduction to adsorption and its definitions is given. The theoretical approach to the investigation of liquid-solid equilibria is much less advanced and much more complex than for gas-solid equilibria. The methods and approaches of gas-solid equilibria were empirically extended to liquid-solid equilibria [66]. Comprehensive standard text books on adsorption are e.g. Ruthven [146] and Oscik [129]. Lets start with a few definitions, which are comprised by the International Union of Pure and Applied Chemistry (IUPAC). "*Adsorption is the enrichment of one or more components in an interfacial layer.*"[27]. The material in the adsorbed state is called *adsorbate* while the one in the bulk phase is called *adsorptive*. For those adsorption processes which occur on solid/fluid interfaces the solid is referred to as the *adsorbent*, while the fluid may be named *adsorbens*. For liquid chromatography or better

for solid/liquid adsorption, the terms adsorbens and adsorptive are referred to as *solvent* and *solute*.

The most prominent adsorption isotherm model is the *Langmuir equation* which can be obtained from several starting points (e.g. chapter 3 in [66]) including statistical thermodynamics, Gibbs-Isotherm and the classical method of an established kinetic equilibrium between an adsorption and a desorption process [103]. It assumes an energetically homogeneous adsorbent surface, monolayer adsorption and no interaction between the adsorbed molecules on the adsorbent surface.

$$
\begin{aligned}
q_i &= q_{s,i} \frac{b_i c_i}{1 + b_i c_i} \\
&= \frac{H_i c_i}{1 + b_i c_i}
\end{aligned}
$$

(2-8)

$q_{s,i}$, b_i and H_i are the saturation capacity of the adsorbent, the equilibrium constant and the Henry coefficient (or constant), respectively. For dilute conditions, where $b_i c_i \ll 1$, Eq. (2-8) reduces to the linear isotherm,

$$
q_i = H_i c_i
$$

(2-9)

Which in analogy to gas absorption is called Henry isotherm. Linear isotherms are typically applicable for small concentrations and have been proven very useful in the field of ion-exchange adsorbers (e.g. sugar purification) – even though the isotherms are not really linear [127, 128]. The Henry coefficient is also referred to as the initial slope of the isotherm.

Thermodynamically consistent competitive isotherms can be obtained from the single component isotherms and the application of the famous ideal adsorbed solution theory [139]. If the saturation capacities of all adsorbable components are equal ($q_{s,1} = q_{s,2} = ... = q_{s,N_C} = q_s$), the single component Langmuir model can be thermodynamic consistently extended to account for multi-component adsorption

$$q_i = q_s \frac{b_i c_i}{1 + \sum_{j=1}^{N_C} b_j c_j} \tag{2-10}$$

Often the Langmuir model is to simple to account for the manifold interactions really happening at the complex adsorbent surface. Especially the assumptions of energetically homogeneous surfaces and monolayer adsorption are often not fulfilled. One method to account for energetically heterogeneous surfaces is the extension by another Langmuirian adsorption center leading to the *multi-bi-Langmuir isotherm*:

$$q_i = q_{s,1} \frac{b_{1,i} c_i}{1 + \sum_{j=1}^{N_C} b_{1,j} c_j} + q_{s,2} \frac{b_{2,i} c_i}{1 + \sum_{j=1}^{N_C} b_{2,j} c_j} \tag{2-11}$$

If the equilibrium constant of the second adsorption center is rather small (i.e. $b_{2,i} c_i \ll 1$) Eq. (2-9) simplifies to

$$q_i = \frac{a_{1,i} c_i}{1 + \sum_{j}^{N_C} b_j c_j} + a_{2,i} c_i \tag{2-12}$$

This *modified Langmuir equation* has been successfully used in a number of applications (e.g. [81])[1]. Jandera *et al.* [86] derived Eq. (2-12) for multi-layer adsorption with a kinetic approach, similar to the derivation of the simple Langmuir model. Gritti and Guiochon [60] derived with the application of the adsorbed solution theory thermodynamically consistent competitive isotherms where one solute is adsorbed by Brunnauer-Emmet-Teller (BET [16]) isotherm and the other is adsorbed by Langmuir isotherms.

Isotherm models are functions used to fit experimental equilibrium data for the purpose of representing this data for further process calculations and process design. A good fit of the simplified yet versatile models does not mean, that the models reflect

---

[1] for a conservative design of a separation process the linear center should be unselective i.e. $a_{2,1} = a_{2,2} = \ldots = a_2$

the real molecular interactions. However, the use of *thermodynamically consistent models* (even if they do not represent the real molecular interactions) *has been proven very successfully for process predictions and process optimizations.*

2.3.2.   Ideal Model of Chromatography

The simplest model of chromatography was formulated first by Wicke [193]. In addition to the assumptions stated above it neglects all mass transfer resistances and back mixing effects. It assumes that both phases are always in equilibrium with each other, leading to the following mass balance for a component i :

$$\frac{\partial c_i}{\partial t} + F \frac{\partial q_i}{\partial t} + u \frac{\partial c_i}{\partial z} = 0 \qquad\qquad i = 1, N_C \qquad\qquad \textbf{(2-13)}$$

c_i and q_i are the concentrations of component i in the fluid and on the solid surface respectively. Since both phases are constantly in equilibrium, the concentration on the solid surface q_i is a function of the liquid phase concentration of all components N_C present:

$$q_i = q_i(c_1, c_2, \ldots, c_i, \ldots, c_{N_C}) \qquad\qquad i = 1, N_C \qquad\qquad \textbf{(2-14)}$$

This model despite its simplifications is of the uttermost importance for the understanding of the basic effects in chromatography, which I will explain in the following. It has been solved and studied extensively by several researches for nonlinear adsorption isotherms. After some initial work of Wicke [193] and Wilson [194], DeVault [23] demonstrated in 1943 that the solution of Eq. (2-13) carries a diffuse boundary at the rear of a profile if the isotherm is convex upward (e.g. Langmuir) and on the front of the profile when the istherm is convex downward (anti-Langmuir). Glueckauf [46-48, 50] measured for the single component problems adsorption isotherms and showed experimentally and theoretically the development of concentration profiles for convex upward, downward and sigmoidal shaped isotherms. Glueckauf's solution was derived without the mathematical methods available and was neglected in the community [66]. Solutions with a given amount of physical insight were obtained by Helfferich [68, 69] for displacement chromatography. Rhee *et al.* [140] provided rigorous solutions for single solutes and multi-

component mixtures with a sound mathematical background. Golshan-Shirazi and Guiochon [51] derived an easier to use equation for the shock location of a single solute for any isotherm without inflection point. Solutions of the ideal model (also known under the name equilibrium theory) were also used to gain physical insight in the performance of counter-current adsorbers and simulated moving bed arrangements [115-118, 123, 141, 177]. Grüner *et al.* and Vu *et al.* extended the equilibrium model by reaction and obtained insight for useful combinations of integrated reactions and separations [61, 62, 190]. Recently, Kaspereit *et al.* and Sainio extended the use of the equilibrium theory to derive design conditions for reduced purity conditions for SMB [97] and steady state recycling [148]. Helfferich and co-authors wrote an interesting series of articles on the solution of the ideal model [71-73]. In the following, I will sketch the main features for the derivation of solutions of Eq. (2-13) with the appropriate initial and boundary conditions appropriate for batch chromatography.

Eq. (2-13) describes a set of homogeneous first order partial differential equations. Its solutions can be constructed using the method of characteristics (for details see section 2.4 below, or chapter 5 in [143]). These solutions may contain discontinuities and are better represented by wave phenomena [72, 143]. Utilizing

$$\frac{\partial q_i}{\partial t} = \frac{dq_i}{dc_i} \frac{\partial c_i}{\partial t}$$

$$\text{with } \frac{dq_i}{dc_i} = \sum_{k=1}^{N_C} \frac{\partial q_i}{\partial c_k} \frac{\partial c_k}{\partial c_i}$$

(2-15)

and inserting it into Eq. (2-13) leads to the wave equation:

$$\frac{\partial c_i}{\partial t} + \frac{u}{1 + F' \frac{dq_i}{dc_i}} \frac{\partial c_i}{\partial z} = 0 \qquad\qquad i = 1, N_C$$

(2-16)

If we introduce the migration or traveling velocity u_c of a constant concentration, we obtain:

$$u_{\mathbf{c}}(c) = \frac{dz}{dt}\bigg|_{\mathbf{c}} = \frac{L}{t_{R,i}} = \frac{u}{1 + F\frac{dq_i}{dc_i}\big|_{\mathbf{c}}} \tag{2-17}$$

From Eq. (2-17) it is obvious that *the migration velocity of a certain concentration depends on the local slope of the isotherm function.* This well known fact is visualized in Figure 2.2 adopted from [66].
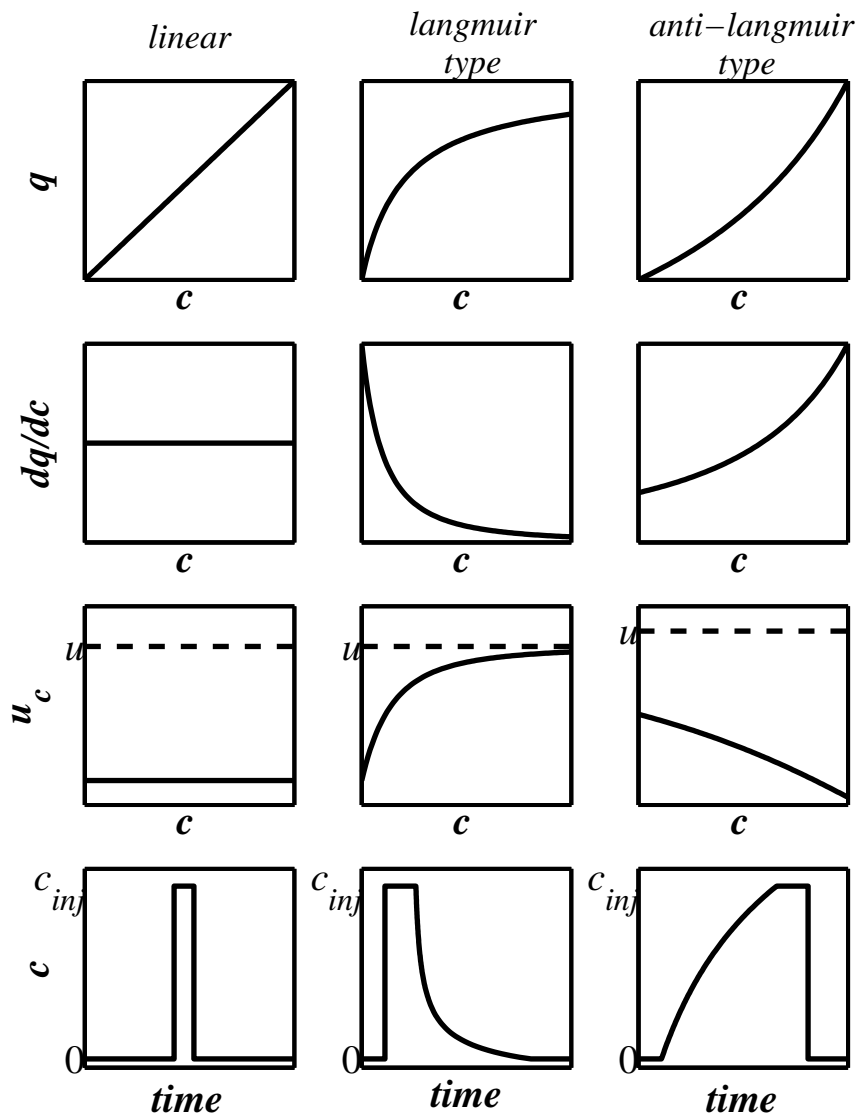
Figure 2.2: Relationship between the shape of the equilibrium isotherm (1st row), its derivative (2nd row), the corresponding migration velocity u_c (3rd row) and concentration profile (last row) at the column outlet for single components.

For linear isotherms (i.e. constant slope) the migration velocity remains independent on the concentration of the solute. Thus, a rectangular injection of an injection concentration c_{inj} migrates unchanged through the column (as long as no mass transfer effects are present). For Langmuirian isotherms the slope of the isotherm decreases with increasing concentration – larger concentrations of the solute are less strongly adsorbed than smaller ones, thus less retained: i.e. larger concentrations have a higher velocity than smaller concentrations. In contrast, for anti-Langmuir type isotherms larger concentrations are stronger adsorbed and more retained than smaller concentrations.
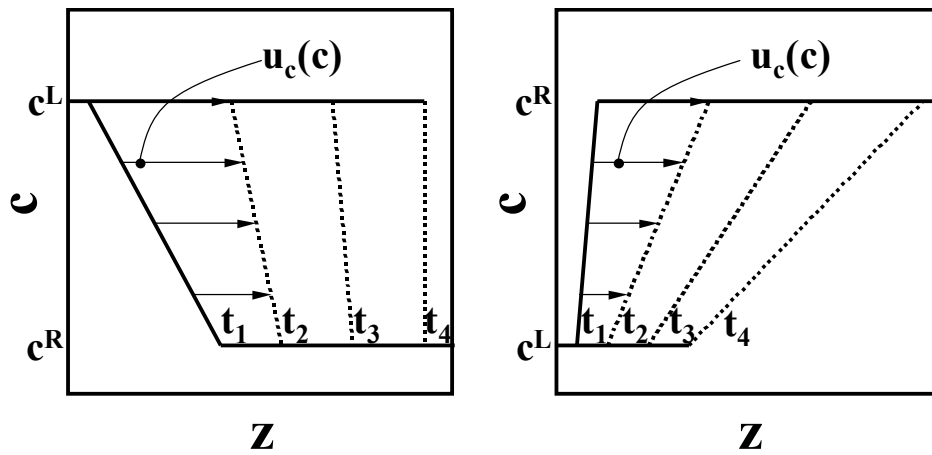
Figure 2.3: Development of an initial concentration profile (solid lines) on its course through a chromatographic column.
left: development of a shock, right: development of a spreading wave.

Consider now a concentration profile as shown in the left diagram of Figure 2.3. Initially, we have a concentration profile where downstream the column is empty (no concentration of the solute). High concentrations travel faster than smaller concentrations, thus the profile sharpens until the point where all smaller concentrations are overtaken by the largest concentration. At this point a discontinuity forms. The propagation speed of the discontinuity can be derived from a mass balance around it (for details see Rhee at al. section 5.4 in [143]).

$$u_Z = \frac{u}{1 + F \dfrac{q^L - q^R}{c^L - c^R}}$$

(2-18)

So, the propagation speed is proportional to the slope of the chord connecting two points on the isotherm. With other words, spreading waves (simple waves, Figure 2.3 right) propagate proportional to the slope of the isotherm, Eq. (2-17), while compressive waves (shocks, Figure 2.3 left) propagate proportional to the chord of the isotherm, Eq. (2-18).

Seidel-Morgenstern [160, 198] introduced the picture of a "rubber band" to explain when the chord, $\frac{\Delta q}{\Delta c}$, and when the derivative, $\frac{dq}{dc}$, of the isotherm determine the traveling velocity of a concentration. For adsorption, the "rubber band", which represents an operating line (dotted lines in Figure 2.4) spans from below the isotherm in the q-c diagram. For desorption the "rubber band" spans from above the isotherm. The "rubber band" always yields the shortest connection between the initial and the feed state and shows whether the propagation velocity is proportional to the chord or the derivative of the isotherm.
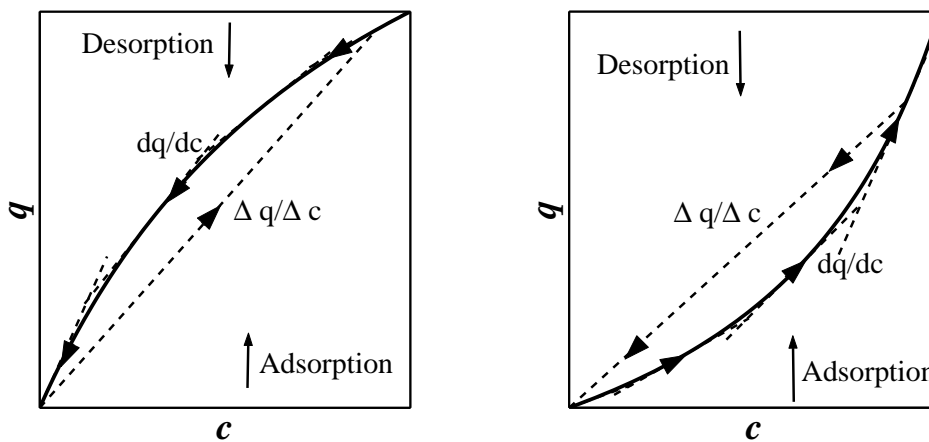
Figure 2.4: Visualization of the "rubber band" (dotted lines) to identify when to use the chord and when to use the derivative of the isotherm to obtain the retention time of a concentration, left for Langmuir-type isotherms and right for anti-Langmuir type isotherms

2.3.3.   Models with Mass Transfer Effects

Comprehensive overviews on the modeling of preparative chromatography are given in e.g. [55, 65, 66]. The most successful and often used extension of the equilibrium model is the equilibrium dispersive model (ED). It is applicable, when the mass transfer kinetics are fast, but finite (e.g. section 2.2.2 in [66]). All contributions of

mass transfer resistances are lumped into in this model into one apparent dispersion coefficient $D_{app,i}$ and Eq. (2-13) becomes:

$$\varepsilon \frac{\partial c_i}{\partial t} + \left(1 - \varepsilon\right) \frac{\partial q_i}{\partial t} + u \frac{\partial c_i}{\partial z} = D_{app,i} \frac{\partial^2 c_i}{\partial z^2} \tag{2-19}$$

with the apparent dispersion coefficient for efficient columns being related to the number of transfer units (Eq. (2-7)) by:

$$D_{app,i} = \frac{uL}{2 NTP_i} \tag{2-20}$$

It is further assumed, that the dispersion coefficient is independent of the concentrations of the components. This assumption is valid since the concentrations of components to be separated are usually smaller than 10 wt.% (typically not applicable for sugar, polymer and protein separations). This model is very versatile and usually applicable in industrial preparative chromatography as long as the plate numbers are above a few hundred and the molecules to be separated are small. This model has been validated with experimental results in numerous publications (see e.g. [55, 65] and references therein). Eq. (2-19) is solved by numerical integration with the simplified boundary conditions for single column batch chromatography:

$$c_i(t, z = 0) = c_i^F(t)$$

$$\left. \frac{\partial c_i}{\partial z} \right|_{t, z = L} = 0 \tag{2-21}$$

Among the numerical methods available, finite differences are the most prominent ones due to their fast solution. The Rouchon algorithm [144] is often used to solve Eq. (2-19) due to its numerical efficiency. In this case, Eq. (2-19) is replaced by Eq. (2-13) and the numerical dispersion is tuned so that it matches the physical dispersion. The direct backward in time (index k), forward in space (index n) finite difference scheme is usually applied. The unknown concentrations, $\mathbf{c}$, can be obtained from the known concentrations and loadings at previous time and space positions:

$$\mathbf{c}_{n+1}^{k} = \mathbf{c}_{n}^{k} - \frac{\Delta z}{u\Delta t}\left(\mathbf{c}_{n}^{k} - \mathbf{c}_{n}^{k-1} + F\left[\mathbf{q}_{n}^{k} - \mathbf{q}_{n}^{k-1}\right]\right) \qquad \text{(2-22)}$$

The time and space increments are obtained from the apparent axial dispersion (expressed by the plate number) and the migration velocities of the components at the equilibrium conditions defined by $\mathbf{c}$:

$$D_{app} = \frac{uL}{2\,NTP} \equiv D_{Num} = \left(u_{\mathbf{c}}\Delta t - \Delta z\right)\frac{u}{2} \qquad \Delta z = \frac{L}{NTP(a_{cou} - 1)}$$

$$\Delta t = a_{cou}\frac{\Delta z}{u_{\mathbf{c}}} \qquad\qquad u_{\mathbf{c}} = \frac{u}{1 + \dfrac{F}{N_C}\displaystyle\sum_{j}^{N_C}\left(\left.\dfrac{dq_i}{dc_i}\right|_{\mathbf{c}}\right)} \qquad \text{(2-23)}$$

In the above Δz and Δt are the space and time increments of the finite difference scheme. The courant number, a_{cou}, is related to a numerical stability criteria and has to be $a_{cou} > 1$ (recommendation $a_{cou} = 2$) for Eqs. (2-22), (2-23).

For more details see e.g. [66, 159]. Even though the solutions obtained from Eq. (2-22), (2-23), carry a certain error for nonlinear isotherms since the numerical dispersion is a function of the local migration velocity of a component, this error is usually negligible [21, 109]. Pitfalls of the Rouchon method and corresponding modifications are reported here [21, 88, 89]. For those cases where the Rouchon method is not applicable to solve Eq. (2-19), in principle three major alternative numerical methods have been shown to overcome the problem:

Orthogonal collocation on finite elements (OCFE see e.g. [11, 90, 109]) – this numerical routine yields the most accurate solution of partial differential equations of the type above. This routine is rather time consuming and thus not often used. It reaches a degree of accuracy, which is seldom needed especially for process optimizations.

Cell-models like the *Craig model* (see e.g. [59, 102, 159, 166]) are usually used when the Rouchon method fails, especially for the modelling of gradient elution [59]. Here the formula Eq. (2-22) becomes implicit and needs to be solved by iteration, which is more time consuming than the Rouchon method but faster than the OCFE. It has been shown, that solutions of the Craig model are often closer to those solutions ob-

tained from OCFE, compared to those obtained from the finite difference scheme defined by Eq. (2-22), (2-23).

The extension of the equilibrium dispersive model Eq. (2-19) to the *Lumped Kinetic Model* by the introduction of an apparent transport term yields an additional equation.

$$\frac{\partial q_i}{\partial c_i} = k\left(q_i^*(\mathbf{c}) - q_i\right)$$ (2-24)

The index * denotes the loadings in equilibrium with the fluid phase concentrations $\mathbf{c}$. For large enough values of the transport coefficient k (typically k>50 s^{-1}), the same results are obtained as for the equilibrium dispersive model solved by the OCFE method (see e.g. section 2.2.3 in [66]). The transport term stabilizes the finite difference scheme defined by Eq. (2-22) and is introduced for numerical reasons only. Kaczmarski and Antos [91] applied this scheme to utilize the fast Rouchon algorithm for implicit isotherms. The time increments are now obtained from:

$$\Delta t = \frac{1}{3\,k}$$ (2-25)

2.3.4.   Modelling Gradient Elution

The application of gradients, that is to change / influence the adsorption equilibria by modifying certain process conditions during the process is commonly used to enhance the performance of liquid chromatography (LC), especially for analytical purposes. In LC, this usually means to change the elution strength of the mobile phase by modifying the mobile phase composition. Other gradients such as temperature gradients are of less importance for liquid preparative chromatography.

For the modelling of gradient elution, two approaches are used to describe the interactions between the components to be separated and the mobile phase constituents. In one approach competition between all adsorbable components in the system is accounted for, i.e. the isotherms of all components (solutes and mobile phase constituents) are connected. The loading of the strong eluent (in the case of binary mobile phases containing an adsorbed strong eluent and an inert weak eluent) should be

modelled by excess loadings Γ_i, since their concentrations, x_i, range from 0-100 mole.% [66].

$$\Gamma_i = q_i - x_i \sum_j^{N_C} q_j \tag{2-26}$$

Excess quantities and their application are comprehensively reviewed by e.g. Oscik [129], Schay [154] and Everett [29]. The loading of the solutes on the other hand are sufficiently modelled by equilibrium loadings (since x_i are small) (see e.g. chapter 3 in [66]). The single component isotherms are coupled via the adsorbed solution theory [139] to obtain the individual loadings of multi component mixtures. This approach is explained and impressively applied in [132-136].

The other (traditional) approach is to model the influence of the strong eluent on the loading of the solutes by an apparent isotherm. In this approach, the isotherm coefficients correspond to the local distribution of the modifier concentration calculated by the use of a dynamic model. For the description of the dependence of the solute loadings on the modifier concentration typically empirical [161] or semi-empirical models [79] are used, such as the Snyder- Soczewinski equation derived for normal phase chromatography:

$$k^{'} = k_0^{'} c_{\text{mod}}^{-m}, \tag{2-27}$$

or the popular linear solvent strength model derived for reversed phase chromatography [24, 164]:

$$\log\left(k^{'}\right) = \log\left(k_0^{'}\right) - m \cdot c_{\text{mod}}. \tag{2-28}$$

Golshan-Shirazi *et al.* [52] have shown for multi-Langmuir isotherms that both approaches (competitive loadings and apparent isotherm parameters) are somewhat similar:

$$q_{solute} = q_s \frac{b_{solute} c_{solute}}{1 + b_{solute} c_{solute} + b_{mod} c_{mod}}$$

$$= q_s \frac{b_{app}(c_{mod}) c_{solute}}{1 + b_{app}(c_{mod}) c_{solute}} \qquad \text{(2-29)}$$

$$\text{with } b_{app}(c_{mod}) = \frac{b_{solute}}{1 + b_{mod} c_{mod}}$$

The result is basically the Scott-Kucera equation (see e.g. [165] and references therein). All of the functions above are often empirically expanded to yield flexible expressions capable to cope for a large range of modifier concentrations. Basically, this approach neglects influence of the solutes on the strong eluent, which is reasonable since the strong eluent is usually present at a much higher concentration. For those cases where the modifier is an additive present at small concentration, this approach is not valid. For those cases where the strong eluent is part of a binary mobile phase, containing both an adsorbable strong eluent and an inert weak eluent, this approach is valid and has been successfully applied to optimize discontinuous [20, 59, 82-85] and continuous preparative gradient processes (see [3, 4, 161] and references therein).

2.3.5.   Determination of Adsorption Isotherms

The adsorption equilibria have to be determined experimentally in liquid chromatography. The steps for the determination are:

1. system characterization (volume of the connecting capillaries, porosity of the column)

2. Analytical and overloaded injections:

   - determination of initial slope of the isotherms ➜ important for fitting of model parameters

   - observation of the peak shape for a pre-choice of suitable adsorption isotherm models

3. Actual experiments to determine adsorption isotherms

4. Fitting of appropriate models (based on first principles) with as few free parameters as possible

Methods to measure adsorption isotherms are comprehensively reviewed here [66, 160]. In our days typically dynamic methods are state of the art. I briefly review the three methods used in this work, while details will be given at their application in chapters 4 and 5.

2.3.5.1.   *Frontal Analysis*

This dynamic method is regarded as the most precise method to obtain adsorption isotherms. A concentration step is introduced at the column entrance so long until this concentration step is observed at the column outlet. Frontal analysis (FA) is independent on mass transfer kinetics and type of isotherm, since it is based on an overall mass balance. For a single component the integral mass balance becomes:

$$
\begin{aligned}
\text{capacity} &\equiv V_0 \left[c_0 \big|_{t<0} - c^F \big|_{z=0} \right] + V_S \left[q\left(c_0 \big|_{t<0} \right) - q\left(c^F \big|_{z=0} \right) \right] \\
&= Q \int_0^\infty \left(c^F \big|_{z=0} - c \big|_{z=L} \right) dt
\end{aligned}
\tag{2-30}
$$

FA can also be used to determine competitive loadings. The necessary theoretical frame work was described by Lisec *et al.* [105]. However, competition results in the development of intermediate plateaus which concentrations need to be determined, either by selective detectors or by sampling and offline analysis. For strong competition, these intermediate plateaus may become unidentifiable. FA is rather material and labor intensive. The latter disadvantage is somewhat relaxed in our days, given the automization of state-of-the-art chromatographic equipment. It biggest advantage is that the loadings are obtained directly and suitable isotherm model can be chosen based on the observed shape of the equilibrium loading.

2.3.5.2.   *Perturbation Method*

The perturbation method is a dynamic method, where the equilibrium at different concentration levels is disturbed by tiny injections and the resulting system responses (peaks at the column outlet) can be related to the slope of the isotherms of the com-

ponents involved. It bases in principle on Eq. (2-17) or rather on (2-37), which can be related to the retention time by

$$t_{R,k} = \frac{L}{u_c} = \frac{t_0 u}{u_c} = t_0 \left(1 + F \left. \frac{dq_i}{dc_i} \right|_{\mathbf{c}} \right) = t_0 \lambda_k(\mathbf{c})$$

(2-31)

with $k = 1..N_c$

$\mathbf{c}$ is the vector of adsorbable components of the length N_c (without the inert mobile phase). A tiny perturbation of an equilibrium state defined by $\mathbf{c}$ yields N_c characteristic responses for each component present in the system. The characteristic times of these responses are synchronized via Eq. (2-31). In this expression, the first derivatives of the adsorption isotherms are included (see e.g. below λ Eq. (2-40) for a binary mixture). The measured retention times for a series of perturbation experiments equilibrated at different concentrations yields the derivatives of the adsorption isotherms at these concentrations. The parameters of appropriate models may be fitted to the experimental data. *The perturbation method for zero equilibrium concentration should be always used to determine the initial slopes of the adsorption isotherms.*

Tondeur *et al*. [185] explained the theory for the area of the perturbation peaks, while Blümel *et al*. [13] presented it for the evaluation of retention times, which is much more practical since the characteristic times can be obtained from simple (unselective) detector responses without calibration. Peak area determination methods require calibrated, substance selective detectors, which must distinguish tiny differences in the concentrations in the presence of large equilibrium concentrations, which is a tough task and seldom applicable in liquid chromatography. For higher equilibrium concentrations and for more pronounced nonlinearity often the problem is met, that the characteristic system responses cancel each other out. This can be overcome with ideal disturbance concentrations as suggested by Forssen *et al*. [34] for binary mixtures. This method was successfully applied by Zhang *et al*. [197]. Even with these improvements, this method lacks applicability for small separation factors (below 2), since the characteristic response times become indistinguishable. The perturbation method has, to my knowledge, not yet been applied to mixtures of more than two components.

2.3.5.3. *Inverse Method*

The so-called *inverse method (IM) is a peak fitting method*. It consists of matching experimental concentration profiles with proper solutions of an appropriate column model. This is typically the equilibrium dispersive model Eq. (2-19). The advantages of this dynamic method are highly condensed information with $c(t)$, which result in just a few experiments (1-3) necessary. The reduced effort of laboratory time has to be compensated by an increased effort of computer time. This is often more than acceptable, since much less material is needed and competitive isotherms – suitable for process optimization – can be extracted directly. A major drawback of this method is, that appropriate adsorption isotherm models have to be chosen indirectly based on peak shapes, which can only give the information whether the isotherms are convex upward, downward or sigmoidal. A further limitation is that a column model must be provided, which has to be validated also.

Since the first reported use of this method [25] it has been successfully applied in a number of applications (e.g. [2, 3, 7, 31, 32, 199, 200]). It has been proven for the IM-method to result in similar isotherms as those obtained from frontal analysis in the concentration range of the elution profiles [1, 8, 18, 78]. Especially competitive isotherms can be extracted in concentration ranges where FA or perturbation methods may fail since the important intermediate plateaus / retention times become indistinguishable. For the determination of competitive isotherms, elution profiles of all components should overlap, only than competitions occur. This is the opposite of the recommendation in [196], but is – besides common sense – in agreement with findings by the other cited resources. Arnell *et al.* [8] recommends the use of the IM on preloaded columns, i.e. utilizing the whole information of a perturbation experiment rather than just the characteristic times. A detailed and practical procedure for the computer implementation of the IM is given by Forssen *et al.* [35]. Some warnings have been given by Kaczmarski [92] for non-Langmuir type isotherms and the use of the Rouchon method [144] for solving the equilibrium dispersive model Eq. (2-19).

2.4. Introduction to Solutions of the Ideal Model and the Hodograph Space

A comprehensive solution of the ideal model based on methods of characteristics is derived in detail in [142, 143]. However, the explanations in these original sources are not easy to understand. I will try to compress the main features of the solution of the ideal model in the following paragraphs. While not always mathematically perfect it may serve the interested reader as a hands-on-solution – ready to be used for specific examples. This section is mainly a derivation of the well-known equations (2-17) and (2-18).

In order to simplify the discussion, commonly a normalization is introduced by defining a dimensionless time τ and a dimensionless column length ζ.

$$\tau = \frac{ut}{L} \qquad\qquad \zeta = \frac{z}{L} \qquad\qquad (2\text{-}32)$$

Typically the characteristic length L of the column is its actual length. Sometimes people do not fix the definition to remain flexible. Inserting Eq. (2-32) into (2-13) yields an expression which can be formulated in the following way (see also page 82 in [142]):

$$\mathbf{A}\frac{\partial \mathbf{c}}{\partial \tau} + \frac{\partial \mathbf{c}}{\partial \zeta} = \mathbf{0} \qquad\qquad \textbf{(2-33)}$$

Where $\mathbf{A}$ and $\mathbf{c}$ are a matrix and a vector, respectively. The matrix $\mathbf{A}$ is referred to as *process matrix* or *process function*, defined as:

$$\mathbf{A} = \begin{bmatrix} 1 + F\dfrac{\partial q_1}{\partial c_1} & \cdots & F\dfrac{\partial q_1}{\partial c_{N_C}} \\[2ex] \vdots & \ddots & \vdots \\[2ex] F\dfrac{\partial q_{N_C}}{\partial c_1} & \cdots & 1 + F\dfrac{\partial q_{N_C}}{\partial c_{N_C}} \end{bmatrix} \qquad\qquad \textbf{(2-34)}$$

i.e.

$$A_{ij} = F \frac{\partial q_i}{\partial c_j} \qquad \text{for } i \neq j, \ i, j = 1..N_C$$

$$A_{jj} = 1 + F \frac{\partial q_j}{\partial c_j} \qquad \text{for } j = 1..N_C$$

For the sake of simplification, the partial derivatives of the loading q are denoted as:

$$q_{ij} = \frac{\partial q_i}{\partial c_j} \qquad \text{for } i, j = 1..N_C \tag{2-35}$$

The characteristic directions (or the slope) of the concentrations in the $\tau - \zeta$ plane are the eigenvalues, λ, of the process function $\mathbf{A}$:

$$\det(\mathbf{A} - \lambda \mathbf{I}) = 0 \qquad \lambda \equiv \frac{d\tau}{d\zeta}\bigg|_{\mathbf{c}} \tag{2-36}$$

where $\mathbf{I}$ is the identity matrix. Since λ represents the slope in the time-space plane it is reciprocal to the migration velocity of a set of concentrations.

$$\tau \sim \lambda \cdot \zeta \tag{2-37}$$

with τ being a vector of characteristic times. Depending on the number of adsorbable components present in the system, λ and τ are N_C-dimensional vectors[2]. In [140, 141] directions are already associated to the eigenvalues λ. I will not do that here – rather I will unambitiously number the individual eigenvalues from $1 \ldots N_C$[3]. This principle is applied in Example 2-1 to a single solute, which adsorbs in a linear fashion to the solid phase. This example visualizes the important fact of *contact discontinuities*. These discontinuities are introduced by the boundary conditions and travel on a characteristic.

---

[2] the mobile phase is regarded as an inert component, so the actual number of components in the system is N_C+1

[3] Note, although the same indices as for the individual components are used, the index of a characteristic has nothing to do with the index of a component

Example 2-1: Propagation of a single solute - linear isotherm - through an initially unloaded column

$$q = Hc \qquad A = 1 + FH \qquad \det(1 + FH - \lambda) = 0 \Rightarrow \lambda = 1 + FH$$

The slopes in the $\tau - \zeta$ plane are constant and are unambitiously sketched. The column is initially equilibrated with solvent, which is treated as an inert (typical for such applications). Between 0 and τ_{inj} a rectangular plug of the solute is introduced at the entrance of the column ($\zeta = 0$, grey region in the figure). Afterwards only pure solvent is applied to the column. The corresponding initial and boundary conditions of this so-called Riemann problem are thus:

$$c(\zeta,\tau) = 0 \quad \tau < 0 \qquad \zeta = [0,1]$$
$$c(\zeta,\tau) = c^F \quad 0 \leq \tau \leq \tau_{inj} \quad \zeta = 0$$
$$c(\zeta,\tau) = 0 \quad \tau > \tau_{inj} \qquad \zeta = 0$$

Note that 2 discontinuities are introduced to the system. Both discontinuities travel along the (constant) characteristics and are called *contact discontinuities*. All characteristics are independent of the solute concentration – another important property of this example. Contact discontinuities are prone to dispersion and often indicate the limitation of the accuracy of the ideal model.

Typical visualizations are time-space (or space-time), concentration-space and concentration-time profiles.
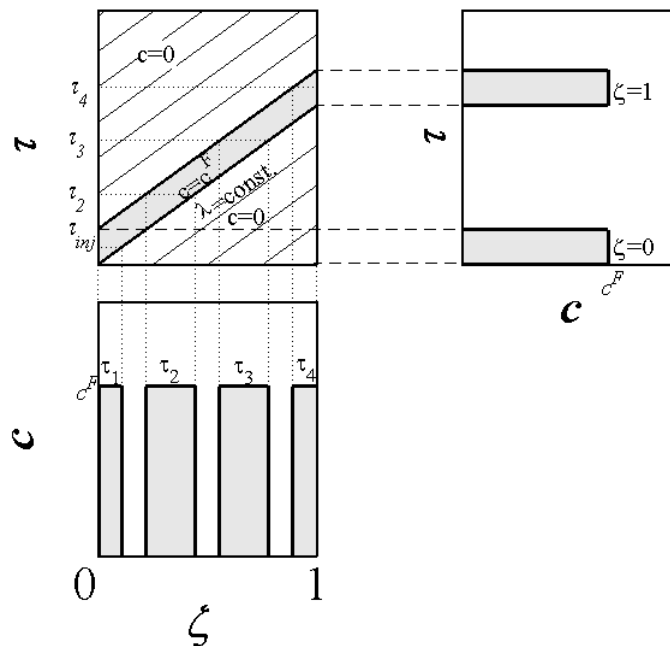
Other typical phenomena are covered in Example 2-2. Here (*centered*) *compressive* and *spreading (expansive) waves* are displayed among the formation of *shocks*. For details see section 'Discontinuities in Solutions' in Rhee's *et al.* book [143]. In all my discussions, I will concentrate on centered waves – a phenomenon which is typically met in chromatography due to the nature of how samples are introduced to the column (as a plug – mathematically this translates to two consecutive *Riemann-problems*).

In Example 2-1 and Example 2-2 always two state changes were considered (from the initial state to the feed state and back from the feed state to the initial state) – i.e. a complete chromatographic cycle. So far interactions between the adsorption and the desorption side of the feed plug were disregarded. For such chromatographic cycles, the speed of the state change at one side of the injection plug will be proportional to the derivative of the isotherm and on the opposite side it will be proportional to the chord of the isotherm. For all nonlinear isotherms it is true:

$$\frac{\Delta q}{\Delta c} \neq \frac{dq}{dc} \tag{2-38}$$

Thus, if the column is long enough or the feed plug small enough at one point interactions between the two state changes will occur. This is sketched in Example 2-3, which is in principle the same as Example 2-2, except that here interactions are happening between the adsorption and the desorption side of the feed plug. The solution of the *shockpath* for centered waves is described exemplarily in Example 2-3.

Example 2-2: Propagation of a single solute - Langmuir isotherm - through an initially unloaded column

$$q = \frac{ac}{1+bc} \qquad\qquad A = 1 + F\frac{a}{\left(1+bc\right)^2} \qquad\qquad \lambda = \lambda(c) = 1 + F\frac{a}{\left(1+bc\right)^2}$$

The same boundary conditions as in Example 2-1 apply. Here, the characteristic slopes in the $\tau - \zeta$ plane are dependent on the concentration of the solute. This is sketched in the figure below.

Prior to the injection, the whole column is in the state where $c = 0$. Thus, the characteristic slopes are $1 + Fa$. At the beginning of the injection the concentration jumps in an infinitesimal small amount of time from 0 to c^F, covering in that time frame all concentrations between 0 and c^F. The characteristic slopes, $\lambda(c) = 1 + F\frac{a}{\left(1+bc\right)^2}$, decrease in that point with increasing concentrations. i.e. higher concentrations travel faster than smaller concentrations and eventually overtake them – at this point we find a *centered compressive wave – a shock*. The inverted shock velocity of the adsorption front with c^F is, according to Eq. (2-18), proportional to the chord of the isotherm between the initial (zero for a not preloaded column) and the feed concentration:

$$\tilde{\lambda}(c^F, c^0) = 1 + F\frac{q(c^F) - \cancel{q(c^0)}^{=0}}{c^F - \cancel{c^0}^{=0}} = 1 + F\frac{a}{1+bc^F}$$

Now, at the end of the injected feed plug the concentrations are changing from the highest concentration c^F to 0. This time the characteristic slopes change from the smallest to the highest value. Thus, the higher concentrations, already faster than the smaller ones, travel ahead of the smaller concentrations. The distance between the smaller and higher concentrations increase as they propagate through the column, i.e. a *spreading (expansive) wave* centered at the column entrance forms.
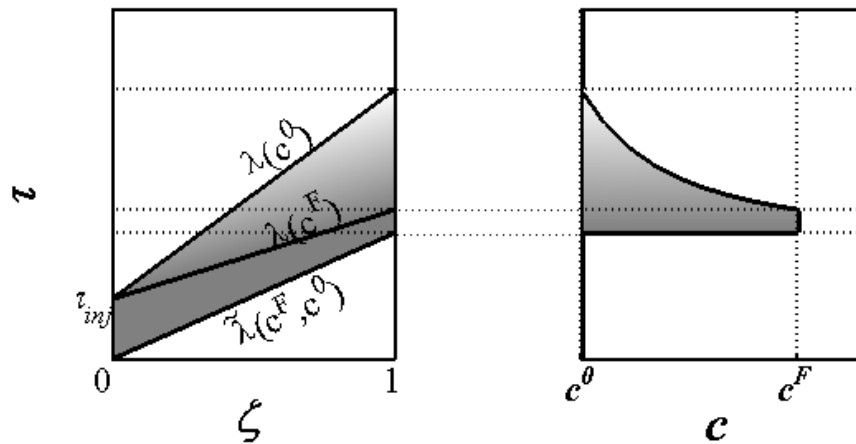
Example 2-3: Propagation of a single solute - Langmuir isotherm - through an initially unloaded column with interactions between the adsorption and the desorption side of the feed state

The same definitions, boundary and initial conditions apply as for Example 2-2. But here the injection is small enough to fulfill (with the dimensionless column length being 1 at the end of the column):

$$\tau_{inj} < \tilde{\lambda}(c^F,c^0) - \lambda(c^F)$$

At the beginning of the column, the same phenomena as described in Example 2-2 are observed. At ζ^* overtake the faster concentrations of the desorption side ($\tau = \tau_{inj} + \lambda(c)\zeta$) the shock of the adsorption ($\tau = \tilde{\lambda}(c^F,c^0)\zeta$). The interaction of the adsorption and desorption front happen for this specific example at:

$$\tilde{\lambda}(c^F,c^0)\zeta^* = \tau_{inj} + \lambda(c^F)\zeta^*$$

$$\Rightarrow \zeta^* = \frac{\tau_{inj}}{\tilde{\lambda}(c^F,c^0) - \lambda(c^F)} \qquad\qquad \tau^* = \tau_{inj}\frac{\tilde{\lambda}(c^F,c^0)}{\tilde{\lambda}(c^F,c^0) - \lambda(c^F)}$$

Note that the equation above is specific for this example (single component and the given boundary and initial conditions), and may have to be modified for another application (e.g. for different number of components, different boundary conditions, etc.). The starting point is always where the characteristics intersect.
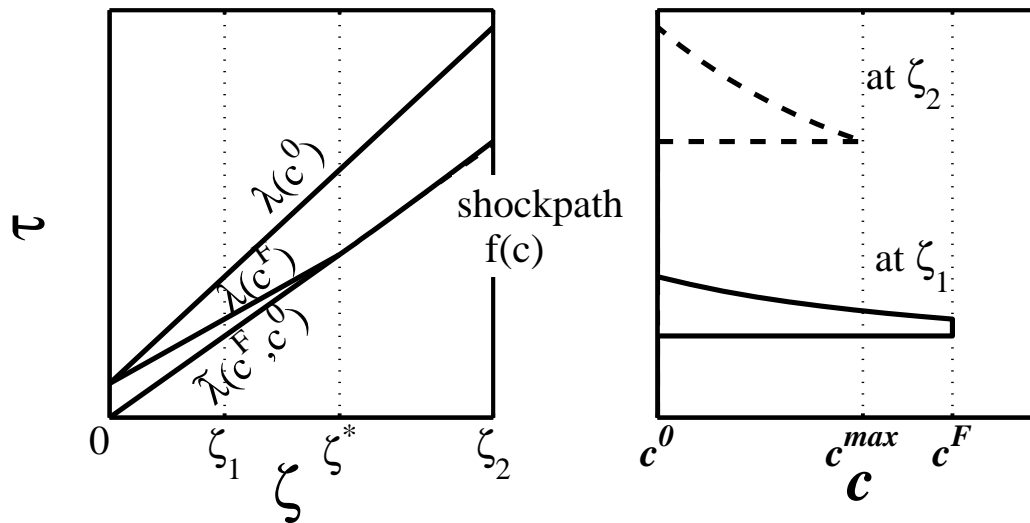
From this point on the shock decelerates as the concentrations decrease. The following describes the derivation of the solution for the shockpath on this example.

Solution of the shockpath:

The slope of the shockpath is still $\dfrac{d\tau}{d\zeta} = \tilde{\lambda}(c,c^0)$.

While for the retention time of the desorption side the following still holds:

$$\tau = \tau_{inj} + \lambda(c)\zeta$$

Differentiating this with respect to c

$$\frac{d\tau}{dc} = 0 + \frac{d\lambda(c)}{dc}\zeta + \frac{d\zeta}{dc}\lambda(c) \quad \text{and rearranging yields}$$

$$\frac{d\tau}{d\zeta} = \frac{d\lambda(c)}{d\zeta}\zeta + \lambda(c)$$

Now replacing $\dfrac{d\tau}{d\zeta}$ by the slope of the shockpath:

$$\tilde{\lambda}(c, c^0) = \frac{d\lambda(c)}{d\zeta}\zeta + \lambda(c)$$

Splitting of the variables:

$$\frac{d\zeta}{\zeta} = \frac{d\lambda(c)}{\tilde{\lambda}(c, c^0) - \lambda(c)}$$

and replacement $d\lambda(c) = \dfrac{d\lambda(c)}{dc} dc$ yields

$$\int_{\zeta^*}^{\zeta} \frac{d\zeta}{\zeta} = \int_{c^F}^{c} \frac{1}{\tilde{\lambda}(c, c^0) - \lambda(c)} \frac{d\lambda(c)}{dc} dc$$

The equation above has to be integrated using the specific isotherm expressions, here:

$$\tilde{\lambda}\left(c^F, c^0\right) = 1 + F\frac{q(c^F) - q(c^0)}{c^F - c^0}$$

$$= 1 + F\frac{a}{\left(1 + bc^F\right)\left(1 + bc^0\right)} \qquad \text{and} \qquad \lambda(c) = 1 + F\frac{a}{\left(1 + bc\right)^2}$$

For the single component Langmuir isotherm this results in the shockpath:

$$\tilde{\zeta}(c) = \zeta^*\left(\frac{(1 + bc)}{(1 + bc^F)}\frac{(c^F - c^0)}{(c - c^0)}\right)^2 \quad \text{with} \quad \zeta^* = \frac{\tau_{inj}}{F \cdot a \cdot b}\frac{\left(1 + bc^0\right)\left(1 + bc^F\right)^2}{c^F - c^0}$$

Usually one is interested in the concentration profile at a given space position or at a given time. Inserting the expression for ζ^* into the solution for the shockpath and solving the resulting expression for c yields an equation for the maximal concentration at a given space position. The resulting solution for the concentration is rather complicated with:

$$C_1 c^2 + C_2 c + C_3 = 0 \qquad\qquad C_1 = (c^F - c^0)(1 + bc^0)\tau_{inj} \cdot b^2 - F \cdot a \cdot b\zeta$$

$$c = -\frac{C_2 \pm \sqrt{\left(C_2\right)^2 - 4C_1 C_3}}{2C_1} \quad \text{and} \quad C_2 = (c^F - c^0)(1 + bc^0)2\tau_{inj} \cdot b + 2c^0 F \cdot a \cdot b\zeta$$

$$C_3 = (c^F - c^0)(1 + bc^0)\tau_{inj} - \left(c^0\right)^2 F \cdot a \cdot b\zeta$$

The unknown concentration is the positive root of the equation above.

In the above, we have seen how we can analyze typical phenomena from the characteristics in the time-space-plane. For multi-component mixtures (more precisely binary mixtures) these phenomena might be easier understood in the *hodograph* space, here the concentration-space. The characteristic directions in the hodograph can be obtained from the Eigenvectors $\mathbf{r}(\lambda_i)$, which are tangent to it [142]. I will explain this methodology on the example of a binary mixture, for which the fully equipped process matrix is:

$$\mathbf{A} = \begin{bmatrix} 1 + Fq_{11} & Fq_{12} \\ Fq_{21} & 1 + Fq_{22} \end{bmatrix}$$

(2-39)

With the definition of the Eigenvalues, Eq. (2-36), we obtain the characteristic directions in the time-space plane

$$\lambda = f(\mathbf{c}) = \begin{bmatrix} \lambda_1 \\ \lambda_2 \end{bmatrix} = \begin{bmatrix} 1 + \dfrac{1}{2}\left(F\left(q_{11} + q_{22}\right) + \sqrt{F^2\left(\left(q_{11} - q_{22}\right)^2 + 4q_{12}q_{21}\right)} \right) \\ 1 + \dfrac{1}{2}\left(F\left(q_{11} + q_{22}\right) - \sqrt{F^2\left(\left(q_{11} - q_{22}\right)^2 + 4q_{12}q_{21}\right)} \right) \end{bmatrix}$$

(2-40)

With the definition of the Eigenvectors $\mathbf{r}(\lambda_i)$

$$\mathbf{A}\mathbf{r}(\lambda_i) - \mathbf{r}\lambda_i = 0$$

(2-41)

two Eigenvectors are obtained for the binary system:

$$\mathbf{r}(\lambda_1) = \begin{bmatrix} 1/2\left(F\left(q_{11} - q_{22}\right) + \sqrt{F^2\left(\left(q_{11} - q_{22}\right)^2 + 4q_{12}q_{21}\right)} \right) \\ Fq_{21} \end{bmatrix} \equiv \begin{bmatrix} dc_1 \\ dc_2 \end{bmatrix}$$

(2-42)

$$\mathbf{r}(\lambda_2) = \begin{bmatrix} 1/2\left(F\left(q_{11} - q_{22}\right) - \sqrt{F^2\left(\left(q_{11} - q_{22}\right)^2 + 4q_{12}q_{21}\right)} \right) \\ Fq_{21} \end{bmatrix} \equiv \begin{bmatrix} dc_1 \\ dc_2 \end{bmatrix}$$

(2-43)

Since the direction of the vectors remain constant if one divides them by an expression, the eigenvectors can be rewritten as[4]:

$$\mathbf{r}^*(\lambda_1) = \begin{bmatrix} \dfrac{1/2\left(q_{11} - q_{22} + \sqrt{(q_{11} - q_{22})^2 + 4q_{12}q_{21}}\right)}{q_{21}} \\ 1 \end{bmatrix} \equiv \begin{bmatrix} \dfrac{dc_1}{dc_2} \\ \dfrac{dc_2}{dc_2} \end{bmatrix}$$

$$= \begin{bmatrix} \dfrac{1}{\dfrac{q_{21}}{1/2\left(q_{11} - q_{22} + \sqrt{(q_{11} - q_{22})^2 + 4q_{12}q_{21}}\right)}} \end{bmatrix} \equiv \begin{bmatrix} \dfrac{dc_1}{dc_1} \\ \dfrac{dc_2}{dc_1} \end{bmatrix}$$

(2-44)

$$\mathbf{r}^*(\lambda_2) = \begin{bmatrix} \dfrac{1/2\left(q_{11} - q_{22} - \sqrt{(q_{11} - q_{22})^2 + 4q_{12}q_{21}}\right)}{q_{21}} \\ 1 \end{bmatrix} \equiv \begin{bmatrix} \dfrac{dc_1}{dc_2} \\ \dfrac{dc_2}{dc_2} \end{bmatrix}$$

$$= \begin{bmatrix} \dfrac{1}{\dfrac{q_{21}}{1/2\left(q_{11} - q_{22} - \sqrt{(q_{11} - q_{22})^2 + 4q_{12}q_{21}}\right)}} \end{bmatrix} \equiv \begin{bmatrix} \dfrac{dc_1}{dc_1} \\ \dfrac{dc_2}{dc_1} \end{bmatrix}$$

(2-45)

The Eigenvectors are tangent to the characteristic directions in the hodograph space. If the Eigenvectors are formulated as depicted in Eq. (2-44), (2-45), integration along one (suited[5]) concentration yield the concentrations pathways $R(\lambda_i)$.

$$R(\lambda_i): \qquad \int_c r^*(\lambda_i)dc$$

(2-46)

The beauty of this method is that it provides immediate inside sight how the concentrations of interest behave.

---

[4] F can be removed from the root, since per definition F is always positive

[5] Attention with the choice of the denominator, consider that it may become zero!

In principle the application of the equilibrium theory to batch elution chromatography can be summarized as follows:

1. Formulate the process matrix $\mathbf{A}$, Eq. (2-34)

2. Solve for Eigenvalues λ ➜ characteristic directions in the time-space-plane

3. Solve for Eigenvectors $\mathbf{r}(\lambda_i)$ ➜ tangent to the directions of the concentrations in the hodograph space (corresponds to $\dfrac{dc_j}{dc_i}$)

4. Integrate $\mathbf{r}(\lambda_i)$ with a suited concentration as a running parameter and plot the resulting concentration pathways $R(\lambda_i)$ in the hodograph

5. In the hodograph space: mark initial and feed state and follow $R(\lambda)$, connected to the smallest Eigenvalue λ_i, from the initial state the until it intersects with the pathway connected to the next larger Eigenvalue and so forth until the feed state is reached. Now we know if:

   - Eigenvalue λ_i increases in the direction of $R(\lambda_i)$ ➜ (simple) spreading waves form

   - Eigenvalue λ_i decreases in the direction of $R(\lambda_i)$ ➜ compressive waves or shocks form – note that the concentration pathway of a shock only overlaps with the characteristic directions $R(\lambda_i)$ for straight lines in the hodograph (e.g. for Langmuir – Isotherms)

   - Eigenvalue λ_i remains constant in the direction of $R(\lambda_i)$ ➜ contact discontinuities form

This methodology is depicted in Example 2-4 for competitive binary interactions, which can be described by Multi-Langmuir isotherms.

Example 2-4: Propagation of a binary mixture - Langmuir isotherms - through an initially preloaded column

$$q_i = \frac{a_i c_i}{1 + \sum_{j=1}^{N_c} b_j c_j} \qquad q_{ij} = -\frac{a_i b_j c_i}{\left(1 + b_1 c_1 + b_2 c_2\right)^2} \qquad q_{ii} = \frac{a_i \left(1 + b_j c_j\right)}{\left(1 + b_1 c_1 + b_2 c_2\right)^2}$$

with $i, j = 1, 2$ $\qquad a_1 = 1$, $a_2 = 2$, $b_1 = 0.1$, $b_2 = 0.2$

initial condition: $c_1^0 = c_2^0 = 1$ $\qquad$ feed condition: $c_1^F = c_2^F = 5$

Inserting these expressions into the expressions for the eigenvectors $\mathbf{r}$ (2-44), (2-45) and integrating them for a set of concentrations yields the concentration pathways in the hodograph (concentration space), depicted in the picture below.

- *thin lines: sets of concentration pathways $R(\lambda_i)$*
- *thick lines: complete chromatographic cycle*
- *0 and F: initial and feed state*
- *I1 and I2: intermediate states*
- *properties of the transitions are described in the table below*

state	λ_1	λ_2	comment	consequence
0	3.17	1.56	$\lambda_1^0 > \lambda_2^0$	start with $R(\lambda_2)$ to receive the state changes $$0 \xrightarrow{\lambda_2} I1$$ $$\lambda_1 \uparrow \qquad \downarrow \lambda_1$$ $$I2 \xleftarrow{\lambda_2} F$$
I1	2.39	1.23	$\lambda_2^0 > \lambda_2^{I1}$	state change from $0 \to I1$ happens with a shock
F	1.54	1.14	$\lambda_1^{I1} > \lambda_1^{F}$	state change from $I1 \to F$ happens with a shock
I2	1.85	1.35	$\lambda_2^F < \lambda_2^{I2}$ $\lambda_1^{I2} < \lambda_1^0$	state change from $F \to I2$ happens with spreading waves state change from $I2 \to 0$ happens with spreading waves

inverted shock velocity from 0→I1:
$$\tilde{\lambda}_{0\to I1} = 1 + F\frac{q_1^{I1}-q_1^0}{c_1^{I1}-c_1^0} = 1 + F\frac{q_2^{I1}-q_2^0}{c_2^{I1}-c_2^0}$$

inverted shock velocity from I1→F:
$$\tilde{\lambda}_{I1\to F} = 1 + F\frac{q_1^F-q_1^{I1}}{c_1^F-c_1^{I1}} = 1 + F\frac{q_2^F-q_2^{I1}}{c_2^F-c_2^{I1}}$$

wave from F→I2:   start: $\lambda_2\left(c_1^F, c_2^F\right)$ end: $\lambda_2\left(c_1^{I2}, c_2^{I2}\right)$

wave from I2→0:   start: $\lambda_1\left(c_1^{I2}, c_2^{I2}\right)$ end: $\lambda_1\left(c_1^0, c_2^0\right)$
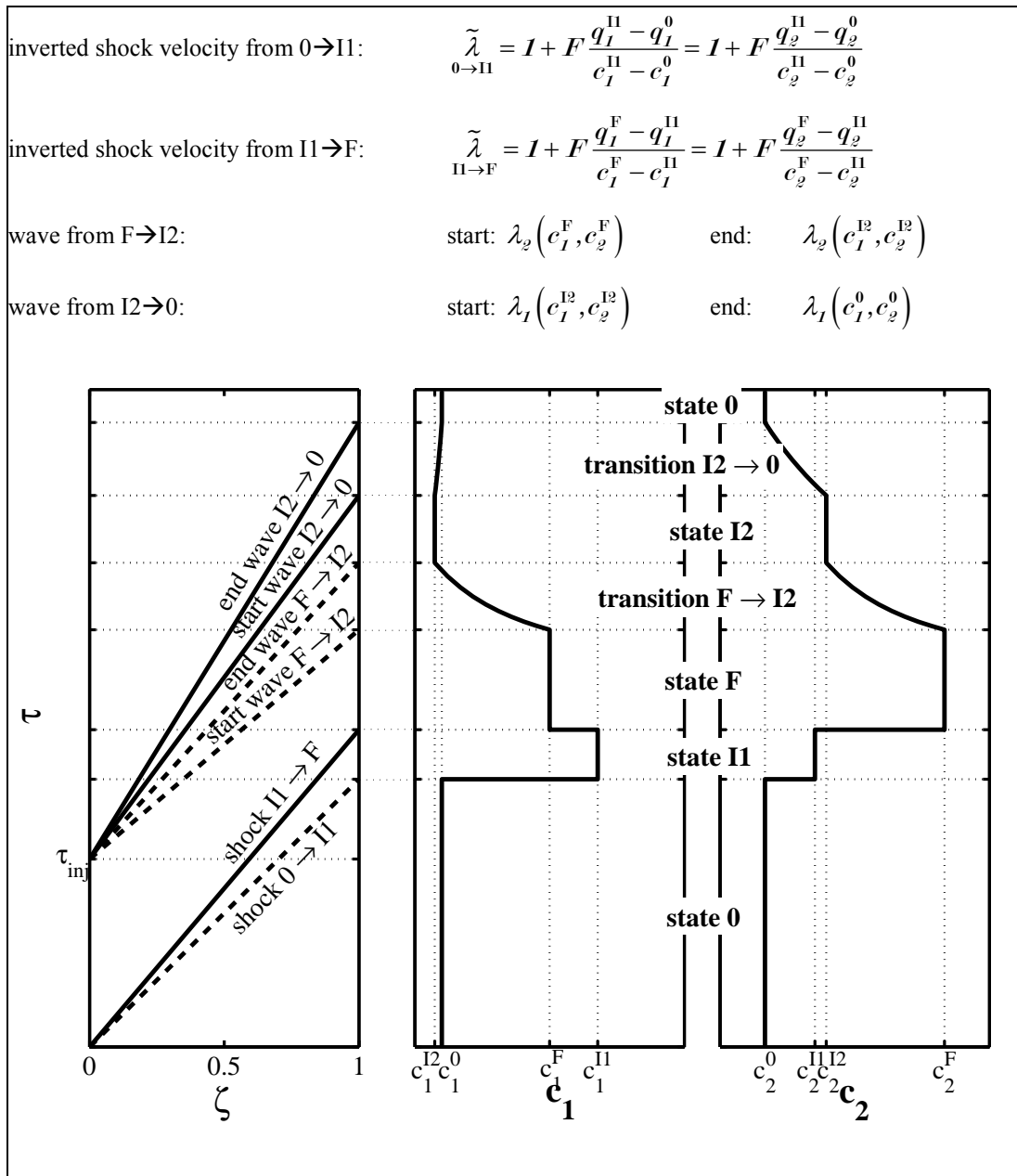
With Example 2-4, I conclude this section. The methodology to analyze the equilibrium model has been introduced in a simplified manner. Based on this methodology key properties of adsorption processes can be analyzed. It has been shown for four examples of increasing complexity that for adsorption processes the shape of the equilibrium loading on the fluid phase concentration has an enormous impact on the shape of elution profiles. Simple changes of the feed conditions may yield rather complicated elution profiles. These elution profiles are caused sole by the shape of the equilibrium function and are not due to mass transfer resistances.

3. Application of Equilibrium Theory for the Analysis of Solvent-Solute Interactions during Gradient Injection

In this chapter, I apply analytical solutions of the ideal model (equilibrium theory) to analyze general solvent-solute interactions of a gradient injection on their course through the chromatographic column. This should give insight on general effects of gradient injection method, such as dilution, concentration and band splitting of the solutes, as experimentally observed for injections in a different mobile phase. I classify this by the nature of the adsorption isotherms. For each type of adsorption isotherm combination I will start with the binary solvent-solute system. For the first isotherm combination the discussion will be extended to ternary solvent-solute-solute systems and the actual impact on the separation. In all cases, I will assume that the solutes have negligible effect on the adsorption of the solvent. This assumption is reasonable, since the solvent is typically present at much larger concentrations compared to the solute.

All solutions of the equilibrium theory presented here were implemented into Matlab scripts (Matlab R13, The Mathworks Inc.) to obtain the schematic figures of this chapter. In that respect, the solutions were also tested by checking the mass balances. The outlet profiles constructed resulted in very small deviations from the mass balance of typically less than 0.1%. In addition, the solutions were qualitatively com-

pared to well-established numerical solutions of column models for gradient elution. Discussion of the results will be typically made from a methodological point of view and be repeated from a more phenomenological point of view.

I will start with the formulation of the general process matrix, the corresponding eigenvalues and eigenvectors for the binary and the ternary system, respectively. We have already seen that the analysis of the interactions in the time-space domain or in the hodograph plane can be obtained from the solution of the process matrix $\mathbf{A}$, which holds for a binary mixture as:

$$\mathbf{A} = \begin{bmatrix} 1 + Fq_{11} & Fq_{12} \\ Fq_{21} & 1 + Fq_{22} \end{bmatrix} \tag{3-1}$$

Since we neglect influence of the solute (index 2) on the modifier (index 1) holds $q_{12} = 0$. Thus, Eq. (3-1) simplifies to

$$\mathbf{A} = \begin{bmatrix} 1 + Fq_{11} & 0 \\ Fq_{21} & 1 + Fq_{22} \end{bmatrix} \tag{3-2}$$

The eigenvalues λ of the process matrix $\mathbf{A}$ (i.e. the characteristic directions of the concentrations in the $\tau - \zeta$ plane) are therefore:

$$\lambda = \begin{bmatrix} \lambda_1 \\ \lambda_2 \end{bmatrix} = \begin{bmatrix} 1 + Fq_{11} \\ 1 + Fq_{22} \end{bmatrix} = 1 + F \begin{bmatrix} q_{11} \\ q_{22} \end{bmatrix} \tag{3-3}$$

The corresponding eigenvectors (tangents of the characteristic directions in the $c_1 - c_2$ hodograph space) are:

$$\mathbf{r}^*(\lambda_1) = \begin{bmatrix} \dfrac{dc_1}{dc_2} \\[2mm] \dfrac{dc_2}{dc_2} \end{bmatrix}_{(\lambda_1)} = \begin{bmatrix} \dfrac{q_{11} - q_{22}}{q_{21}} \\[2mm] 1 \end{bmatrix} \quad \text{or} \quad \mathbf{r}^*(\lambda_1) = \begin{bmatrix} \dfrac{dc_1}{dc_1} \\[2mm] \dfrac{dc_2}{dc_1} \end{bmatrix}_{(\lambda_1)} = \begin{bmatrix} 1 \\[2mm] \dfrac{q_{21}}{q_{11} - q_{22}} \end{bmatrix} \tag{3-4}$$

$$\mathbf{r}^{*}(\lambda_{2}) = \begin{bmatrix} \dfrac{dc_{1}}{dc_{2}} \\[6pt] \dfrac{dc_{2}}{dc_{2}} \end{bmatrix}_{(\lambda_{2})} = \begin{bmatrix} 0 \\[6pt] 1 \end{bmatrix} \qquad (3\text{-}5)$$

Note that it might be more appropriate to express $\mathbf{r}(\lambda_{1})$ with respect to dc_{1} since q_{21} can be become zero.

Consider now a ternary mixture consisting of the modifier (index 1) and two solutes (indices 2, 3). Lets use the assumption again that the solutes have no influence on the adsorption of the modifier, i.e. $q_{12} = q_{13} = 0$. Using this assumption, the process matrix $\mathbf{A}$ becomes:

$$\mathbf{A} = \begin{bmatrix} 1 + Fq_{11} & 0 & 0 \\ Fq_{21} & 1 + Fq_{22} & Fq_{23} \\ Fq_{31} & Fq_{32} & 1 + Fq_{33} \end{bmatrix} \qquad (3\text{-}6)$$

The corresponding eigenvalues of Eq. (3-6) can then be derived:

$$\lambda = \begin{bmatrix} \lambda_{1} \\ \lambda_{2} \\ \lambda_{3} \end{bmatrix} = 1 + F \begin{bmatrix} q_{11} \\[6pt] \dfrac{1}{2}\left(q_{33} + q_{22} - \sqrt{\left(q_{33} - q_{22} \right)^{2} + 4q_{23}q_{32}} \right) \\[6pt] \dfrac{1}{2}\left(q_{33} + q_{22} + \sqrt{\left(q_{33} - q_{22} \right)^{2} + 4q_{23}q_{32}} \right) \end{bmatrix} \qquad (3\text{-}7)$$

This in turn delivers the following eigenvector corresponding to λ_{1}:

$$\mathbf{r}(\lambda_{1}) = \begin{bmatrix} dc_{1} \\ dc_{2} \\ dc_{3} \end{bmatrix}_{(\lambda_{1})} = \begin{bmatrix} (q_{11} - q_{22})(q_{11} - q_{33}) - q_{32}q_{23} \\ q_{21}(q_{11} - q_{33}) + q_{31}q_{23} \\ q_{31}(q_{11} - q_{22}) + q_{21}q_{32} \end{bmatrix} \qquad (3\text{-}8)$$

Here it is convenient to express dc_{2} and dc_{3} with respect to dc_{1}.

The eigenvectors corresponding to λ_{2} and λ_{3} become:

$$\mathbf{r}(\lambda_2) = \begin{bmatrix} dc_1 \\ dc_2 \\ dc_3 \end{bmatrix}_{(\lambda_2)} = \begin{bmatrix} 0 \\ 1/2\left(q_{22} - q_{33} - \sqrt{(q_{22} - q_{33})^2 + 4q_{32}q_{23}}\right) \\ q_{32} \end{bmatrix} \tag{3-9}$$

$$\mathbf{r}(\lambda_3) = \begin{bmatrix} dc_1 \\ dc_2 \\ dc_3 \end{bmatrix}_{(\lambda_3)} = \begin{bmatrix} 0 \\ 1/2\left(q_{22} - q_{33} + \sqrt{(q_{22} - q_{33})^2 + 4q_{32}q_{23}}\right) \\ q_{32} \end{bmatrix} \tag{3-10}$$

The expressions given above can be used for any isotherm combination which holds $q_{12} = q_{13} = 0$.

3.1.   Analysis of Systems with Linear - Linear Isotherms

In the case of linear isotherms for both, the modifier (index 1) and the solute (index 2), the isotherms and their derivatives are quite simple. However, the Henry coefficient of the solute (H_2) depends on the concentration of the modifier (c_1):

$$q_1 = H_1 c_1 \tag{3-11}$$

$$q_2 = H_2(c_1)c_2 \tag{3-12}$$

$$q_{11} = H_1 \qquad\qquad q_{12} = 0 \tag{3-13}$$

$$q_{21} = \frac{dH_2(c_1)}{dc_1}c_2 \qquad q_{22} = H_2(c_1) \tag{3-14}$$

Substituting these expressions into the equations for the eigenvalues Eq. (3-3) yields:

$$\lambda = \begin{bmatrix} \lambda_1 \\ \lambda_2 \end{bmatrix} = 1 + F \begin{bmatrix} H_1 \\ H_2(c_1) \end{bmatrix} \tag{3-15}$$

The corresponding eigenvectors Eqs. (3-4) and (3-5) in turn become:

$$\mathbf{r}^*(\lambda_1) = \begin{bmatrix} \dfrac{dc_1}{dc_1} \\ \dfrac{dc_2}{dc_1} \end{bmatrix}_{(\lambda_1)} = \begin{bmatrix} 1 \\ \dfrac{c_2}{H_1 - H_2(c_1)} \dfrac{dH_2(c_1)}{dc_1} \end{bmatrix} \qquad (3\text{-}16)$$

$$\mathbf{r}^*(\lambda_2) = \begin{bmatrix} \dfrac{dc_1}{dc_2} \\ \dfrac{dc_2}{dc_2} \end{bmatrix}_{(\lambda_2)} = \begin{bmatrix} 0 \\ 1 \end{bmatrix} \qquad (3\text{-}17)$$

It is now obvious that $\lambda_1 = constant$, thus resulting in contact discontinuities for the concentrations in the $\tau - \zeta$-plane along the characteristics belonging to λ_1. On the other hand, the trajectory of the concentrations in the $c_1 - c_2$-hodograph plane ($\mathbf{r}(\lambda_1)$, Eq. (3-16)) is a curve which shape depends on the usually strong nonlinear dependence of the Henry coefficient of the solute on the modifier concentration ($H_2(c_1)$).

$\lambda_2 = f(c_1)$ is changing with the modifier concentration. However, the trajectories in the hodograph plane ($\mathbf{r}(\lambda_2)$, Eq. (3-17)) are just parallel to the axis of the solute concentration, i.e. $c_1 = constant$ thus $\lambda_2 = constant$. Again, contact discontinuities are present, since the eigenvalues λ_2 are constant along its trajectory in the hodograph plane.

The actual solution depends heavily on the dependence of the Henry coefficient of the solute on the modifier concentration, $H_2(c_1)$. The Henry coefficient typically decreases with increasing modifier concentration in a strong nonlinear manner. Thus, the derivative of the Henry coefficient is smaller than zero. For the mathematical description of that functional relation typically a number of different empirical equations are applied for the description of gradient elution [66]. Among the most prominent ones is the logarithmic-linear function often used in reversed-phase gradient chromatography. Power laws are also often used, e.g. in [66, 79]. Exemplary, I will use a flexible expansion of the Snyder-Soczewinski function (Eq. (2-27)), which will be used also for the experimental system, discussed in chapter 5:

$$H_2 = p_1 c_1^{-p_2} + p_3 \qquad \text{with} \quad \frac{dH_2}{dc_1} = -p_1 p_2 c_1^{(-p_2-1)} \qquad (3\text{-}18)$$

It holds $\dfrac{dH_2}{dc_1} < 0$, since in the equation above $p_1 > 0$ and $p_2 > 0$, i.e. decreasing

adsorption of the solute with increasing modifier concentration.

3.1.1.   Binary System – General Effects for a Single Solute

A equilibrium theory based discussion of the effects for a single solute for linear-linear isotherms was independently done also by Ströhlein *et al.* [180-182]. I will exemplary summarize the most important parts of the analysis here. Although I mainly discuss the injection in a stronger solvent in this work, I will also consider the injection in a weaker solvent. A couple of scenarios are possible for such systems. The general effects on the peak shape will depend on:

- the elution order of the modifier and the solute,

- whether a stronger or a weaker solvent is used for the injection.
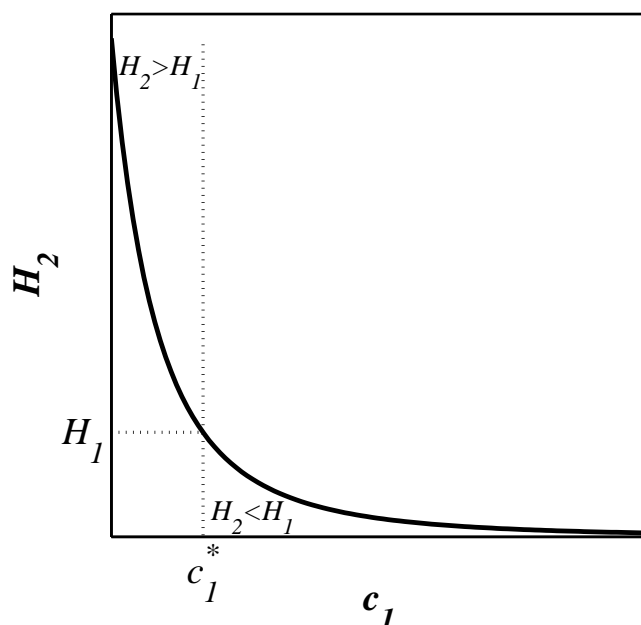
Figure 3.1: Typical dependence of the Henry coefficient of the solute on the modifier concentration.

Typical dependence of the Henry coefficient on the modifier concentration is shown in Figure 3.1. There may exist a modifier concentration c_1^*, which indicates the change of the elution order. Below c_1^* the solute is the stronger adsorbed component and above c_1^* the solute is the less adsorbed component. Based on these the following cases are possible:

case a) The modifier is always the least retained component: $H_2(c_1) > H_1$, $c_1 < c_1^*$. I regard this case to be the most relevant one for preparative chromatography, where the modifier is part of a mixed binary solvent mixture.

case b) The modifier is always the strongest retained component: $H_2(c_1) < H_1$, $c_1 > c_1^*$. Though this happens, e.g. in displacement chromatography and biochromatography, it seams a less frequent case compared to case a).

case c) Mixed elution order: $H_2(c_1) \leq H_1 \leq H_2(c_1)$, $c_1^* \leq c_1 \leq c_1^*$. Solute has smaller and larger retentions than the solute, depending on the modifier concentration. Such a case can be observed, however it has to be avoided, since it will make such a system unsuitable for separation of more component systems.

These three cases will be discussed below.

3.1.1.1. *Modifier is the Least Retained Component - Case a)*

This case is applicable if $c_1 < c_1^*$ (Figure 3.1). Let us consider a column of an arbitrary length ζ. In that case we can study injections large enough to reach the feed state and injections small enough to capture the interactions between the adsorption branch and the desorption branch of an injection plug in the same diagram. We will consider a column that is equilibrated initially with a uniform concentration of the modifier and the solute. The following discussion will be limited to initially not preload columns with respect to the solute ($c_2^0 = 0$), although the applied methodology is capable of analyzing preloaded columns. The initial concentration of the modifier on the other hand is usually not unity ($c_1^0 \neq 0$). This is the typical initial state of a

batch chromatographic process. Thus, the injection of a finite plug is defined by the following initial and boundary conditions:

$$\tau < 0: \qquad \zeta = 0..end: \quad c_1(\zeta) = c_1^0 \quad c_2(\zeta) = c_2^0$$
$$0 \le \tau < \tau_{inj}: \quad \zeta = 0: \qquad c_1(\zeta) = c_1^F \quad c_2(\zeta) = c_2^F \qquad \textbf{(3-19)}$$
$$\tau_{inj} < \tau: \qquad \zeta = 0: \qquad c_1(\zeta) = c_1^0 \quad c_2(\zeta) = c_2^0$$

The two characteristic curves R in the hodograph plane $R(\lambda_1)$ and $R(\lambda_2)$ are obtained from integration of $\mathbf{r}(\lambda_1)$ (Eq. (3-16)) and $\mathbf{r}(\lambda_2)$ ((3-17)).

$$R(\lambda_1): \qquad \int_{c_1} \mathbf{r}^*(\lambda_1) dc_1$$
$$R(\lambda_2): \qquad \int_{c_2} \mathbf{r}^*(\lambda_2) dc_2 \qquad \textbf{(3-20)}$$
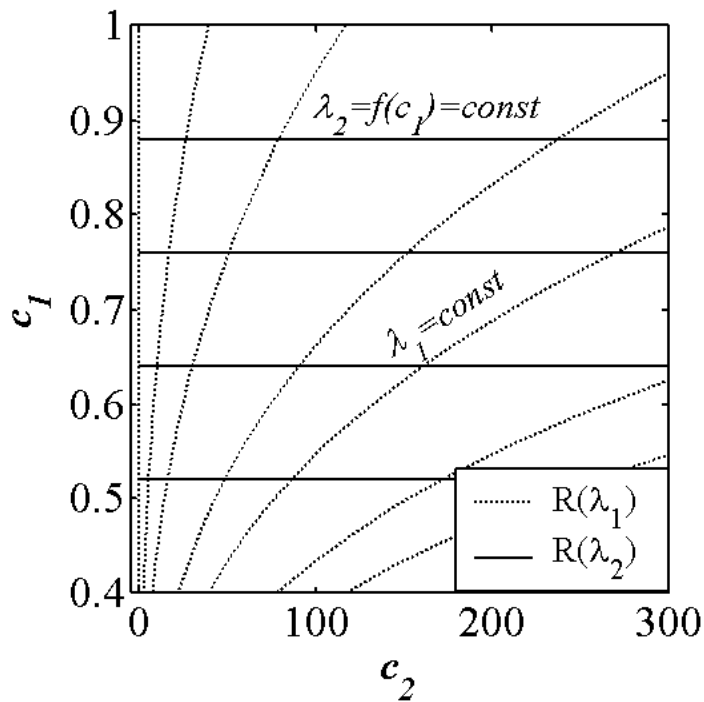
Figure 3.2: Trajectories of the concentrations in the hodograph plane for case a). Linear isotherms of the modifier and the solute, modifier is always the less adsorbed component.

An exemplary result of the trajectories is shown in Figure 3.2. The dotted lines in Figure 3.2 are the characteristic curves belonging to λ_1 while the solid lines are the

characteristics belonging to λ_2. It is an interesting feature of such systems that the eigenvalues λ remain constant along their trajectories in the hodograph plane. While λ_1 is constant by definition, λ_2 is a function of the modifier concentration (Eq. (3-15)). However, the modifier concentration c_1 remains constant along the characteristics belonging to λ_2, and so does λ_2. All concentration changes are therefore happening as contact discontinuities.

Lets discuss now the case that the solute is injected in a modifier surplus ($c_1^F > c_1^0$). The trajectories are shown in Figure 3.3. The initial and the feed state are indicated by $\mathbf{0}$ and $\mathbf{F}$. These states are steady states, while the intermediate states $\mathbf{I}$, which will be simply numbered, are dynamic states.

The pathway of the chromatographic cycle starts at the initial point. From here we have to follow the characteristic belonging to the smallest eigenvalue λ to the first intermediate state $\mathbf{I1}$. In the case that the modifier is always the least retained component this is in general $\lambda_1 = 1 + FH_1 < \lambda_2 = 1 + FH_2(c_1)$. To complete the adsorption pathway we follow the $R(\lambda_2)$ characteristic from state $\mathbf{I1}$ to the feed state $\mathbf{F}$. The solution has now reached the new steady state $\mathbf{F}$. For desorption we follow again at first the characteristic curve belonging to the smallest eigenvalue, i.e. λ_1, from the feed state to the intermediate state $\mathbf{I2}$, which has a smaller concentration of the solute than the feed. The chromatographic cycle is summarized with:

- $\mathbf{0} \rightarrow \mathbf{I1}$ along $R(\lambda_1 = const) \rightarrow$ contact discontinuity

- $\mathbf{I1} \rightarrow \mathbf{F}$ along $R(\lambda_2 = const) \rightarrow$ contact discontinuity

- $\mathbf{F} \rightarrow \mathbf{I2}$ along $R(\lambda_1 = const) \rightarrow$ contact discontinuity

- $\mathbf{I2} \rightarrow \mathbf{0}$ along $R(\lambda_2 = const) \rightarrow$ contact discontinuity
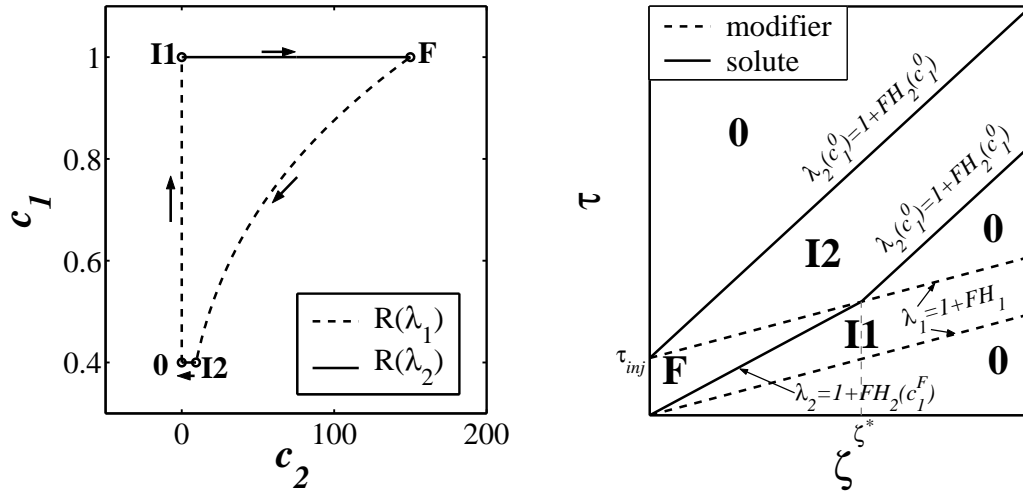
Figure 3.3: Hodograph of a gradient injection with a modifier surplus for linear-linear isotherms, when the modifier is always the least retained component (left). Right picture shows the construction of the characteristics in the space-time domain. The dashed lines correspond to the modifier, while the solid lines correspond to the solute.

Lets now translate the results into the space-time domain. From the hodograph plane we now know that all concentration changes happen with contact discontinuities. We also know the characteristic slopes in the $\zeta - \tau$-plane, which are just the eigenvalues λ of the process matrix. At the very beginning of the injection the column is equilibrated with the modifier concentration c_1^0. Since the modifier is the least retained component it starts to travel ahead of the solute with the velocity characteristic to the modifier, i.e. $\lambda_1 = 1 + FH_1$. Thus, the solute on the adsorption side of the injection is in contact only with the modifier concentration of the injection c_1^F. Therefore, the solute on the adsorption side of the injection travels initially with the velocity $\lambda_2 = 1 + FH_2(c_1^F)$. On the desorption side of the injection, starting at τ_{inj}, the modifier travels again with the velocity according to $\lambda_1 = 1 + FH_1$. The solute on the rear end of the injection is slower and immediately leaves the modifier plug. It enters a region of the column in which the modifier concentration is equal to the initial state of the column. The rear part of the injection of the solute travels now with a velocity corresponding to reciprocal of the slope $\lambda_2 = 1 + FH_2(c_1^0)$. The rear part of the modifier plug travels with a higher velocity (a smaller slope in the $\zeta - \tau$

plane) than the adsorption side of the solute and overtakes the adsorption branch of the solute at ζ^*. The following equalities hold for this point of interaction:

$$\tau_{inj} + \left(1 + FH_1\right)\zeta^* = \left(1 + FH_2(c_1^F)\right)\zeta^* \tag{3-21}$$

$$\zeta^* = \frac{\tau_{inj}}{FH_2(c_1^F) - FH_1} \tag{3-22}$$

$$\tau^* = \tau_{inj} + (1 + FH_1)\zeta^* = (1 + FH_2(c_1^F))\zeta^* \tag{3-23}$$

Beyond this dimensionless length ζ^* interactions of the desorption and the adsorption branch of the chromatographic cycle are present and the feed state is not reached anymore. At this space position, where the solute leaves the modifier feed plug, the concentration of the solute drops instantaneously from the feed state c_2^F to a intermediate state c_2^{I2}, while the concentration of the modifier at $I2$ is equal to the initial state 0 ($c_1^{I2} = c_1^0$). The concentration of the solute c_2^{I2} can be calculated by an integration of the trajectory in the hodograph plane (Eq. (3-16)) from the feed state F to state $I2$:

$$\frac{dc_2}{dc_1} = \frac{c_2}{H_1 - H_2(c_1)} \frac{dH_2(c_1)}{dc_1}$$

$$\int_{c_2^F}^{c_2^{I2}} \frac{1}{c_2} dc_2 = \int_{c_1^F}^{c_1^0} \frac{dH_2(c_1)}{dc_1} \frac{1}{H_1 - H_2(c_1)} dc_1 \tag{3-24}$$

$$\ln c_2 \Big|_{c_2^F}^{c_2^{I2}} = -\ln \left(H_1 - H_2(c_1)\right)\Big|_{c_1^F}^{c_1^0}$$

$$\Rightarrow c_2^{I2} = c_2^F \frac{H_1 - H_2(c_1^F)}{H_1 - H_2(c_1^0)}$$

During the elution of the solute a dilution is happening. This dilution is due to the different migration velocities of the modifier and the solute. The moment the solute leaves the high modifier concentration it is diluted below the feed concentration. This is visualized in Figure 3.4, where the characteristic plot of the space-time domain is shown again as well as the extracted concentration-time plots (left diagram) and con-

centration-space plots (bottom diagram). Drop lines are shown in grey to visualize the connection of these diagrams.

The concentration-time plots are shown at two different space positions ζ_1 and ζ_2.

One space position $\zeta_1 < \zeta^*$ is before the adsorption and the desorption characteristics start to interact (solid lines). Thus, in the concentration profiles all four states (0, $I1$, F, $I2$) can be observed. At first elutes the modifier with its feed concentration. Then, within this elution plug, elutes the solute also with its feed concentration. The moment the concentration of the modifier goes back to its initial value, the concentration of the solute drops to c_2^{I2}. The elution time is larger than the injection time, which indicates already, that the solute must be diluted compared to the feed concentration.
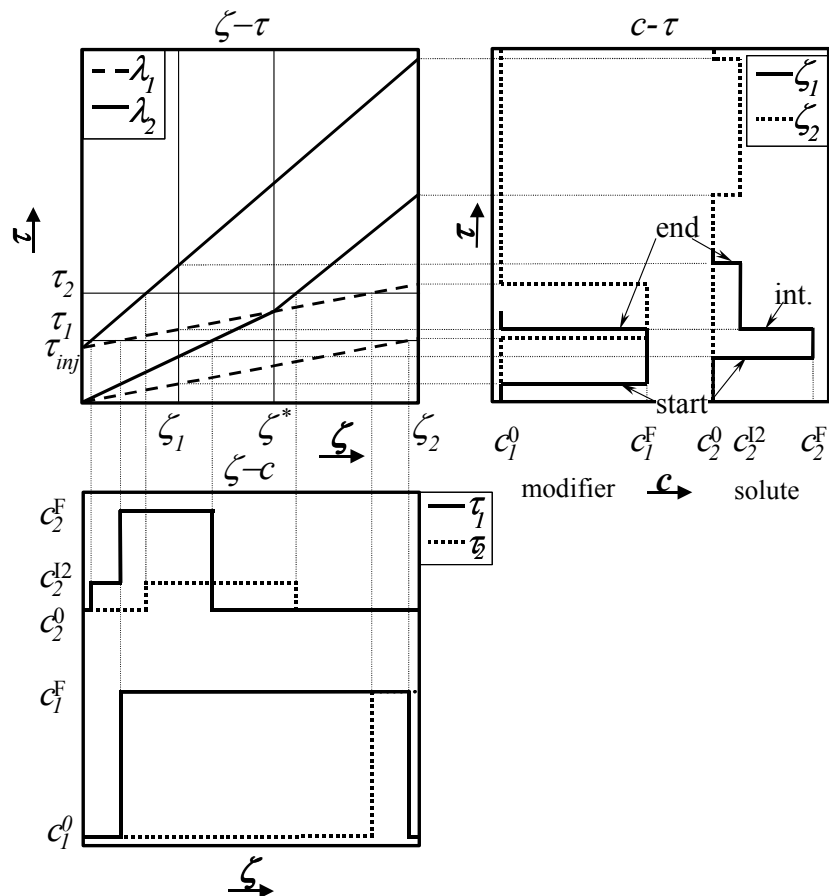
Figure 3.4: Plot of the characteristics in the space-time domain. Extracted concentration-time profiles of the modifier and the solute at two space positions ζ_1 (solid lines) and ζ_2 (dotted lines) are shown right, while concentration-space profiles at two different times τ_1 (solid lines) and τ_2 (dotted lines) are shown in the bottom diagram.

The dotted lines in the same diagram (Figure 3.4, left) depict the concentration profiles at a column length $\zeta_2 > \zeta^*$. In that case interactions between the adsorption and the desorption characteristics have taken place, resulting in complete separation of the solute and the modifier and in erosion of the feed state of the solute. The solute elutes now only with the concentration of state $I2$. In principle, the same results are shown over the column length at two specific times in the bottom diagram of Figure 3.4. The characteristic times for the construction of a chromatogram at a given column length are defined in

Table 3.1. This information can be easily rearranged for the construction of a chromatogram at a given time.

Table 3.1: Construction of a chromatogram for case a) and an initially not preloaded column. Linear-linear isotherms and modifier is the fastest component
$$(\lambda_1 = 1 + FH_1 \text{ and } \lambda_2(c_1) = 1 + FH_2(c_1))$$

	modifier		solute	
	τ	c_1	τ	c_2
start	$\lambda_1 \zeta$	c_1^{F}	$\begin{cases} \lambda_2(c_1^{\mathrm{F}})\zeta & \text{for } \zeta < \zeta^* \\ \lambda_2(c_1^{\mathrm{F}})\zeta^* + \lambda_2(c_1^0)\left(\zeta - \zeta^*\right) & \text{for } \zeta > \zeta^* \end{cases}$	$\begin{cases} c_2^{\mathrm{F}} \\ c_2^{I2} \end{cases}$
int.	-	-	$\tau_{inj} + \lambda_1 \zeta \quad \text{for } \zeta < \zeta^*$	c_2^{I2}
end	$\tau_{inj} + \lambda_1 \zeta$	c_1^0	$\tau_{inj} + \lambda_2(c_1^0)\zeta$	c_2^0

$$\zeta^* = \frac{\tau_{inj}}{\lambda_2(c_1^{\mathrm{F}}) - \lambda_1}$$

$$\tau_{inj}^* = \left(\lambda_2(c_1^{\mathrm{F}}) - \lambda_1\right)\zeta$$

Let us now discuss the gradient injection of a solute dissolved in solvent with less modifier ($c_1^{\mathrm{F}} < c_1^0$). The corresponding hodograph and characteristic plot are shown in Figure 3.5. In the hodograph plane we start at the initial state $\mathbf{0}$ and follow the

characteristic with the smallest eigenvalue to the intermediate state $\mathbf{I1}$. The corresponding characteristic $R(\lambda)$ is again the one connected to λ_1, since the modifier is the least retained component. The concentration of the solute c_2^{I1} remains at its initial value for the initially not preloaded column, i.e. $c_2^{I1} = c_2^0$ if $c_2^0 = \boldsymbol{0}$. From the intermediate state $\mathbf{I1}$ we follow the characteristic $R(\lambda_2(c_1^F))$ towards the feed state. For the desorption we have to follow alternatively the characteristic $R(\lambda_1)$ to the intermediate state $\mathbf{I2}$. The initial concentration of the modifier is already reached at this state. The concentration of the solute on the other hand is larger than the feed concentration c_2^F. This time an *on-column concentrating effect* of the solute is observed, contrary to the case discussed above, i.e. the injection of a modifier surplus, where an *on-column diluting effect* is happening. From state $\mathbf{I2}$ the concentrations return to the initial state along the $R(\lambda_2(c_1^0))$ characteristic. The concentration c_2^{I2} can be calculated with Eq. (3-24) also.
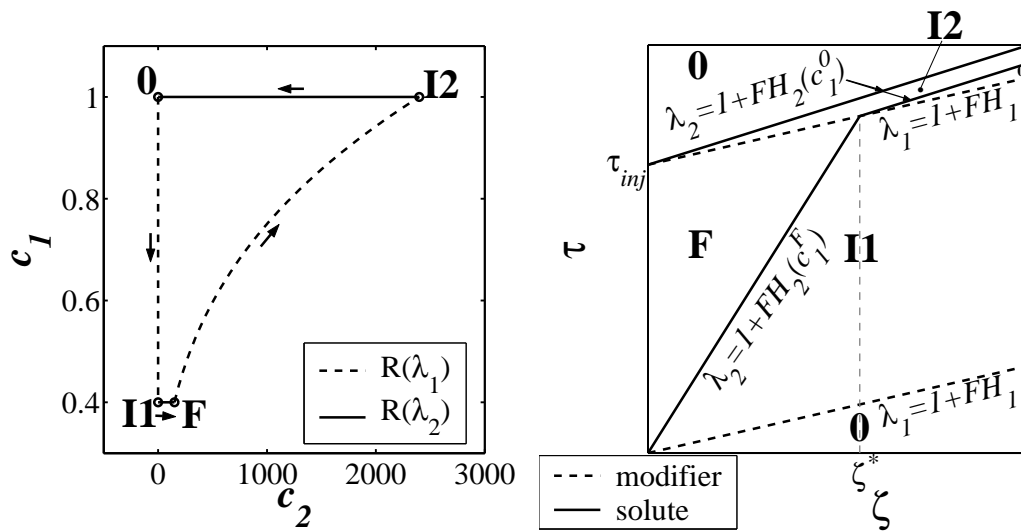
Figure 3.5: Hodograph of a gradient injection with a modifier deficit for linear-linear isotherms, when the modifier is always the least retained component (left). Right picture shows the construction of the characteristics in the space-time domain. The dashed lines correspond to the modifier, while the solid lines correspond to the solute.

The corresponding characteristics in the physical plane are shown in the left diagram of Figure 3.5. The characteristics of the modifier are again those with the smallest slope (dotted lines). The modifier travels as a retained plug through the column, which is neither concentrated nor diluted. Thus, the elution time of the modifier is

equal to the injection time. The solute on the other hand has a higher slope in the smaller modifier concentration of the injection, compared to the slope in the modifier concentration of the initial state, thus the solute gets concentrated in the initial part of the column. On the desorption side (starting at τ_{inj}) the solute immediately leaves the injection plug with the lower modifier concentration, thus the solute travels with a velocity connected to the initial modifier concentration. The modifier characteristic of the desorption branch (starting at τ_{inj}) has a smaller slope than the solute characteristic of the adsorption branch (origin at $\mathbf{0}$). As it was the case for the injection of a modifier surplus, both characteristics intercept at ζ^* (Eq. (3-22)). From this point on, the concentration of the solute is c_2^{I2}. The elution time of the solute is smaller compared to the injection time τ_{inj}, already indicating the on-column concentrating effect.

The construction of the chromatogram can be done for both types of injection with the equations given in

Table 3.1. The injection of the solute in a modifier deficit compared to the initial state will result in the elution of more concentrated solutes compared to the injection, while the injection in a modifier surplus will result in the elution of more diluted samples at the column outlet. In addition, double peaks can be observed if the column length ζ is smaller than a critical length ζ^*. This is the case when the injection time exceeds:

$$\tau_{inj} > \left(H_2(c_1^{\mathrm{F}}) - H_1 \right) \zeta \tag{3-25}$$

3.1.1.2.   *Modifier is the Strongest Retained Component - Case b)*

This second case results if $c_1 > c_1^*$ (Figure 3.1). Let us follow the same procedure as used for case a). Now the solute is always the least retained component in the system, i.e. $H_1 > H_2(c_1)$ and $\lambda_2(c_1) = 1 + FH_2(c_1) < \lambda_1 = 1 + FH_1$. Thus, we have to follow first the characteristic curves $R(\lambda_2)$ in the hodograph space. An example of the characteristic curves is given in Figure 3.6.
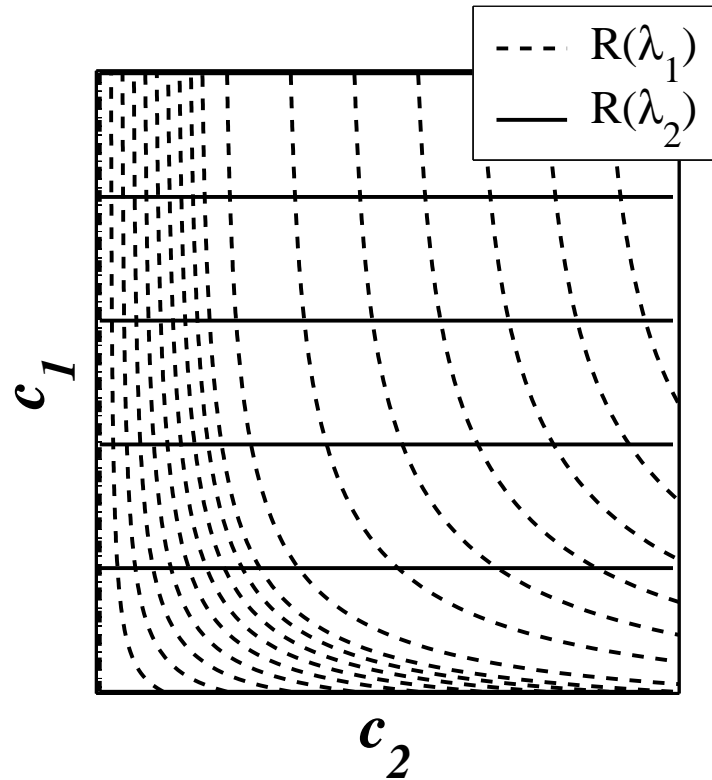
Figure 3.6: Trajectories of the concentrations in the hodograph plane for case b). Linear isotherms of the modifier and the solute, modifier is always the strongest adsorbed component.

In principle the same properties apply to case b) as to case a). All concentration changes happen instantaneously with contact discontinuities. Let us start the discussion with the solute being dissolved in a modifier surplus compared to the initial modifier concentration, i.e. $c_1^F > c_1^0$.

As already mentioned we have to follow at first the $R(\lambda_2)$ characteristics. Thus, the following chromatographic cycle develops:

- $\mathbf{0 \to I1}$ along $R(\lambda_2 = const) \to$ contact discontinuity

- $I1 \to F$ along $R(\lambda_1 = const) \to$ contact discontinuity

- $F \to I2$ along $R(\lambda_2 = const) \to$ contact discontinuity

- $I2 \to 0$ along $R(\lambda_1 = const) \to$ contact discontinuity

Figure 3.7: Hodograph of a gradient injection with a modifier surplus for linear-linear isotherms, when the modifier is always the most retained component (right). Left picture shows the construction of the characteristics in the space-time domain. The dashed lines correspond to the modifier, while the solid lines correspond to the solute.

It can be deducted from the hodograph in Figure 3.7 that the concentration of the solute on the intermediate state **I1** on the adsorption branch is larger than the feed concentration, while the modifier concentration remains constant here. This concentration increase is indirectly visible in the left diagram of Figure 3.7. The elution time of the solute is markedly smaller compared to the injection time. In order to fulfill the mass balance, the elution concentration of the solute, i.e. c_2^{I1}, has to be larger than the injection concentration.

This on-column concentrating effect can be explained with the characteristics in the physical $\zeta - \tau$ plane (Figure 3.7, right). The solute travels always faster than the modifier. The solute injected at the origin will immediately separate from the modifier injection plug and enter a region of the column in which the initial (smaller) modifier concentration is present. Since the solute possesses a larger Henry coefficient at smaller modifier concentrations, its traveling velocity will decelerate (larger slope in $\zeta - \tau$ plane). Thus, the solute is transported slower away from a certain spot, than it arrives there, resulting in a concentration increase.

The concentration of the solute at **I1** can be obtained from an integration of Eq. (3-16) from the feed state **F** to state **I1** (a procedure similar to the one shown above in more detail for Eq. (3-24)). The results is:

$$c_2^{I1} = c_2^{F} \frac{H_1 - H_2(c_1^{F})}{H_1 - H_2(c_1^{0})} \tag{3-26}$$

Note that this result is identical with the result obtained for c_2^{I2} for case a), when the modifier is always the least retained component. The construction rule for case b), summarized in Table 3.2 is somewhat the opposite of the rule given in

Table 3.1.

Table 3.2: Construction of a chromatogram for case b) and an initially not preloaded column. Linear-linear isotherms and modifier is the strongest retained component ($\lambda_1 = 1 + FH_1$ and $\lambda_2(c_1) = 1 + FH_2(c_1)$)

	modifier		solute	
	τ	c_1	τ	c_2
start	$\lambda_1\zeta$	c_1^{F}	$\lambda_2(c_1^{0})\zeta$	c_2^{I1}
int.	-	-	$\lambda_1\zeta$ for $\zeta < \zeta^*$	c_2^{F}
end	$\tau_{inj} + \lambda_1\zeta$	c_1^{0}	$\tau_{inj} + \begin{cases} \lambda_2(c_1^{F})\zeta & \text{for } \zeta < \zeta^* \\ \lambda_2(c_1^{F})\zeta^* + \lambda_2(c_1^{0})\left(\zeta - \zeta^*\right) & \text{for } \zeta > \zeta^* \end{cases}$	c_2^{0}

The injection of the solute dissolved in a modifier deficit is depicted in Figure 3.8. As expected, we observe here an on-column dilution effect.

Concluding this section, we have seen for case b) that the injection in a weak solvent leads to an on-column dilution and the injection in a strong solvent causes an on-column concentrating effect. This is contrary to case a), where the opposite behavior is encountered.
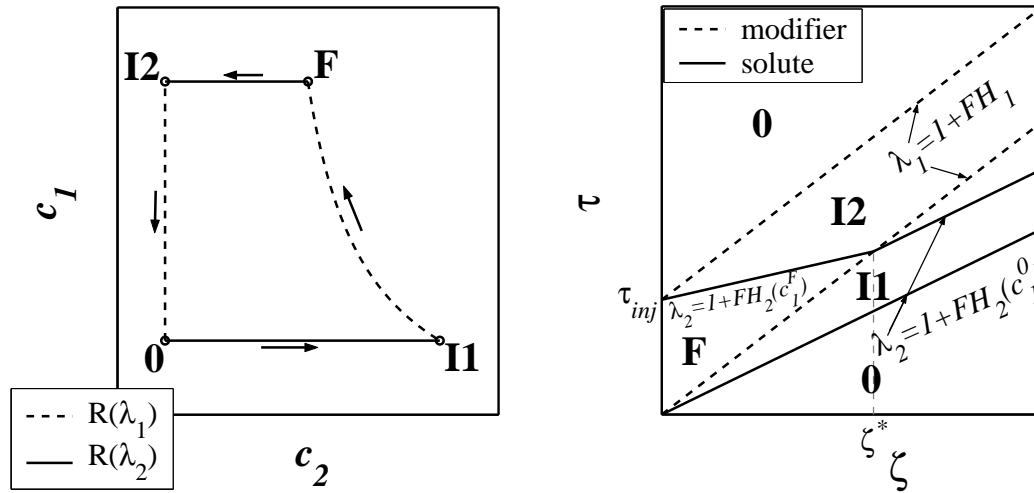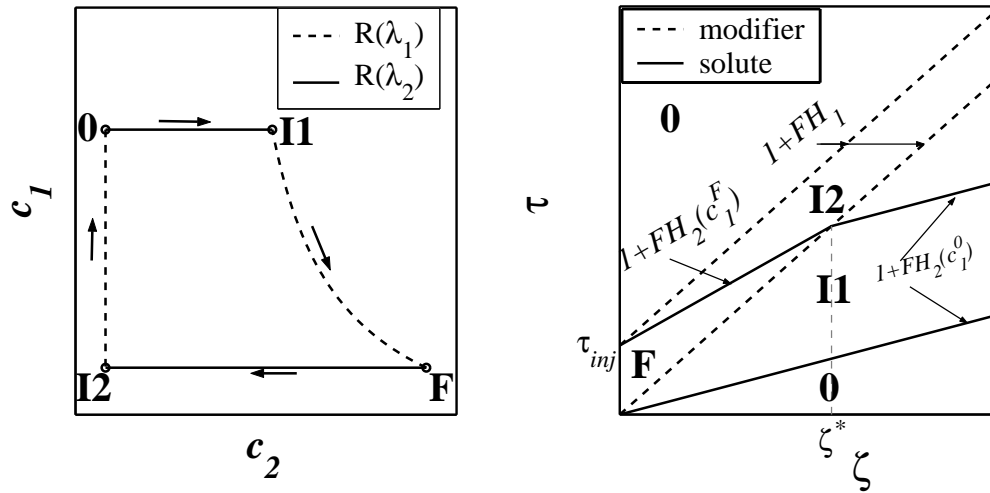
Figure 3.8: Hodograph of a gradient injection with a modifier deficit for linear-linear isotherms, when the modifier is always the strongest retained component (right). Left picture shows the construction of the characteristics in the space-time domain. The dashed lines correspond to the modifier, while the solid lines correspond to the solute.

3.1.1.3. *Mixed Elution Order - Case c)*

Finally, let us consider the scenario, where the modifier concentration of the feed and the initial states lay on opposite sides of the critical modifier concentration c_1^* depicted in Figure 3.1. Again two sub scenarios are possible, either $c_1^F > c_1^* > c_1^0$ or $c_1^F < c_1^* < c_1^0$. The first case would result in $H_2(c_1^F) < H_1 < H_2(c_1^0)$, meaning that the solute in the injection media travels faster than the modifier, while the solute in the initial modifier concentration travels slower then the modifier. In the latter case holds $H_2(c_1^F) > H_1 > H_2(c_1^0)$, thus the solute travels slower than the modifier in the injection plug, while it travels faster than the modifier in the initial modifier concentration.

The hodograph plot for such a system is depicted in Figure 3.9. The dashed line indicates the critical modifier concentration c_1^*. At this concentration the order of the characteristics change. This situation corresponds to the water shed point introduced in [143]. In the previous examples the order of the eigenvalues remained constant, i.e. $\lambda_2 > \lambda_1$ in for case a) and $\lambda_2 < \lambda_1$ for case b). In this example, the elution order changes during the process. In the upper part of the hodograph in Figure 3.9 the sol-

ute is less retained than the modifier, i.e. $\lambda_2(c_1) < \lambda_1$. So the concentrations should start changing along the $R(\lambda_2)$ characteristic. More precisely, at the critical concentration we have $\lambda_2(c_1^*) = \lambda_1$ and the order of the characteristics changes. In the bottom part of the hodograph in Figure 3.9 holds $\lambda_2(c_1) > \lambda_1$ and the opposite behavior should be observed. However, the characteristics above and below the critical modifier concentration never intercept. The consequences of that specific property are explained below.
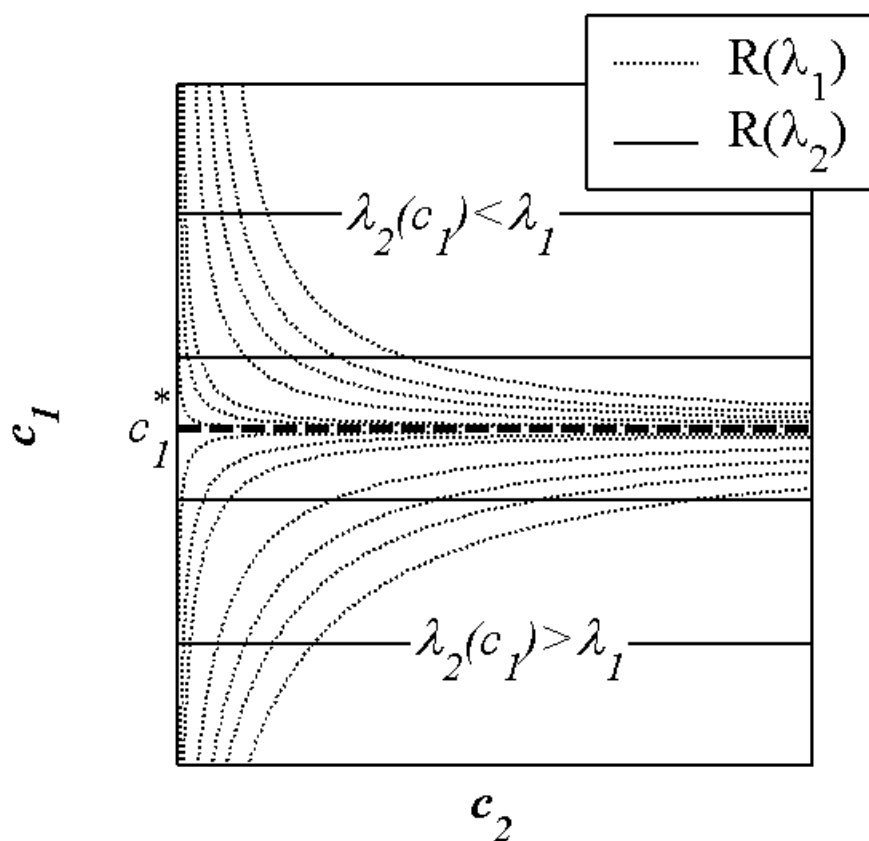
Figure 3.9: Hodograph for linear-linear isotherms case c). The critical modifier concentration c_1^* indicating the change of the elution order is depicted by the dashed line. Above this concentration, the modifier is the strongest adsorbed component. Below this concentration, the modifier is the least adsorbed component.
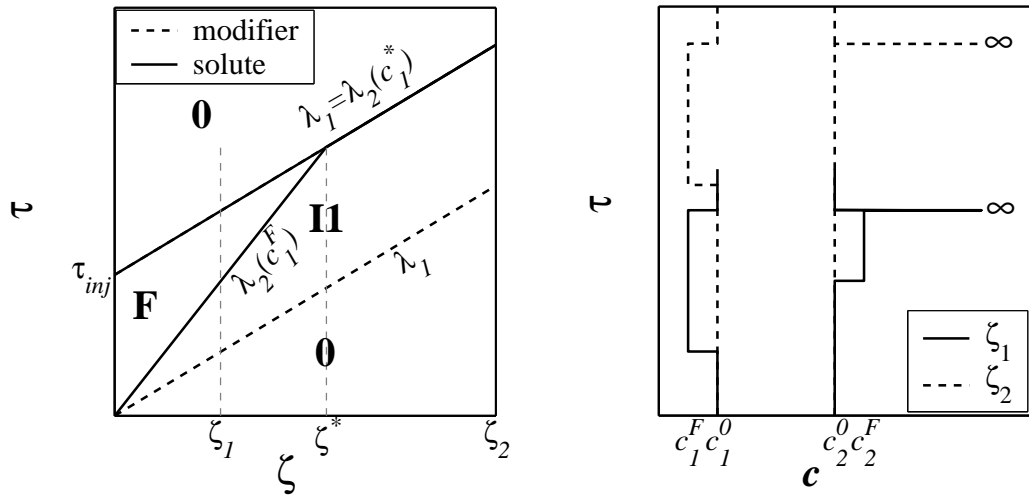
Figure 3.10: Plot of the characteristics for a gradient injection of the solute in a modifier deficit in the $\tau - \zeta$ physical plane (left). The corresponding concentration profiles at two length positions ζ are shown in the $\tau - c$ diagram (right).

Let us start the discussion this time in the physical plane. To construct the characteristics, we start at the origin and draw two lines with the slopes of λ_1 and $\lambda_2(c_1^F)$. The traveling velocity of the solute in the low modifier concentration of the injection plug is smaller than the one of the modifier. The solute on the adsorption branch is eventually overtaken by the desorption branch of the modifier (at ζ^*), which starts at τ_{inj} and has also the slope of λ_1. Up to the critical column length ζ^*, we will observe the feed state. The solute on the desorption branch travels also faster than the modifier, so it immediately leaves the injection plug of the low modifier concentration and enters a region with a high modifier concentration. But, the traveling velocity of solute in this modifier concentration is larger than the one of the modifier itself. Thus, the solute enters again the plug with the low modifier concentration. In that manner the solute gets focused on the rear flank of the modifier plug. A double peak will be observed if the column length is below the critical column length (i.e. $\zeta < \zeta^*$ or $\tau_{inj} > \tau_{inj}^*$). This double peak consists of the feed concentration of the solute at the front of the peak (Figure 3.10, right, solid lines) and an infinite concentration of the solute at the rear flank of the solute peak. For columns with a larger column length than the critical length or for shorter injections, the feed state vanishes

completely and the solute elutes as an infinite short and infinite high peak at the rear end of the modifier plug (Figure 3.10, right, dotted lines).
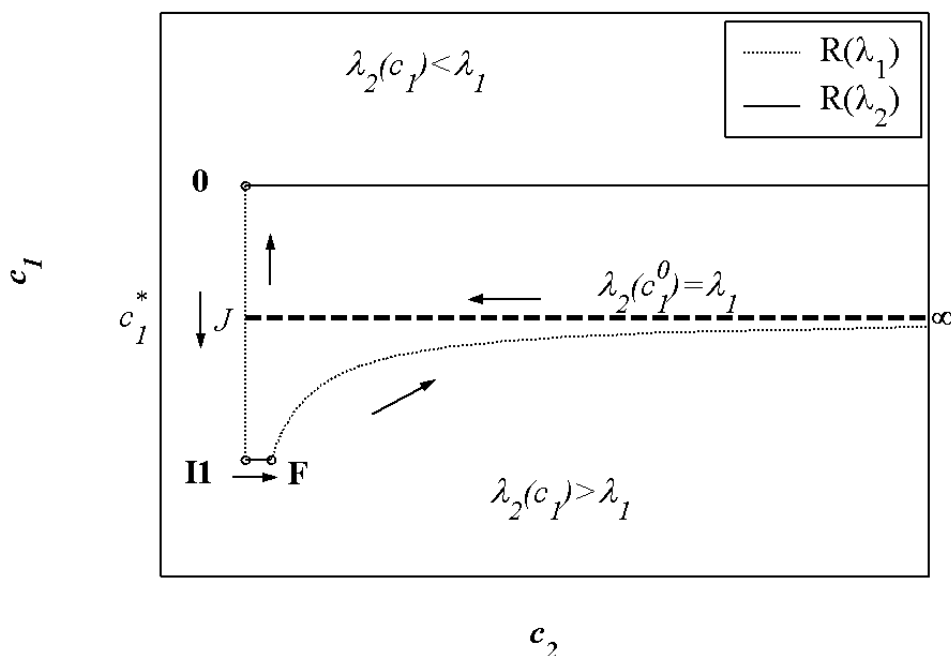
Figure 3.11: Plot of the characteristics in the hodograph plane for gradient injections of the solute in a modifier deficit.

Figure 3.11 shows the corresponding hodograph plot for the gradient injection in a modifier deficit. From the initial state $\mathbf{0}$ we should follow the characteristic belonging to the smaller eigenvalue, $R(\lambda_2)$, since $\lambda_2(c_1^0) < \lambda_1$. This characteristic nowhere intersects with a $R(\lambda_1)$ characteristic connecting it to the feed state. Thus, let us follow the $R(\lambda_1)$ characteristic until it intersects a $R(\lambda_2)$ characteristic at state $\mathbf{I1}$ that connects it to the feed state $\mathbf{F}$. For the desorption cycle we start at the feed state and follow the $R(\lambda_1)$. Along this trajectory the concentration of the solute increases up to infinity. At the same time it asymptotically closes to the characteristic at which $R(\lambda_1) = R(\lambda_2)$. From infinity we follow the trajectory $R(\lambda_1) = R(\lambda_2)$ towards the point J. From there we follow the $R(\lambda_1)$ characteristic towards the initial state $\mathbf{0}$.

The injection of a modifier plus results in the opposite behavior, as depicted for the physical plane in Figure 3.12. The solute in the modifier rich injection travels faster

than the modifier itself. Thus, the front of the solute plug leaves the modifier rich solution and enters a region in the column where the initial modifier concentration is present. Here, the traveling velocity of the solute is smaller than the one of the modifier, thus it enters again the modifier rich injection plug. In that manner the solute gets concentrated at the front of the modifier injection plug (as depicted in the right plot of Figure 3.12). The solute on the desorption branch is initially traveling also with a velocity larger than the modifier migration velocity. It overtakes the adsorption branch of the modifier at ζ^{*}. If the actual column length is smaller than this critical length, a split peak of the solute will appear, with an infinite concentration eluting at the same time as the modifier followed by the feed concentration (solid lines in Figure 3.12, right). If the column length is larger than the critical column length only one infinite high and short peak of the solute will be observed (dotted lines in Figure 3.12, right).
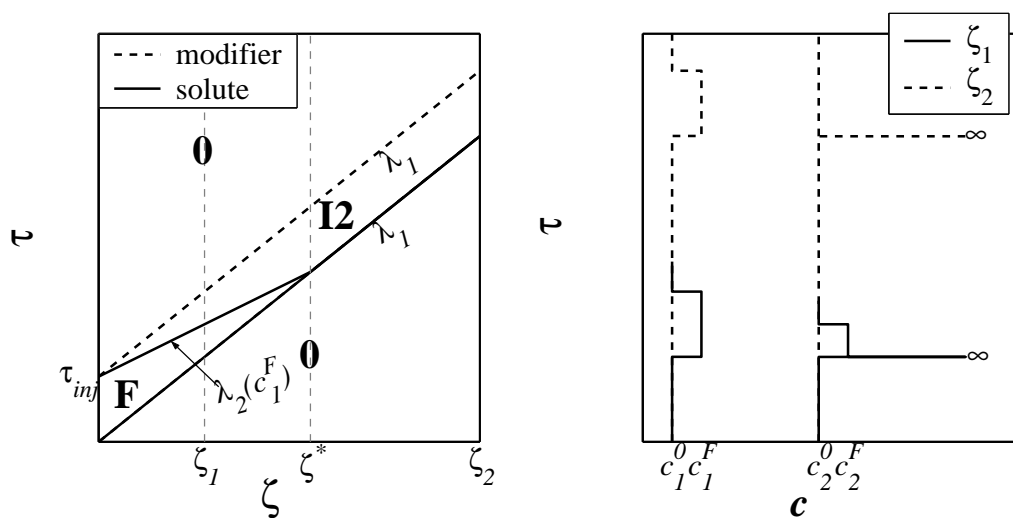
Figure 3.12: Plot of the characteristics for a gradient injection of the solute in a modifier surplus in the $\tau - \zeta$ physical plane (left). The corresponding concentration profiles at two length positions ζ are shown in the $\tau - c$ diagram (right).

3.1.1.4. *Summary of Binary Systems with Linear - Linear Isotherms*

We have seen that gradient injection can result in strong dilution of the solute or in strong concentration increases, depending on the elution order and the elution strength of the injection solvent. The following table summarizes the interesting effects for the two relevant cases a) and b), i.e. where the elution order of the modifier

and the solute does not change throughout the elution. Depending on the size of the injection, split or distorted peaks of the solute may be observed.

Table 3.3: Summarizing the essential effects of a solute during the elution if it was injected in a different solvent than used for elution (gradient injection).

elution strength of the injection solvent / elution order of the modifier compared to the solute	stronger than eluent	weaker than eluent
modifier is the least retained component, case a)	on-column dilution	on-column concentration
modifier is the most retained component, case b)	on-column concentration	on-column dilution

It can be deducted that the injection of a solute dissolved in a stronger solvent, with an injection concentration higher than the solubility in the solvent used for elution will most likely be applicable a system where the modifier is the least retained component. Here, the solute is injected at a concentration larger than the solubility in the mobile phase. However, the moment the solute leaves the high modifier concentration, its concentration decreases strongly (maybe even below the solubility limit in the mobile phase), thus reducing the level of super saturation with respect to the mobile phase. On the other hand, in a system where the modifier is the strongest retained component, the injection concentration (already above the solubility in the mobile phase) will further increase during the elution. Thus, it will be largely above the solubility limit the instant the solutes enter the in the mobile phase used for elution. Thus, crystallization in the column or in the connecting pipes may occur. *This discussion leaves the scenario where the modifier is the least retained component as suitable for the injection in a different solvent, for cases where such gradients injections should be used to overcome solubility problems.* For the rest of this work I will primarily concentrate on the most relevant case that the modifier always possesses the highest migration velocity, i.e. case a).

An attractive injection method seems to be also the injection in a weak solvent and the elution with a stronger solvent, if the modifier is the least retained component, since in that case the solute can be collected with a higher concentration, than it was applied. A drawback of that method is that the injection concentration is limited by

the solubility in the weak solvent, which is typically low. Thus, it remains to be seen for specific cases if the injection in a weak solvent is really a good option. This aspect will be discussed also in the following where the concept of gradient injection is applied to the separation of two solutes.

3.1.2. Ternary System – Application of Gradient Injections to Separation

In the section above we have learned that the injection in a different mobile phase gives rise to the interesting phenomena of on-column dilution and on-column concentration. It is obvious from different scenarios discussed above, that only those cases where the elution order does not change throughout the experiment (cases a) and b)) are suitable for separation. In case c), no or only incomplete separation for the solutes to be separated is achievable. Another reason of not following this path is the danger of precipitation if the concentration of the solutes is increased that much. However, case b), where the modifier is the strongest retained component, is also not suitable for the injection with a stronger solvent to overcome limited solubility of the solute in the mobile phase. In this case, the concentration is also further increased during the elution, increasing the possibility of solubility/precipitation problems.

Table 3.4: Isotherm equations and their derivatives for the ternary system of linear–linear isotherms.

	modifier (index 1)	less retained solute (index 2)	stronger retained solute (index 3)
q_i	$H_1 c_1$	$H_2(c_1)c_2$	$H_3(c_1)c_3$
$\dfrac{dq_i}{dc_1} = q_{i1}$	H_1	$\dfrac{dH_2(c_1)}{dc_1}c_2$	$\dfrac{dH_3(c_1)}{dc_1}c_3$
$\dfrac{dq_i}{dc_2} = q_{i2}$	0	$H_2(c_1)$	0
$\dfrac{dq_i}{dc_3} = q_{i3}$	0	0	$H_3(c_1)$

The indications less and stronger retained solute in Table 3.4 refer only to the elution order of the solutes. The modifier may be stronger or less adsorbed then the solutes. It can be further deducted from the partial derivatives that the solutes are assumed not to interact with each other. Therefore, the elution profiles can be obtained from two individual applications of the equilibrium theory for the two binary modifier–solute systems 1-2 and 1-3, with the same procedures as explained in section 3.1.1. In addition, we could apply the expressions in Table 3.4 to the equations of the equilibrium theory of the ternary system (Eqs. (3-5)-(3-10)). This involves expanding the hodograph space to a third dimension. This is shown in Appendix B 1 on page 149.

Let us define some criteria to evaluate the possibility of performing the injection in the same, a stronger or a weaker solvent than used for the elution. Let us further assume we have one chromatographic column of fixed dimensions, packed with a certain amount of stationary phase. Finally, we assume that there are no significant viscosity effects limiting the flow rate or the causing back mixing due to viscous fingering. It is our goal to separate perfectly the two solutes from each other. Perfect means with a purity of 100 % and a recovery of 100% (note the purely theoretical values). The ideal amount injected for a 100% purity and 100% recovery is, when there is no time lag between the desorption front of the first eluting compound and the adsorption front of the later elution compound (i.e. touching band separation [66]), which results in:

$$\tau_2^{des} = \tau_3^{ads} \Rightarrow \tau_{inj}^{opt} = \frac{\left(\lambda_3^0 - \lambda_2^0\right)\left(\lambda_3^F - \lambda_1\right)}{\left(\lambda_3^0 - \lambda_1\right)} \tag{3-27}$$

Fulfilling the condition given in (3-27) the goal of the separation is reached in an optimized manner. Since in chromatography typically more than one injection is performed, we need to specify the cycle time (τ_c) after which we perform the next injection. This time should be decreased in order to increase the productivity, which is proportional to:

$$PR_i \sim \frac{\tau_{inj}}{\tau_c} c_i^{inj} \tag{3-28}$$

In order to leave out interactions of consecutive injections the minimal cycle time is obtained in the following way.

$$\tau_c = \max\left(\tau_i^{des}\right) - \min\left(\tau_i^{ads}\right) \qquad\qquad i = 1, 2, 3 \qquad\qquad \textbf{(3-29)}$$

Another method to define the cycle time is explained in appendix A 2 on page 134. There, interactions between consecutive injections are allowed. However, that method described there results in the same general results only with much more lengthy expressions and is thus omitted here.

Let us now compare three scenarios:

    i.   the injection in a weaker solvent (modifier deficit),

    ii.   the isocratic injection, and

    iii.   the injection in a stronger solvent (modifier surplus).

Figure 3.13 shows the general trends for the separation of two solutes. The injection in a weaker solvent (Figure 3.13, left) results in a concentration of the solutes to be separated, as expected from the results for the binary system. The solutes are mainly separated in the weak solvent used for injection. After the solutes leave the injection plug of the modifier, the mobile phase, which has here a higher elution strength, quickly transports the solutes towards the column outlet. The cycle time τ_c is dominated by the injection time τ_{inj}.

During an isocratic injection (Figure 3.13, middle), the samples are continuously separated as they migrate through the column. Since the injection concentration of the modifier is equal to the concentration of the mobile phase, no injection band of the modifier is present. Thus, the cycle time is just two times the optimal injection time (for a two solute system).

The injection in a stronger solvent (Figure 3.13, right) results in strong dilution of the solutes. Only a very narrow band of the solutes can be injected, while the elution band is rather broad. The solutes migrate more or less unseparated (depending on the separation factor in the strong solvent) in the injection band of the modifier. After the solutes leave the injection plug, they enter the weaker mobile phase, where the sol-

utes are finally separated. The cycle time is dominated by the time needed for elution.
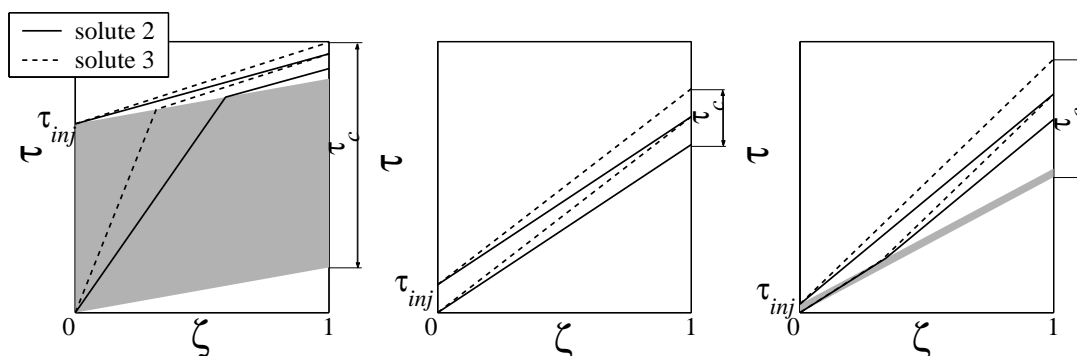
Figure 3.13: Schematic representation of the chromatographic batch separation of two solutes (2 solid lines, 3 dashed lines) with three different injection concentrations of the modifier. The injection plug of the modifier is shown in grey. Injection of i) modifier deficit (left), ii) isocratic injection (middle) and iii) injection of a modifier surplus (right).

From this perspective, the injection in a strong solvent seems to be the least efficient method to separate two solutes, since the ratio of injection time over cycle time τ_{inj} / τ_c is the smallest. The injection in a weak solvent with the highest ratio of τ_{inj} / τ_c seems more efficient. However, the injection concentration has not been considered so far. If we include the maximal possible injection concentration (dependent on the solubility), the picture may reverse, depending on the specific solubility functions. For a given example, each of the three injection methods might be the optimal one. If we set the isocratic injection as a reference, we obtain the following condition for a gradient injection to be more efficient than the isocratic injection:

$$\frac{\tau_{inj}}{\tau_c}\bigg|_{grad} c_{grad}^{F} > \frac{\tau_{inj}}{\tau_c}\bigg|_{iso} c_{iso}^{F} \tag{3-30}$$

This expression is made under the assumption of a constant mobile phase velocity. In this study we do not take into account effects of:

- viscosity changes with the modifier content in the mobile phase (resulting in possible changes of the applicable mobile phase velocity)

- viscosity effects due to the high solute concentrations in the feed solution (viscous fingering)

The injection time and the cycle time are functions of the separation factors between the modifier and the nearest solute and the separation factors between the solutes. For the gradient injections we need a certain separation factor (larger than 1) of the solutes and the modifier. However, these separation factors should not be too large since this would increase corresponding the cycle time unduly. All separation factors are functions depending on the modifier concentration. There are too many possibilities of diverging, constant or increasing separation factors with increasing modifier concentration, to be covered in a systematic parametric study. I discuss below for the sake of illustration an example that covers the interplay of the solubility function and the productivity. For this I will vary for an example the dependence of the solubility on the modifier concentration. The solubility shall increase by a factor of 150 between the minimal and the maximal modifier concentration applicable. The solubility shall increase in one case exponentially and in another case linearly with increasing modifier concentration. The separation factors of the solutes realistically decrease with increasing modifier concentration. The separation factor is maximal (2) at the minimal modifier concentration applicable ($c_1^{\min}$), while it is minimal (1, thus no separation) at the maximal applicable modifier concentration $c_1^{\max}$. For the dependence of the Henry coefficients on the modifier concentration of the less adsorbed solute I use exemplary the values for phenol found in [85]. The Henry coefficients of the stronger adsorbed component are calculated according to the separation factor. Details on the physical data are given in Appendix A 1.

Figure 3.14 and Table 3.5 summarize for this example the relevant physical data (Henry coefficients, separation factor, solubility), the ratio of optimal injection time over cycle time and the resulting productivity for the three injection methods. As mentioned above, the ratio τ_{inj}/τ_c is increasing for the injection in the weak solvent with increasing modifier content. Eventually it overtakes the constant ratio for isocratic injections. The ratio τ_{inj}/τ_c for the injection in a stronger solvent is always the smallest, but it is also increasing with increasing modifier content in the mobile phase.
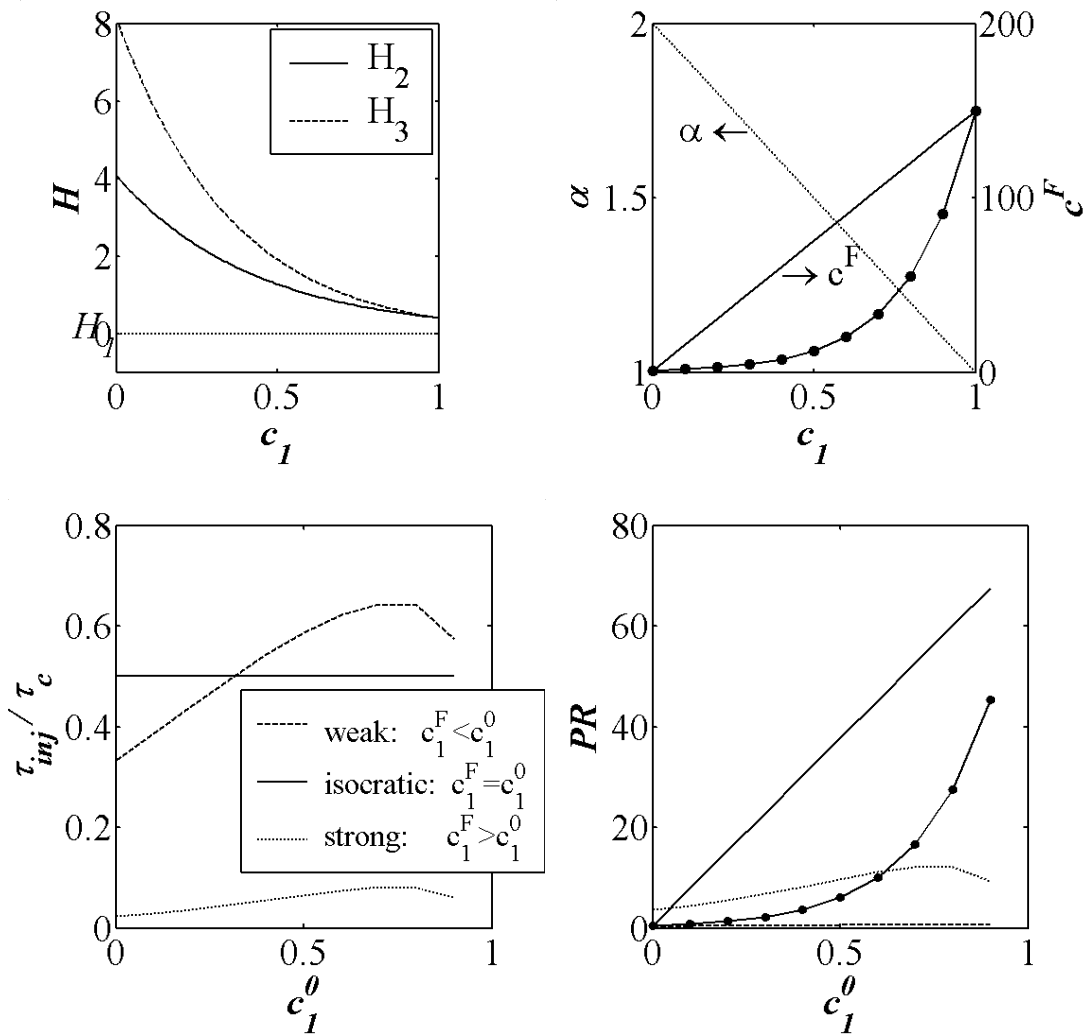
Figure 3.14: Henry coefficients of the solutes (upper left) and the corresponding separation factor and applicable feed concentration (solibility) (upper right) for linear dependence and an exponential dependence on the modifier concentration. Ratio of injection time over cycle time (bottom left) and the corresponding productivity (bottom right) for the three injection methods. The productivity of the isocratic injection is shown for a linear dependence of the solubility on the modifier concentration (solid lines, no symbols) and for an exponential dependence (solid lines, circles).

Table 3.5: Summary of optimal injection time and optimal cycle time for the separation of two solutes using gradient injection in a weak solvent, isocratic injection and gradient injection in a strong solvent. The separation factor is increasing from 1 to 2. The solubility is increasing by a factor of 150 over the range of modifier concentrations

	$c_I^F = 0$ & $c^F = 1$				$c_I^0 = c_1^0$ & $c^F = f(c_1)^{(1)}$					$c_I^F = 1$ & $c^F = 150$			
c_1^0	τ_{inj}	τ_c	$\dfrac{\tau_{inj}}{\tau_c}$	$\dfrac{\tau_{inj}}{\tau_c}c^F$	τ_{inj}	τ_c	$\dfrac{\tau_{inj}}{\tau_c}$	c^F	$\dfrac{\tau_{inj}}{\tau_c}c^F$	τ_{inj}	τ_c	$\dfrac{\tau_{inj}}{\tau_c}$	$\dfrac{\tau_{inj}}{\tau_c}c^F$
0.0	1.91	5.74	0.33	0.33	1.91	3.83	0.50	1 (1)	0.5 (0.5)	0.093	3.92	0.024	3.6
0.1	1.81	4.69	0.39	0.39	1.36	2.73	0.50	1.7 (16)	0.8 (8.0)	0.089	2.97	0.030	4.5
0.2	1.70	3.86	0.44	0.44	0.96	1.92	0.50	2.7 (31)	1.4 (15.4)	0.083	2.25	0.037	5.5
0.3	1.58	3.19	0.49	0.49	0.67	1.33	0.50	4.5 (46)	2.2 (22.9)	0.077	1.70	0.045	6.8
0.4	1.44	2.64	0.54	0.54	0.45	0.91	0.50	7.4 (61)	3.7 (30.3)	0.070	1.28	0.055	8.2
0.5	1.28	2.17	0.59	0.59	0.30	0.60	0.50	12.3 (76)	6.1 (37.8)	0.062	0.96	0.065	9.7
0.6	1.09	1.76	0.62	0.62	0.19	0.38	0.50	20.2 (90)	10.1 (45.2)	0.053	0.72	0.074	11.2
0.7	0.88	1.37	0.64	0.64	0.11	0.23	0.50	33.4 (105)	16.7 (52.7)	0.043	0.53	0.081	12.2
0.8	0.64	1.00	0.64	0.64	0.06	0.12	0.50	55.1 (120)	27.5 (60.1)	0.031	0.39	0.080	12.0
0.9	0.35	0.61	0.57	0.57	0.02	0.05	0.50	90.9 (135)	45.4 (67.6)	0.017	0.28	0.061	9.2
1.0	0.00	0.19			-	-		-	-	-	-	-	-

(1)　The injection concentration is calculated based on an exponential increase between the minimal solubility at $c_1^F = 0$ and the maximal solubility at $c_1^F = 1$ (Eq. (A-3) on page 134). In brackets a linearly dependent solubility (Eq. (A-4)) and the corresponding productivity to that solubility is shown.

For isocratic injections both the injection time and the cycle time decrease with increasing modifier due to the decreasing retention. The productivity of such an idealized manner depends solely on the injection concentration, since the ratio of τ_{inj}/τ_c remains constant at *0.5*. The productivity of the isocratic injection is thus continuously increasing with increasing modifier concentration[6].

For the injections in the weak solvent it can be observed, even though the ratio τ_{inj}/τ_c is larger at a certain point compared to the isocratic injections, its productivity is not. Only very small concentrations of the solutes to be separated can be proc-

---

[6] In reality, there would be an optimal modifier concentration since back mixing would severely diminish separation for those very narrow bands (Table 3.5) obtained for high modifier concentrations.

essed here. At best, the ratio of τ_{inj}/τ_c approaches one, i.e. twice the value of the isocratic injection.

The gradient injection in a strong solvent outperforms (for this example) up to a modifier concentration of about 0.6 the isocratic injection, if the solubility follows an exponential dependency. Note, that this is possible even though the solutes are not separated at all in the modifier injection concentration ($\alpha^F = 1$). If the solubility is linearly dependent on the mobile phase composition, the isocratic injection outperforms over a large range of modifier concentrations the injection in a strong solvent.

Generalized it can be stated for a two solute system: i) *The gradient injection in a weaker solvent can only outperform the isocratic injection if the solubility does not increase over the range of modifier concentrations above a factor of 2. ii) The gradient injection in a strong solvent can outperform isocratic injections depending on the solubility function.* The statements made here are also valid for different separation factors and more sophisticated production methods. See Appendix A 3 for more examples.

3.2. *Analysis of Systems with Linear - Langmuir Isotherms*

The discussion in this section is expanded to nonlinear isotherms of the solute. The isotherm of the modifier remains linear, while the solute isotherm is described by the Langmuir equation. The discussion will be limited to binary systems with a single solute.

3.2.1. Binary System - General Effects for a Single Solute

For the dependence of the isotherm of the solute on the modifier concentration we assume that the modifier just influences the adsorption constant $b_2 = b_2(c_1)$ of the solute, while the saturation capacity $q_{s,2} \neq q_{s,2}(c_1)$ shall not be affected by the modifier. For the dependence of the Henry coefficient, $H_2 = H_2(c_1)$, of the solute on the modifier we use the same exponentially decreasing expression already used for the linear-linear system (Eq. (3-18) on page 46). With the adsorption constant defined as:

$$b_2(c_1) = \frac{H_2(c_1)}{q_{s,2}} \qquad (3\text{-}31)$$

the Langmuir isotherm equation of the solute can be formulated as stated in Table 3.6. Here, all isotherm equations and their derivatives are listed for a binary system consisting of a modifier – adsorbed linearly – and a solute – adsorbed according to a Langmuir type isotherm.

Table 3.6: Isotherm equations and their derivatives for a binary system of linear–Langmuir isotherms.

	modifier (index 1)	solute (index 2)
q_i	$H_1 c_1$	$\dfrac{H_2(c_1)c_2}{1 + \dfrac{H_2(c_1)}{q_s}c_2}$
$\dfrac{dq_i}{dc_1} = q_{i1}$	H_1	$\dfrac{\dfrac{dH_2(c_1)}{dc_1}c_2}{\left(1 + \dfrac{H_2(c_1)}{q_s}c_2\right)^2}$
$\dfrac{dq_i}{dc_2} = q_{i2}$	0	$\dfrac{H_2(c_1)}{\left(1 + \dfrac{H_2(c_1)}{q_s}c_2\right)^2}$

Now we apply the expressions of Table 3.6 into the equations for the eigenvalues $\boldsymbol{\lambda}$ (Eq. (3-3) on page 42) and the corresponding eigenvectors $\mathbf{r}$ (Eqs. (3-4)-(3-5) on page 42). Let us first check the dependence of the eigenvalues on the concentrations:

$$\boldsymbol{\lambda} = \begin{bmatrix} \lambda_1 \\ \lambda_2 \end{bmatrix} = 1 + F \begin{bmatrix} H_1 \\ \dfrac{q_s^2 H_2(c_1)}{\left(q_s + H_2(c_1)c_2\right)^2} \end{bmatrix} \qquad (3\text{-}32)$$

The eigenvalues λ_1 are independent on the modifier and solute concentrations (thus constant), while λ_2 ($\lambda_2 = f(c_1, c_2)$) decreases with increasing solute concentration c_2 and with increasing modifier concentration c_1. Integration of the eigenvectors

$$\mathbf{r}^*(\lambda_1) = \begin{bmatrix} 1 \\ \dfrac{dc_2}{dc_1} \end{bmatrix} = \begin{bmatrix} 1 \\ \dfrac{dH_2(c_1)}{dc_1} \dfrac{q_s^2 c_2}{H_1(q_s + H_2(c_1)c_2)^2 - q_s^2 H_2(c_1)} \end{bmatrix} \qquad (3\text{-}33)$$

and

$$\mathbf{r}^*(\lambda_2) = \begin{bmatrix} \dfrac{dc_1}{dc_2} \\ 1 \end{bmatrix} = \begin{bmatrix} 0 \\ 1 \end{bmatrix} \qquad (3\text{-}34)$$

yields the concentration trajectories, $R(\lambda_i(c_1, c_2))$, in the $c_1 - c_2$ hodograph plane. They are depicted in Figure 3.15. Again we have to make a case distinction. The local derivative of the adsorption isotherm of the solute may be larger or smaller than that of the modifier as the solute migrates through the column. Contrary to the linear-linear case, where this just depends on the modifier concentration, here both concentrations influence the trajectories:

- $\lambda_1 < \lambda_2(c_1, c_2)$, is fulfilled for $c_1 < c_1^*$ and $c_2 < c_2^*(c_1)$

- $\lambda_1 > \lambda_2(c_1, c_2)$. This case is always fulfilled for $c_1 > c_1^*$

Inserting the expressions for the eigenvalues (Eq. (3-32)) into the inequalities results in an expression for a critical concentration $c_2^*(c_1)$ at which the relative size of the eigenvalues change, i.e. $\lambda_1 = \lambda_2$.

$$H_1 = \frac{q_s^2 H_2(c_1)}{\left(q_s + H_2(c_1)c_2^*\right)^2}$$

$$\Rightarrow c_2^*(c_1) = q_s\left(-\frac{1}{H_2(c_1)} \pm \frac{1}{\sqrt{H_1 H_2(c_1)}}\right) \qquad (3\text{-}35)$$

Hereby, only the positive root is the physically relevant solution.
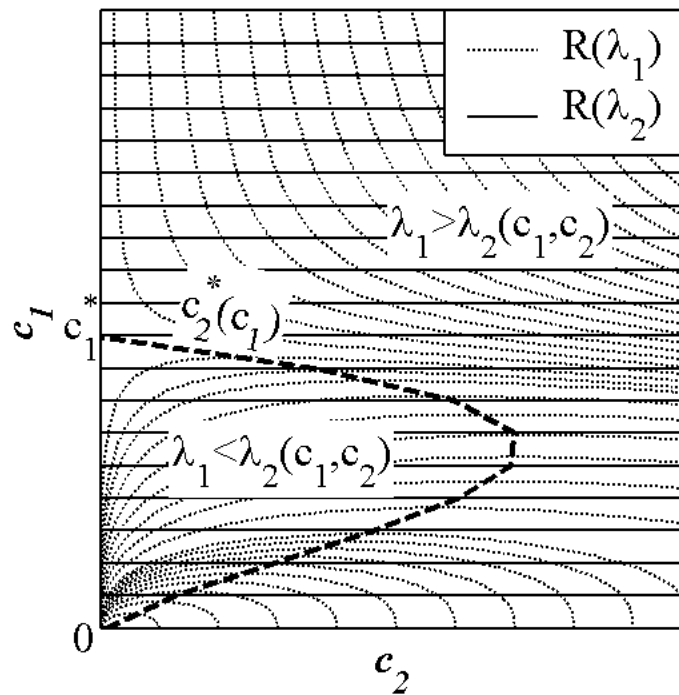
Figure 3.15: Schematic of a typical hodograph for a binary linear-Langmuir system. The fat dashed line encloses the region (calculated with Eq. (3-35)) where the modifier is always the fastest migrating component.

The hodograph looks in principle not much different compared to those obtained for the binary linear-linear system (Figure 3.9). Thus, the solutions will feature the same phenomena as observed for the strictly linear isotherms, i.e. on-column dilution and on-column concentrating effects. Given the nature of the nonlinear isotherm of the solute more complicated elution shapes can be expected this time, as well as nonlinear phenomena such as shocks and spreading waves.

Again, numerous combinations could be discussed.

case a) modifier is always the least retained component: $\lambda_2(c_1, c_2) > \lambda_1$ for $c_1 < c_1^*$ and $c_2 < c_2^*$ (inside the dashed region in Figure 3.15).

case b) modifier is always the strongest retained component: $\lambda_2(c_1, c_2) < \lambda_1$ for $c_1 > c_1^*$ and $c_2 > c_2^*$ (outside the dashed region in Figure 3.15).

case c) mixed elution order: $\lambda_2(c_1, c_2) \leq \lambda_1 \leq \lambda_2(c_1, c_2)$ for $c_1^* \leq c_1 \leq c_1^*$

and/or $c_2^* \leq c_2 \leq c_2^*$. Solute is less and more retained than the modifier, depending on the modifier and/or solute concentration. Such a case is possible but it should be avoided, since this will make such a system unsuitable for separation of more component systems.

Contrary to the linear-linear interaction, we will discuss below only the relevant cases a) and b). Each case will be discussed for gradient injections of:

- modifier deficit, $c_1^F < c_1^0$

- modifier surplus, $c_1^F > c_1^0$

The effect of the solute concentration will be mainly disregarded for the sake of a focused discussion.

Analytical solutions will not be provided here since they strongly depend on the function used to describe the dependence of the isotherm parameters on the mobile phase composition.

3.2.1.1.   Modifier is the Least Retained Component - Case a)

This case is applicable in the range when the modifier and the solute concentrations are both below the critical concentrations c_1^* and $c_2^*(c_1)$. Remember that the critical solute concentration, Eq. (3-35), is a function of the modifier concentration. Lets apply now the same procedure as shown above for the binary linear-linear system and start with the gradient injection in a surplus of modifier. The corresponding hodograph plots will typically look like the one sketched in Figure 3.16.

Note, that the hodograph above looks in principle like the one for linear-linear isotherms (Figure 3.3 on page 50). The only difference is, that here the eigenvalue λ_2 is also function of the solute concentration, i.e. $\lambda_2 = \lambda_2(c_1, c_2)$. Since the eigenvalue λ_1 is always smaller than λ_2 we have to start at the initial state, $\mathbf{0}$, and follow the concentration pathway belonging to λ_1. This pathway is parallel to the c_1-axis for a not preloaded column with respect to the solute ($c_2^0 = \mathbf{0}$). The corresponding eigenvalue remains constant along $R(\lambda_1)$. At the intersection of the concentration path-

way ($R(\lambda_1)$) through the initial state with the concentration pathway ($R(\lambda_2)$) through the feed state, an intermediate state **I1** is observed. From here we follow $R(\lambda_2)$ towards the feed state. The transition from **I1** to **F** happens with a shock, since the eigenvalues $\lambda_2(c_1, c_2)$ decrease with increasing solute concentration. The chromatographic cycle is completed from the feed state along the concentration pathway belonging to λ_1 towards the intermediate state **I2** and from there back to the initial state **0** along $R(\lambda_2)$.
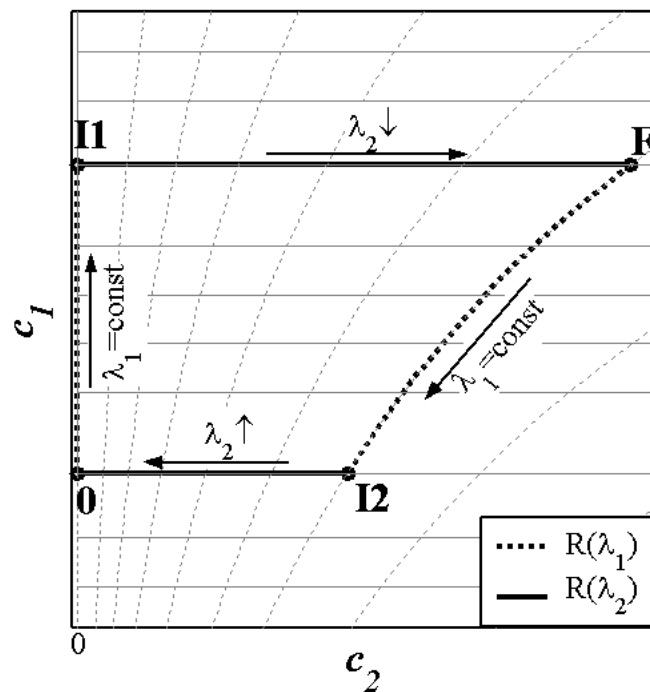
Figure 3.16: Hodograph of the injection of a modifier surplus for linear-Langmuir isotherms, when the modifier is always the least retained component.

The chromatographic cycle is summarized with:

- $\mathbf{0} \rightarrow \mathbf{I1}$ along $R(\lambda_1 = const) \rightarrow$ contact discontinuity

- $\mathbf{I1} \rightarrow \mathbf{F}$ along $R(\lambda_2 \downarrow)$ $\rightarrow$ shock

- $\mathbf{F} \rightarrow \mathbf{I2}$ along $R(\lambda_1 = const) \rightarrow$ contact discontinuity

- $\mathbf{I2} \rightarrow \mathbf{0}$ along $R(\lambda_2 \uparrow)$ $\rightarrow$ spreading wave

The unknown concentrations **I1** respectively **I2** are the intersections of the two concentration pathways through the feed state and the initial state. On the other hand, we know from the special properties, the initial and final modifier concentrations of the intermediate states. Thus, the intermediate states can be obtained from an integration of $\mathbf{r}^*\left(\lambda_1\right)$ over the modifier concentration, c_1 :

$$R(\lambda_1): \qquad \int_{c_2^{start}}^{c_2^{final}} dc_2 = \int_{c_1^{start}}^{c_1^{final}} \mathbf{r}^*\left(\lambda_1\right) dc_1 \qquad\qquad (3\text{-}36)$$

here with: $\qquad c_2^{start} = c_2^0, \; c_1^{start} = c_1^0, \; c_2^{end} = c_2^{I1}, \; c_1^{end} = c_1^{I1} = c_1^F$

or $\qquad c_2^{start} = c_2^F, \; c_1^{start} = c_1^F, \; c_2^{end} = c_2^{I2}, \; c_1^{end} = c_1^{I2} = c_1^0$

Inserting the specific interactions defined by Eq. (3-31) and Table 3.6 into Eq. (3-33) and integrating the resulting expression yields for the unknown concentration of the solute:

$$c_2^{end} = \frac{1}{2H_1 H_2(c_1^{end})}\Bigg\{ -H_1 q_s + \frac{\left(c_2^{start}\right)^2 H_1 H_2(c_1^{start}) + \left(q_s\right)^2 + H_1 q_s c_2^{start}}{\left[q_s + c_2^{start} H_2(c_1^{start})\right] H_2(c_1^{end})} \dots$$

$$\dots + \sqrt{ \begin{aligned} &\left(H_1 q_s\right)^2 - 4\left(q_s\right)^2 H_1 H_2(c_1^{end}) \dots \\ &\dots + \frac{2 q_s H_1 H_2(c_1^{end})\left[\left(q_s\right)^2 + q_s H_1 c_2^{start} + \left(c_2^{start}\right)^2 H_1 H_2(c_1^{start})\right]}{q_s + c_2^{start} H_2(c_1^{start})} \dots \\ &\dots + \frac{\left[\left(q_s\right)^2 + q_s H_1 c_2^{start} + \left(c_2^{start}\right)^2 H_1 H_2(c_1^{start})\right]^2 \left[H_2(c_1^{end})\right]^2}{\left[q_s + c_2^{start} H_2(c_1^{start})\right]^2} \dots \end{aligned} } \Bigg\} \qquad (3\text{-}37)$$

The usefulness of the expression above is limited, since it represents a solution <u>only</u> for those solvent-solute interactions defined by Eq. (3-31) and Table 3.6. This is one of the algebraic solutions, where it may be more expedient just to settle for a numerical evaluation of Eq. (3-36).

Let us now translate the results from the hodograph into the time-space domain (Figure 3.17). The modifier travels always faster than the solute. If the initial concen-

tration of the solute is not zero ($c_2^0 \neq \mathbf{0}$ i.e. a preloaded column) solute will be desorbed at the boundary between the initial state and the feed state of the modifier, since $q_2(c_1^0, c_2^0) > q(c_1^F, c_2^0)$. A preloaded column with respect to the solute is not common for preparative batch chromatography, thus, we will disregard this in the further discussion and will concentrate on the case where $c_2^0 = \mathbf{0}$, thus $c_2^{I1} = c_2^0 = \mathbf{0}$. The concentrations of the solute increase within the injection plug of the modifier from c_2^{I1} to the feed concentration c_2^F. Since the traveling velocity of the solute decreases with increasing solute concentration, c_2, a shock forms at the beginning of the injection, with the inverse velocity proportional to:

$$\underset{I1 \to F}{\widetilde{\lambda}} = \mathbf{1} + F \frac{q_2(c_1^F, c_2^F) - q_2(c_1^F, c_2^{I1})}{c_2^F - c_2^{I1}} \tag{3-38}$$
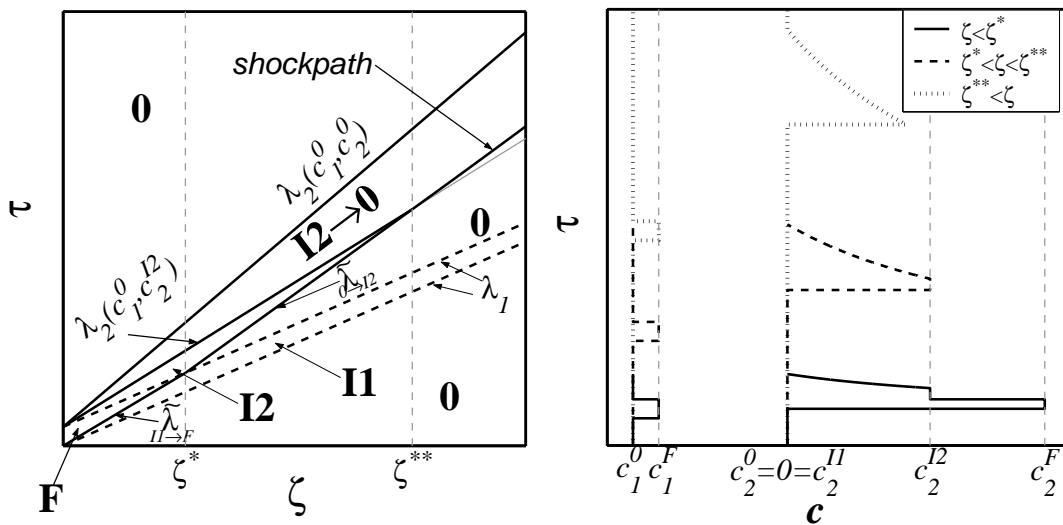
Figure 3.17: Characteristics in the space-time domain for a gradient injection of a modifier surplus for linear-Langmuir isotherms, when the modifier is always the least retained component (left). Right figure shows the corresponding concentration-time profiles for a not preloaded column at three different space positions.

On the rear side of the injection, the modifier plug travels uninterrupted by the solute (due to the linear isotherm of the modifier) through the column with the inverse velocity proportional to λ_1. All solute concentrations propagate slower than the modifier, thus they immediately leave the higher modifier concentration of the injection plug. Within the injection plug, the solute is transported faster away from a certain

space position, compared to outside the injection media. Thus, a dilution of the solute happens at the boundary of the modifier between the feed and the initial state in form of a contact discontinuity from $c_2^F \rightarrow c_2^{I2}$. After that the solute is in media with the modifier concentration of c_1^0 and the solute concentrations decrease from $c_2^{I2} \rightarrow c_2^0$ in form of a spreading wave with $\lambda_2(c_1^0, c_2)$. This is the complete cycle as observed in the hodograph in Figure 3.16, as long as interactions between the front and the rear of the injection plug are not present.

The shock from the intermediate state $\mathbf{I1}$ to the feed state $\mathbf{F}$ travels slower than the modifier. At a certain space position, let us denote it by ζ^*, this shock will interact with the rear part of the injection plug (the modifier).

$$
\tau_{inj} + \lambda_1 \zeta^* = \underset{I1 \rightarrow F}{\tilde{\lambda}} \zeta^*
$$

$$
\Rightarrow \zeta^* = \frac{\tau_{inj}}{\underset{I1 \rightarrow F}{\tilde{\lambda}} - \lambda_1} \tag{3-39}
$$

Beyond this point ζ^* the feed state, c_2^F, is not reached anymore. The solute concentration will drop at the rear end of the modifier injection plug to the initial state, c_2^0, with a contact discontinuity. The front of the intermediate state I2 with its origin at τ_{inj} has also reached that space position ζ^* and another shock forms proportional to:

$$
\underset{0 \rightarrow I2}{\tilde{\lambda}} = 1 + F \frac{q_2(c_1^0, c_2^{I2}) - q_2(c_1^0, c_2^0)}{c_2^{I2} - c_2^0} \tag{3-40}
$$

This shock propagates slower through the column than the fastest wave of $\lambda_2(c_1^0, c_2^{I2})$ (origin at $\zeta = 0, \tau = \tau_{inj}$). The shock will be overtaken at a certain space position, let us denote it by ζ^{**}:

$$\tau_{inj} + \lambda_2\left(c_1^0, c_2^{I2}\right)\zeta^{**} = \underset{I1\to F}{\tilde{\lambda}}\,\zeta^* + \underset{0\to I2}{\tilde{\lambda}}\left(\zeta^{**} - \zeta^*\right)$$

$$\Rightarrow \zeta^{**} = \frac{\tau_{inj}\left(\underset{0\to I2}{\tilde{\lambda}} - \lambda_1\right)}{\left(\underset{I1\to F}{\tilde{\lambda}} - \lambda_1\right)\left(\underset{0\to I2}{\tilde{\lambda}} - \lambda_2\left(c_1^0, c_2^{I2}\right)\right)} \tag{3-41}$$

From this point on the solute concentration of the shock decreases and the shock decelerates as described in Example 2-3 on page 34. The shockpath $\tilde{\zeta}$ is in principle the same as the one derived for the Langmuir example, only the start points have to be adopted (i.e. starting concentrations, initial space position).

$$\tilde{\zeta}(c) = \zeta^{**}\left(\frac{\left(1 + b(c_1^0)c_2\right)\left(c_2^{I2} - c_2^0\right)}{\left(1 + b(c_1^0)c_2^{I2}\right)\left(c_2 - c_2^0\right)}\right)^2 \tag{3-42}$$

Inserting Eqs. (3-32), (3-38), (3-40), (3-41) into Eq. (3-42) and solving it with respect to c_2 - typically unknown at a given space position - yields the following lengthy algebraic expression for the maximum concentration of the shockpath at a certain space position, ζ :

$$C_1 c_2^2 + C_2 c_2 + C_3 = 0$$

$$c_2 = -\frac{C_2 \pm \sqrt{\left(C_2\right)^2 - 4C_1 C_3}}{2C_1}$$

$$C_1 = \zeta^{**}\left(b_2(c_1^0)\right)^2\left(c_2^{I2} - c_2^0\right)^2 - \zeta\left(1 + b_2(c_1^0)c_2^{I2}\right)^2 \tag{3-43}$$

$$C_2 = \zeta^{**}\,2b_2(c_1^0)\left(c_2^{I2} - c_2^0\right)^2 + \zeta\,2\left(1 + b_2(c_1^0)c_2^{I2}\right)^2 c_2^0$$

$$C_3 = \zeta^{**}\left(c_2^{I2} - c_2^0\right)^2 - \zeta\left(1 + b_2(c_1^0)c_2^{I2}\right)^2\left(c_2^0\right)^2$$

The same phenomena in terms of on-column dilution of the feed state, as observed for the completely linear case, are present here in the case of linear – Langmuir interactions of solvent and solute and a gradient injection in a modifier surplus.

The injection of a modifier deficit results, as we would expect from the linear-linear interaction, in an on-column concentrating effect (Figure 3.18). The chromatographic

cycle is identical with the one described on page 77 (contact discontinuity, shock, contact discontinuity, spreading wave), only the concentration of the intermediate desorption state I2 is this time larger than the feed concentration. The complete chromatographic cycle is sketched in Figure 3.19.

Figure 3.18: Hodograph for an injection of a modifier absence for linear-Langmuir isotherms, when the modifier is always the least retained component.

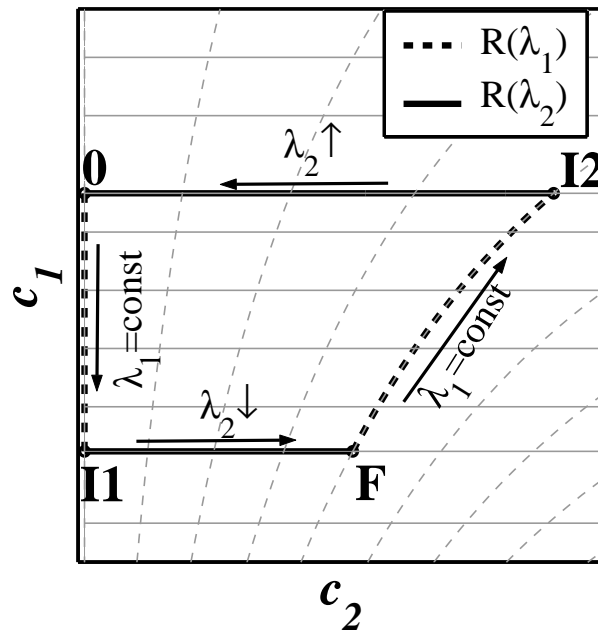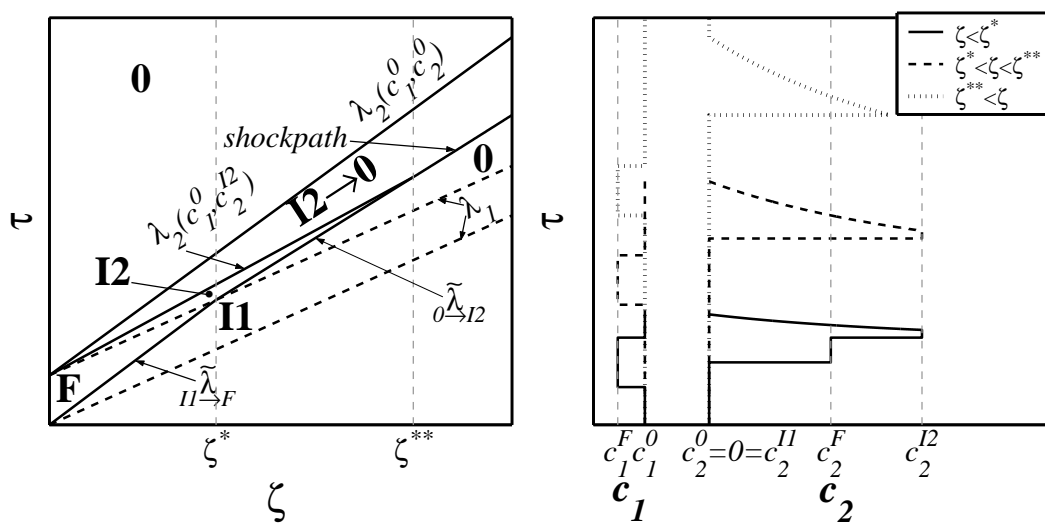**Figure 3.19: Characteristics in the space-time domain for a injection of a modifier absence for linear-Langmuir isotherms, when the modifier is always the least retained component (left). Right figure shows the corresponding concentration-time profiles at three different space positions.**

3.2.1.2. *Modifier is the Strongest Retained Component - Case b)*

This scenario is valid outside the dotted region in Figure 3.15. We will only discuss it here for $c_1 > c_1^*$ since this work concentrates on batch chromatography, where typically the initial concentration of the solute is zero. The consideration of effects of preloaded columns (with respect to the solute), though interesting and applicable especially for isotherm determination (frontal analysis, perturbation method, frequency response, etc.) and continuous chromatographic processes, would unnecessarily complicate the discussion below.

The corresponding part of the hodograph of Figure 3.15 above c_1^* is sketched in Figure 3.20. The eigenvalues λ_2 are always smaller than λ_1. Thus, the concentrations propagate from the initial state **0** along the $R(\lambda_2)$ characteristic to the intermediate state **I1**. Along this characteristic, the concentration of the modifier remains constant at its initial value c_1^0. The state change happens with a shock , since the eigenvalues λ_2 decrease between 0 and I1,. The state transitions along the $R(\lambda_1)$ characteristics from I2 to F and from I2 back to the initial state happen as contact discontinuities (since $\lambda_1 = const$).

Figure 3.20: Hodograph of a gradient injection of a modifier surplus (left) and a modifier deficit (right) for Linear – Langmuir Isotherms when the modifier is always the strongest retained component – case b).
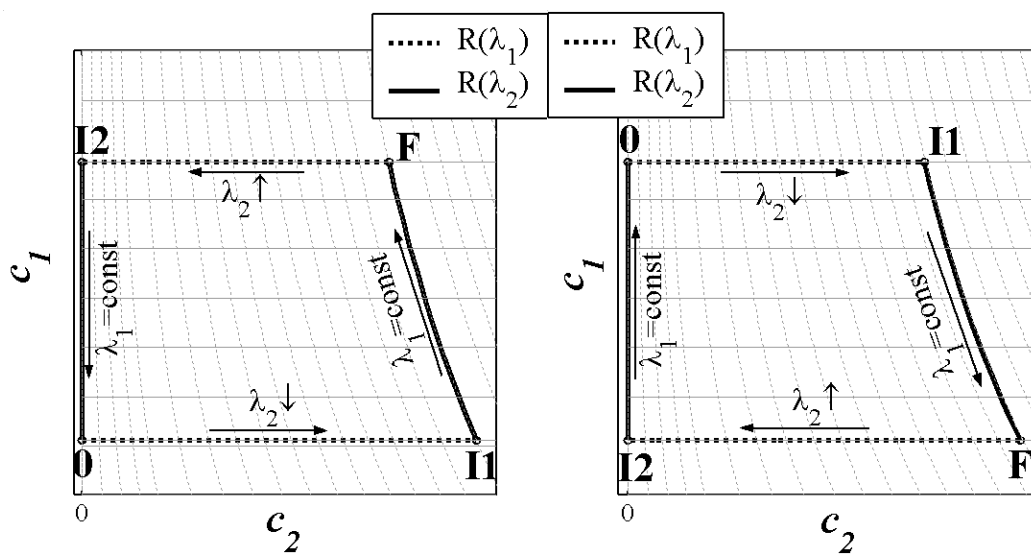
The chromatographic cycle is summarized with:

- $0 \rightarrow I1$ along $R\left(\lambda_2 \downarrow\right)$ $\rightarrow$ shock

- $I1 \rightarrow F$ along $R\left(\lambda_1 = const\right)$ $\rightarrow$ contact discontinuity

- $F \rightarrow I2$ along $R\left(\lambda_2 \uparrow\right)$ $\rightarrow$ spreading wave

- $I2 \rightarrow 0$ along $R\left(\lambda_1 = const\right)$ $\rightarrow$ contact discontinuity

In the case of the injection of a modifier surplus (Figure 3.20, left) a concentration above the feed concentration is observed. For the gradient injection of a modifier deficit a dilution of the solute occurs, as expected from the results for the linear – linear case.

The unknown intermediate concentrations c_2^{I1} and c_2^{I2} can be calculated from the solution of Eq. (3-36) with the following boundaries:

- for c_2^{I1}: $c_2^{start} = c_2^{F}$, $c_1^{start} = c_1^{F}$, $c_2^{end} = c_2^{I1}$, $c_1^{end} = c_1^{I1} = c_1^{0}$

- for c_2^{I2}: $c_2^{start} = c_2^{0}$, $c_1^{start} = c_1^{0}$, $c_2^{end} = c_2^{I2}$, $c_1^{end} = c_1^{I2} = c_1^{F}$

Let us now do the same discussion from the physical point of view. The migration velocity of the solute is here always larger than the one of the solvent. Thus, the solute leaves the injection media immediately at the beginning of the feed plug. In the case of the injection of a modifier surplus, the traveling velocity of solute outside the injection media is smaller compared to inside the injection plug. Thus, the solute is transported faster to a certain position, than it is transported away – the concentrating effect beyond the feed concentration of the solute occurs (and vice versa for the injection of a modifier deficit). Additionally, all concentrations between the initial state of the solute and the intermediate state are present. This results (as we know for Langmuir type isotherms) in a shock with the velocity corresponding to:

$$\tilde{\lambda}_{0 \rightarrow I1} = 1 + F \frac{q_2(c_1^{0}, c_2^{I1}) - q_2(c_1^{0}, c_2^{0})}{c_2^{I1} - c_2^{0}} \tag{3-44}$$

The concentrations of the components jump from the state I1 to the feed state F at the boundary of the injection plug, which migrates through the column with the inverse

velocity proportional to λ_1. At the rear end of the injection, the solute takes all values between the feed state and the intermediate state, I2, and forms a spreading wave bounded by $\lambda_2(c_1^F, c_2^F)$ and $\lambda_2(c_1^F, c_2^{I2})$ (Figure 3.21, left). For a not preloaded column is $c_2^{I2} = c_2^0$. For a preloaded column the modifier acts as a displacer resulting in a smaller concentration than the feed concentration of the solute for the injection of a modifier plus (solute is transported slower to the interface outside the injection media, than it is transported away inside) and vice versa for the injection of a modifier deficit. Finally, the modifier drops to its initial value. This summarizes the complete chromatographic cycle in the physical plane, if no interactions between the adsorption and desorption side of the injection are present .

These interactions shall start at column length ζ^*, where the characteristic λ_1 is overtaken by the faster characteristic $\lambda_2(c_1^F, c_2^F)$ with its origin at τ_{inj}.

$$\lambda_1 \zeta^* = \tau_{inj} + \lambda_2(c_1^F, c_2^F) \zeta^*$$

$$\Rightarrow \zeta^* = \frac{\tau_{inj}}{\lambda_1 - \lambda_2(c_1^F, c_2^F)} \tag{3-45}$$

Beyond this space position (dashed line Figure 3.21, right) the feed state is not observed anymore. The concentrations of the solute within the injection plug decrease further until the transition from the feed state F to the intermediate state I2 has completely vanished (dotted line in Figure 3.21) and leaves only the state I2, which is from there on transported through the column and bounded by the characteristics λ_1.

This space position is arbitrarily called ζ^{***} and fulfills the condition:

$$\lambda_1 \zeta^{***} = \tau_{inj} + \lambda_2(c_1^F, c_2^{I2}) \zeta^{***}$$

$$\Rightarrow \zeta^{***} = \frac{\tau_{inj}}{\lambda_1 - \lambda_2(c_1^F, c_2^0)} \tag{3-46}$$

The corresponding concentration of the solute left and right of I2 is the initial concentration c_2^0. Note that $\zeta^{**} > \zeta^{***}$ or $\zeta^{**} < \zeta^{***}$, depending on the isotherm parameters, feed and initial conditions.

Figure 3.21: Characteristics in the space-time domain for a injection of a modifier surplus for linear-Langmuir isotherms, when the modifier is always the strongest retained component (left). Right figure shows the corresponding concentration-time profiles for a not preloaded column at four different space positions.

The concentration of the solute jumps with a contact discontinuity from $c_2^F \rightarrow c_2^{I1}$ at the interface (solid lines in Figure 3.21, right). Beyond this point, this concentration of the solute migrates further in the initial mobile phase proportional to $\lambda_2(c_1^0, c_2^{I1})$ (Figure 3.21, left). The slope of this characteristic is smaller than the corresponding slope of the shock $\tilde{\lambda}_{0 \rightarrow I1}$, and it will overtake it at a space position arbitrary called ζ^{**} (to remain consistent with the previous section).

$$\tilde{\lambda}_{0 \rightarrow I1} \zeta^{**} = \tau_{inj} + \lambda_2(c_1^F, c_2^F)\zeta^* + \lambda_2(c_1^0, c_2^{I1})\zeta^{**}$$

$$\Rightarrow \zeta^{**} = \frac{\tau_{inj}\left[\lambda_1 - \lambda_2(c_1^0, c_2^{I1})\right]}{\left(\tilde{\lambda}_{0 \rightarrow I1} - \lambda_2(c_1^0, c_2^{I1})\right)\left(\lambda_1 - \lambda_2(c_1^F, c_2^F)\right)} \qquad \text{(3-47)}$$

From this point on the shock decelerates (dash-dotted line in Figure 3.21). Here, the decelerating concentrations are not centered as it is so well known from the Langmuir Example 2-3 on page 34 and for case a) in the previous section. Each decelerating concentration leaves the injection plug at a different space position, in principle $\zeta^*|_{c_2} = f(c_2^{in})$, where the superscript *'in'* denotes the concentration within the injection media. At the boundary of the injection media and the initial solvent, the con-

centrations of the solute jump in form of a contact discontinuity from c_2^{in} to c_2^{out}, with the superscript *'out'* denoting the corresponding concentration of the solute outside the injection media (see enlarged region in Figure 3.21). Both concentrations are connected via Eq. (3-33). All concentrations decelerating the shock have a different origin at the interface of the injection media and the original mobile phase, which makes the derivation of the shockpath somewhat complicated. This time, no useful algebraic solution for the shockpath can be found. The application of the procedure for the derivation of the shockpath is explained in detail for the interested user in Appendix B 2 on page 151.

Figure 3.22 presents the corresponding figures for the gradient injection of a modifier deficit. The same phenomena described for the gradient injection of a modifier surplus are of course also present. Only that here the feed state represents the highest concentration.
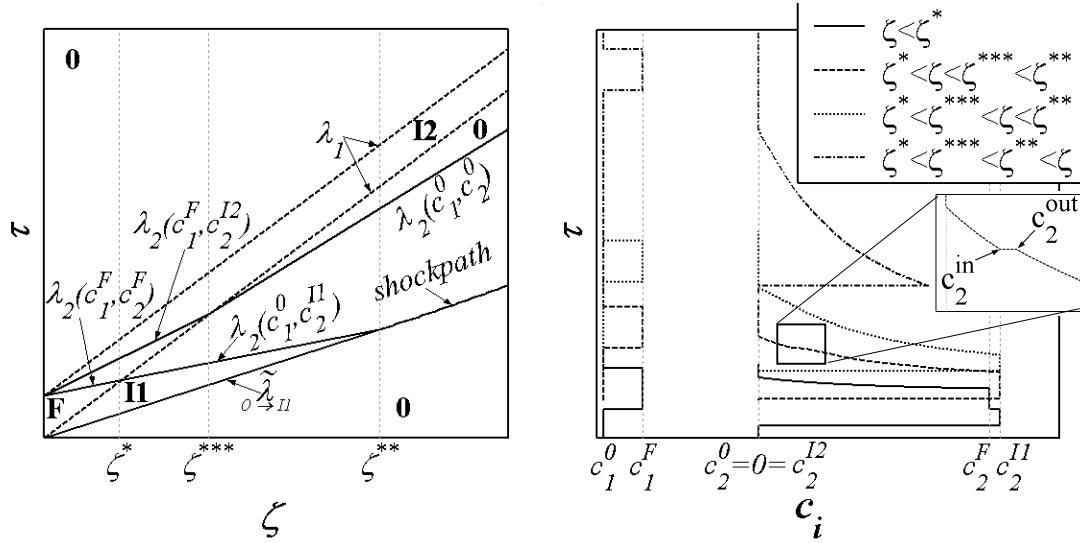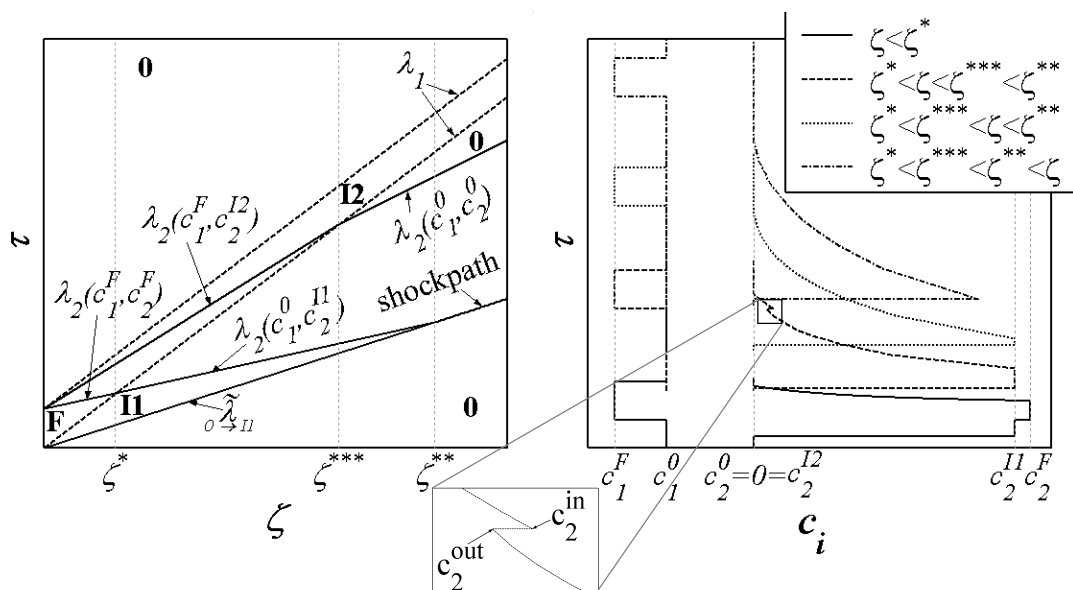

Figure 3.22: Characteristics in the space-time domain for a gradient injection of a modifier deficit for linear-Langmuir isotherms, when the modifier is always the strongest retained component (left). Right figure shows the corresponding concentration-time profiles for a not preloaded column at four different space positions.

3.2.2.   Summary of Binary Systems with Linear - Langmuir Isotherms

It can be concluded that the same essential effects in terms of on-column dilution and on-column concentration as summarized in Table 3.3 on page 64 for the linear – linear case can be also expected for non-linear isotherms of the solutes. Additional effects, due to the non-linearity of the solute isotherms, such as shocks and disperse

boundaries are now also present. However, those are in principle the same effects as already known for nonlinear isocratic injections.

3.3.   Summary

The equilibrium theory was applied to extract and analyze general effects of gradient injections of solutes in a different mobile phase than used for the elution. The study was performed exemplary for different isotherm combinations for the modifier and the solutes (linear – linear and linear – Langmuir). Both isotherm combinations resulted in the same general effects for the peak profiles.

It can be deducted, just based on the variation of the adsorption isotherms with the mobile phase composition, that on-column dilution, on-column concentration and split/distorted peaks of the solutes can be expected for such a gradient injection. If the column is long enough or the injection small enough, the band profile of the solute may be mistaken with the one for an isocratic injection. On-column dilution and on-column concentrating effects depend on the elution strength of the injection solvent and its relative retention compared to the solutes. This is summarized in Table 3.3 on page 64.

The gradient injection is only applicable to overcome solubility issues of the mobile phase, if the modifier is the least retained component. The general assumption behind this finding is that with increasing modifier concentration, both, the solubility of the solutes as well as the elution strength increase. If, in such a case, the modifier would be stronger retained compared to the solutes, than the concentration of the solutes would increase even above the injection concentration and may trigger undesired precipitation. Such a combination of a stronger injection eluent and a stronger retention of the former may make sense for certain applications, where the desired solute is very diluted and needs to be concentrated.

The dependence of the solubility on the modifier concentration is of the uttermost importance for the productivity. The most productive injection method depends on the function of the solubility of the solutes on the modifier concentration. A positive effect for a gradient injection can be expected only for strong nonlinear dependences of the solubility on the modifier concentration. The isocratic injection is the better choice if this strong nonlinear increase is not observed. The injection in a weaker solvent may be only desirable if the solubility of the components to be separated is

not an issue and posses markedly different elution times (large separation coefficient). This injection method corresponds then to a typical gradient operation, where the elution strength of the mobile phase is immediately increased after the injection.

This work could be extended towards nonlinear isotherms of the solutes for ternary systems. Another extension should be the incorporation of nonlinear isotherms for solvent components. Here, the consequent application of the adsorbed solution theory for the prediction of loadings of the solutes as a function of the solvent composition could enhance the state-of-the-art. The analysis could also be extended to preloaded columns, for the determination of characteristic effects due to the solute concentrations, as they might be observed for perturbation experiments.

> *To understand gradient elution, one must begin with a good picture of isocratic elution.*
>
> L.R. Snyder, in *High performance Liquid Chromatography - Advances and Perspectives,* C. Horváth, Editor. 1980, Academic Press: New York. p. 207-216.

4. Gradient Injection and the Effect of Solvent-Solute Interactions – 1st Case Study

In this chapter, solvent-solute interactions during gradient injection are experimentally tested on the example of overloading a chromatographic column with a compound possessing low solubility in the mobile phase. In order to increase the concentration of injection a strong solvent for dissolving the feed was used. From the theoretical results of the previous chapter, it is known that the modifier should travel faster through the column than the solute to avoid that the concentration of the solute increases even more above the local solubility. The example studied corresponds in principle to the cases a) of chapter 3. The injection of such concentrated samples brings the risk of triggering undesired crystallization processes.

In this chapter a model system has been investigated with ethanol-water as the mobile phase and DL-threonine as the sample dissolved in the strong solvent (pure water). Under extreme overloaded conditions band splitting was observed, as expected from the previous chapter 3. Measurements of the adsorption isotherms and systematic solubility studies have been carried out. For the process analysis, a simplified mathematical model as it is often used for the description of gradient chromatography was applied. The simulations of the band profiles were compared with the experimental data. A detailed description of this work has been published in [41]. The results will be summarized below.

4.1.   Chemicals and Experimental Procedures

A summary of the chromatographic system chosen for the investigation is given in Table 4.1. Ethanol was of HPLC grade (Merck, Darmstadt, Germany). Deionized water was used and further purified using a Milli-Q-Gradient system (Millipore, Billerica, MA, U.S.A.). DL-threonine (>99%) was obtained from Merck (Darmstadt, Germany). Lichroprep NH_2 25-40 µm (Merck, Darmstadt, Germany) was used as achiral stationary phase capable to retain DL-threonine. The column was packed in our laboratory by subsequent filling and compression (due to slight thumping on the column) of dry stationary phase.

The solubility of DL-threonine in solvents of different water contents was measured in our laboratory in the framework of an independent study. The results are published in detail by Sapoundjiev *et al.* in [151, 152]. In a series of experiments, a surplus of DL-threonine was equilibrated with solvent at 20°C for 24 *h*. The temperature of the stirred suspension was controlled (+/-0.1 *K*) with a Polystat CC3 thermostat (Peter Huber Kältemaschinenbau, Offenburg, Germany). Samples of 10 to 20 *ml* of the liquid were taken after equilibration. The liquid was completely evaporated and the threonine content was determined gravimetrically [151]. The masses of the samples before and after evaporation were measured (+/-0.1 *mg*) with a microbalance AT261 by Mettler Toledo (Giessen, Germany).

Table 4.1: Summary of the experimental system

solute	mobile phase	feed solvent	stationary phase and column
DL-threonine	*water:ethanol of various compositions*	*water*	*LiChroprep NH₂, 24-40µm, 0.46x25cm, ε=0.792*

For the chromatographic elution experiments, a conventional HPLC system was used, consisting of a Waters 600E quaternary low-pressure gradient pump (Waters, Milford, MA, U.S.A.) and a UV-detector (Knauer, Berlin, Germany). The detection was done at a wavelength of 215 *nm*. The temperature of the column and the manual injection valve (integrated in the thermostat) was controlled at 20°C (Jetstream II, Knauer, Berlin, Germany). Only full loop injections were performed with sample loops of 10, 100, 1000 and 2000 *µl*, respectively. Each experiment was repeated at least twice.

The experimental chromatographic setup is sketched in Figure 4.1 below. The additional 6-port / 2-way valve with the bypass allows for extremely sharp step changes of the feed for frontal analysis experiments.

Frontal analysis experiments of consecutive breakthroughs (20 steps) were carried out at nine different volume fractions of water in the mobile phase (i.e. g=0.2-1). The maximum concentrations of these experiments were close to the solubility limit of threonine in the mobile phase. These experiments have been performed using the low-pressure gradient of the pump and were used also to calibrate the detector at different water contents. The flow rate in all experiments was 1.97 *ml/min* as permanently verified with a flow meter (Phase Separations, Deeside, U.K.).
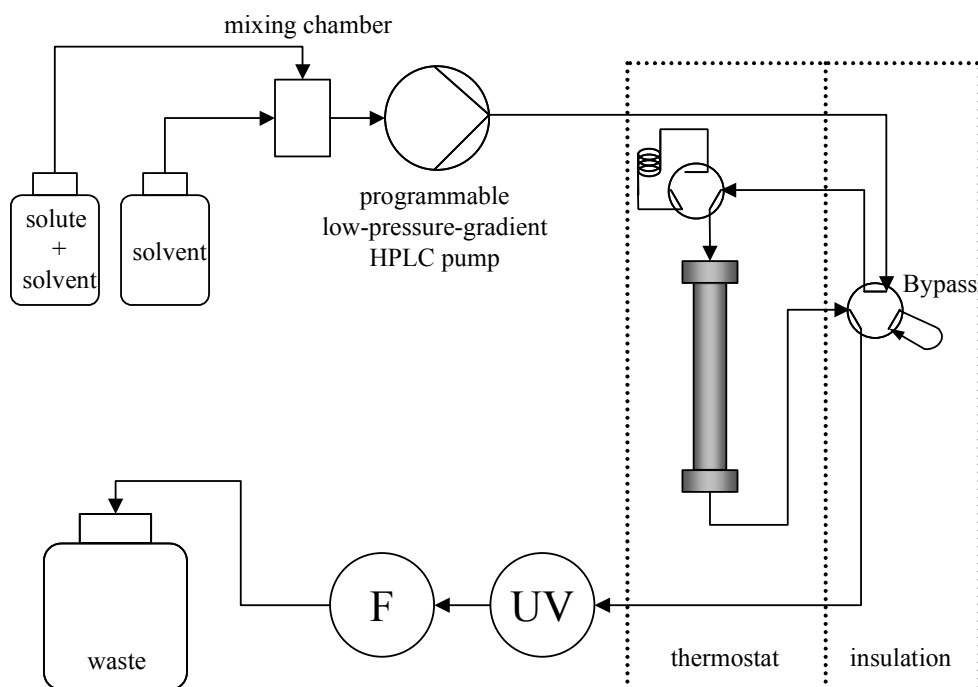
Figure 4.1: Schematic of the experimental setup for the chromatographic experiments.

4.2. Results

4.2.1.   Solubility of DL-threonine in the Mobile phases and in the Injection Media

Figure 4.2 shows the solubility of DL-threonine at $20°C$ for different water contents in the solution. The constant injection concentration applied in the chromatographic experiments is also depicted. The solubility was approximated with an empirical

function fitted to the experimental data using a nonlinear curve fit (see Table 4.2 for details, correlation coefficient $r^2=0.998$).

$$c_{S,DL} = 0.77 * \exp(6.01 y_{H2O})$$

(4-1)

$c_{S,DL}$ and y_{H2O} are the saturation concentration of DL-threonine in g/l and the volume fraction of water in the solution at $T=20°C$, respectively.

Table 4.2: Solubility of DL-threonine in ethanol/water mixtures at $T=20°C$.

$H_2O{:}EtOH_{v/v}$	y_{H2O}	$c_{S,DL}{}^{exp}$	$c_{S,DL}$ calc. with Eq. (4-1)
20:80	0.20	2.4	2.6
40:60	0.40	10.3	8.5
60:40	0.59	29.3	26.7
80:20	0.76	78.2	74.2
100:0	0.89	165.7	162.0
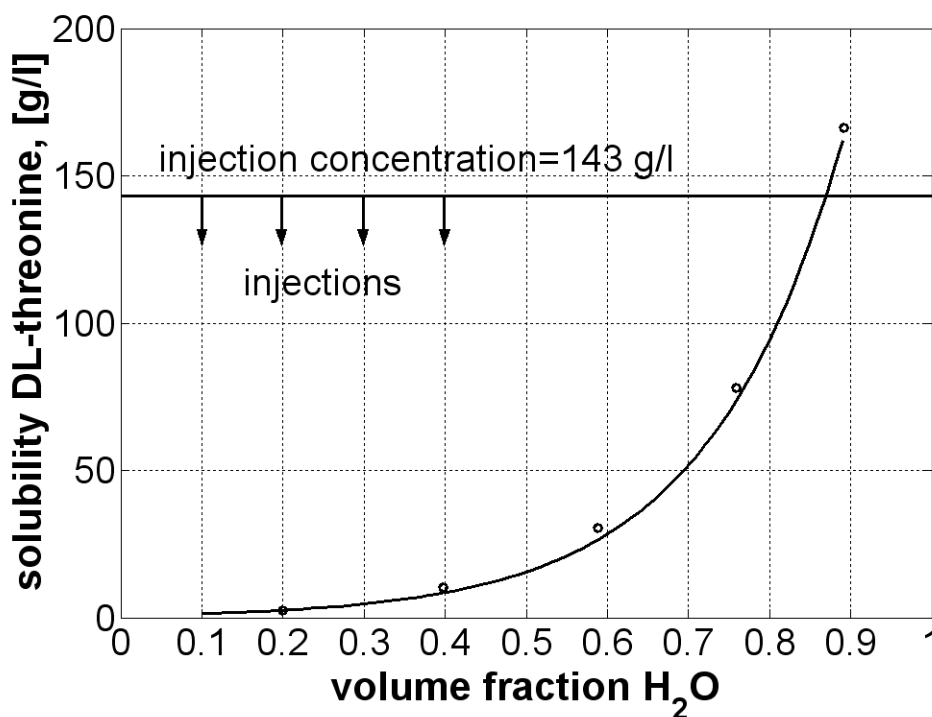
Figure 4.2: Solubility of DL-threonine at 20°C in ethanol-water mixtures. Symbols: experimental data points, line: empirical function (Eq. (4-1)). The arrows indicate the water content of the mobile phases at which elution experiments were performed, while the horizontal line depicts the injection concentration in water.

4.2.2. Elution Profiles

The mobile phase compositions of the overloaded elution experiments were $g_{H2O} = 0.1, 0.2, 0.3$ and 0.4 volume fraction of water and the corresponding solubility (Eq. (4-1)) in the mobile phase were $c_{S,DL} = 1.4, 2.5, 4.6$ and 8.4 *g/l*, respectively. The injection solvent was water and the injection concentration of DL-threonine was 143 *g/l* for all experiments. Note that this injection concentration was much higher than the solubility of DL-threonine in the mobile phase. Significant precipitation or at least crystallisation of threonine large enough to reduce the permeability of the column (thus increasing the pressure drop) was not observed during these experiments. This was surprising, since broad injections were performed up to 60 % of column fluid volume (3.29 *ml*). Due to the large surface area provided by the stationary phase, crystallisation can be expected to occur instantaneously once a super saturation is present with the system. Nevertheless, our results of an absence of this effect are in agreement with the observations reported earlier by Szanya *et al.* [183] for the separation of two steroids, where the displacement of the less adsorbed component by the stronger adsorbed component caused precipitation of the former one within the column. However, for this system blocking has not been reported either.

Figure 4.3 shows the evolution of the elution profiles of threonine with increased injection volume. At the chosen wavelength of 215 nm the signal of threonine was independent of the water content in the mobile phase (see also Appendix A 4). Blank injections of water (without threonine) resulted in negligible detector responses. The retention of the sample increased with decreased amount of the strong solvent water (evident especially for 100 *μl* injections, Figure 4.3-a to d, left plot). The sample elutes as a single peak for 100 *μl* injections. For larger injection volumes a part of the sample travels faster with the injection solvent water resulting in a peak splitting, which becomes more pronounced for decreased water contents in the mobile phase (see Figure 4.3 a-d, middle and right plots). Note that the enantiomers of DL-threonine are not separated in this achiral chromatographic system. In this environment the enantiomers behave as a single component.

This band splitting phenomenon is in agreement with results reported by Jandera and Guiochon [80] for non-aqueous reversed-phase chromatography and by Feng *et al.*

[33] for hydrophobic interaction chromatography of proteins. Note, that this system corresponds in principle to case a) explained in the previous chapter 3 –The experimental results (especially for the largest injections) demonstrate clearly the phenomena expected from chapter 3 for the gradient injection of a solute in a less retained, stronger eluent (here water):

- breakthrough of the feed state,

- sudden decrease of the solute concentration,

- constant intermediate state,

- elution of a dispersed rear part of the peak

- for smaller injections peak profiles are observed like a isocratic injections

a) volume fraction of H_2O g_{H2O}=0.4, $c_{S,DL}$=8.4 g/l

b) volume fraction of H_2O g_{H2O}=0.3, $c_{S,DL}$=4.6 g/l

c) volume fraction of H_2O g_{H2O}=0.2, $c_{S,DL}$=2.5 g/l

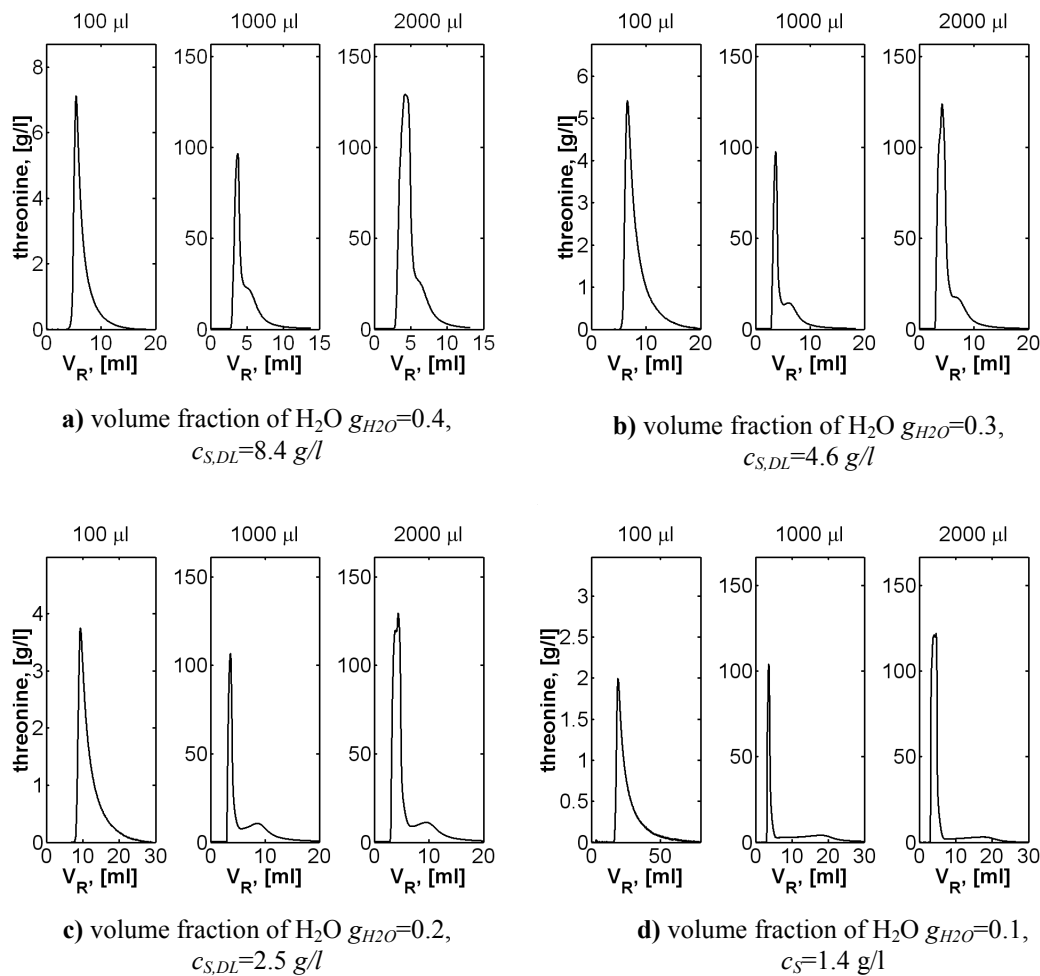d) volume fraction of H_2O g_{H2O}=0.1, c_S=1.4 g/l

Figure 4.3: Evolution of experimental elution profiles of threonine with increasing injection volume (c_{inj}=143 g/l) and for decreasing water contents in the mobile phase (a-d). $c_{S,DL}$ denotes the saturation concentration of DL-threonine in the applied mobile phase calculated with Eq. (4-1).

4.2.3.   Determination of Adsorption Isotherm

To gain further insight in the phenomena observed we determined the adsorption isotherms of the sample at nine different water contents in the mobile phase. The loading of water could be neglected since pulse experiments at different water contents in the mobile phases investigated (i.e., 0.2-0.9 volume fraction of water in the mobile phase) showed no retention. During the experiments, the mobile phase component water was found to deactivate progressively the adsorbent and to reduce the adsorption capacity of the polar adsorbent (although the manufacturer recommends water as a mobile phase for this stationary phase). Nevertheless, for the purpose of this study this system was found to be a good example for studying possible crystallisation because of high solubility of the sample in water and reasonable retention times in the ethanol-water mobile phases.

Frontal analysis required a number of experiments involving equilibration of the adsorbent with the water-rich mobile phases and could, due to the mentioned deactivation, not be successfully used to determine the adsorption equilibria on the stationary phase precisely. These FA experiments were utilized to obtain initial information on the shape of the isotherms at different water contents in the mobile phase.

Three parameter modified Langmuir equation Eq. (2-12) was found to be sufficient to correlate the concentration of the sample in the mobile and the solid phase. The model assumes adsorption mechanism on the heterogeneous surface containing two energetically different adsorption sites: site "1" with high adsorption energy accounted for by a larger equilibrium constant b_1 and site "2" with a low adsorption energy and a negligible equilibrium constant b_2, resulting in the following simplified expression of the Bi-Langmuir equation:

$$q_{DL} = \frac{a_1(g_{H_2O})c_{DL}}{1 + b(g_{H_2O})c_{DL}} + a_2(g_{H_2O})c_{DL} \tag{4-2}$$

where: c_{DL} is the concentration of the sample in the mobile phase, q_{DL} is the concentration in the solid phase at equilibrium with c_{DL}. Further, g_{H_2O} is the volume fraction of water in the mobile phase. a corresponds to retention of the solute on site 1 or 2 and b corresponds to the equilibrium constant for site 1.

For a multi-component mobile phase (here ethanol-water) the isotherm coefficients can be considered as apparent factors lumping the contributions of all constituents of the mobile phase to the adsorption equilibrium. These coefficients are functions of the mobile phase composition, in our case expressed as a function of the water content g_{H2O}.

After accomplishing the frontal analysis experiments, the retention time of small pulses of the sample were measured again in a second set of experiments for various mobile phase compositions. Due to the adsorbent deactivation, mentioned above, some differences in retention have been found for the pulses recorded before and after frontal analysis (see also Figure A.10 in Appendix A 4). Therefore, finally for evaluation of the isotherm coefficients a peak fitting method (e.g. James *et al*. [78]) evaluating the shapes chromatograms registered before frontal analysis experiments was employed. For peak fitting overloaded chromatograms registered at different water contents were selected, for which solvent and sample were well separated at the column outlet, i.e., interactions between sample and solvent could be neglected. The overloaded band profiles exhibited strong peak tailing (see e.g., Fig. 2,4) characteristic for heterogeneous adsorption mechanism. Such a peak shape was not reproduced correctly by the use of the Langmuir model, while the three parameter bi-Langmuir model (Eq. (4-2) was found to be sufficiently accurate.

The isotherm coefficients of Eq. (4-2) were determined by the use of a standard optimization tool (Levenberg-Marquardt optimization routine [137]), for each volume fraction of water in the mobile phase. The following empirical extension of the Snyder-Soczewinski equation functions were fitted to the obtained isotherm parameters of threonine.

$$a_1 = p_{a1} g_{H2O}^{-m_{a1}} + r_{a1}$$

$$a_2 = p_{a2} g_{H2O}^{-m_{a2}} + r_{a2} \tag{4-3}$$

$$b = p_b g_{H2O}^{-m_b} + r_b$$

The coefficients of these functions are shown in Table 4.3 and the resulting isotherms are depicted in Figure 4.4.

Table 4.3: Coefficients of Eq. (4-3) correlating the isotherm parameters of threonine (Eq. (4-2)) with the water content in the solution

isotherm parameter Eq. (4-2)	p	m	r
a_1, [-]	1.302	1.278	-1.202
b [l/g]	0.101	1.482	-0.092
a_2, [-]	0.359	1.702	-0.339
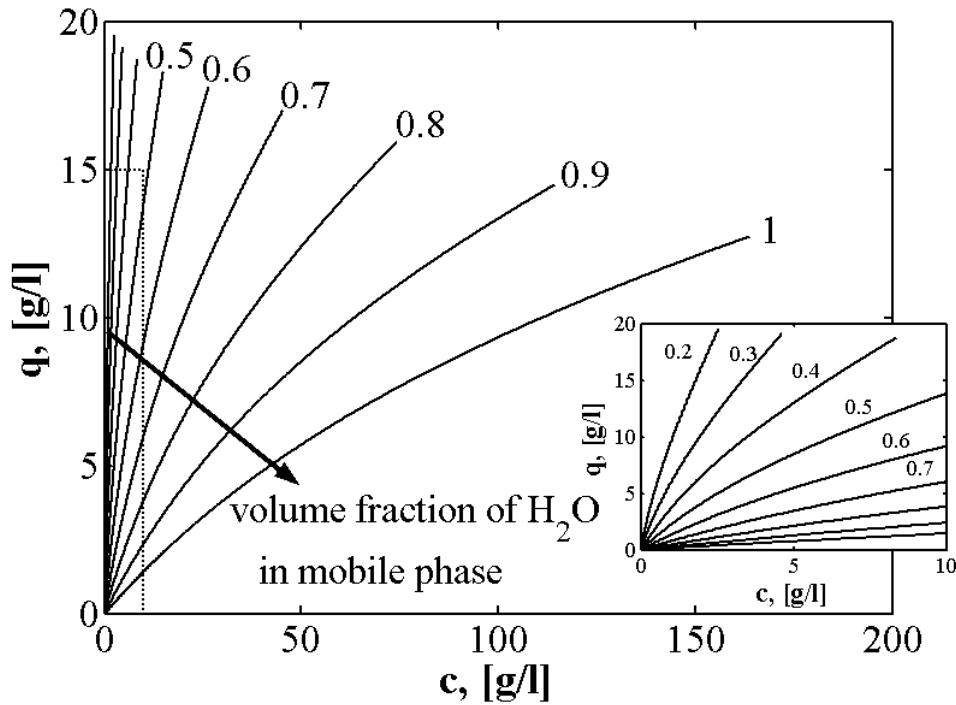
Figure 4.4: Isotherms of threonine at 20°C as calculated (Eqs. (4-2) and (4-3)) based on the results of the peak fitting method. Parameters as listed in Table 4.3. Isotherms are extrapolated up to the specific solubility limits in the mobile phase.

4.2.4. Column model

The well-known equilibrium dispersive model, Eq. (2-19), already used for the peak fitting method has been used to simulate a larger amount of elution profiles of the solute and the strong solvent water. The required apparent dispersion coefficients of the strong solvent water and the solute threonine were estimated from the plate numbers and Eq. (2-20). The number of theoretical plates has been determined experimentally and was 250 for water and 90 for threonine. This model coupled with adequate initial and boundary conditions, Eq. (2-21), was discretized by the use of the method of orthogonal collocation on fixed elements and solved with the VODE procedure (procedure available in http://www.netlib.org), which automatically chooses

the time increment in order to guarantee the required accuracy of the solution. The number of collocations points was high enough to assure numerical convergence of the solution. Details of the discretization method of orthogonal collocation used in this work can be found elsewhere [90, 91].

4.3.   Discussion

The band profiles of threonine as well as the injection solvent water were calculated (numerical solution of Eqs. (4-2)-(4)) and are depicted for selected examples in Figure 4.5 and Figure 4.6.

Directly after injection the front part of DL-threonine travels with a velocity corresponding to the retention behavior of DL-threonine in water. If the sample volume is large enough, that non-retained water and DL-threonine do not separate, then some amount of DL-threonine elutes together with water (see Figure 4.6). The rear part of the sample separates from the injection solvent (as it is the case also for small injection volumes, Figure 4.5) and travels then with a lower velocity corresponding to the adsorption isotherm valid for the mobile phase composition. These different traveling velocities cause the observed band splitting (see Figure 4.3 and Figure 4.6).

The agreement between the calculated and the experimental elution profiles is satisfactory, considering that the isotherm parameters reflect just a 'snapshot' of the mentioned complex transient adsorption behavior (due to the aforementioned temporal degradation of the stationary phase). The agreement for $100 \, \mu l$ injections (Figure 4.5) is better than the agreement for the larger $2000 \, \mu l$ injection volumes (Figure 4.6), because the $100 \, \mu l$ injections were used the estimation of the isotherm parameters for the peak fitting method. Apparently, the mathematical strategy, applied already for prediction of gradient elution [2, 6] is capable to account for the band splitting observed for large injection volumes. In our model precipitation was not taken into account, contrary to Jandera and Guiochon [80], who used a similar model. These authors reported qualitative agreement of the model predictions with their experimentally determined elution profiles, once the model also accounts for precipitation (for details see [80]). The incorporation of this additional effect was not necessary in our case, where already band profiles predicted with the fitted isotherm data and without a limitation of a maximal fluid phase concentration showed qualitative similar shapes like the experimental elution profiles.

Figure 4.5: Experimental (symbols) and simulated (solid line) elution profile of threonine at the column outlet for 100 *μl* injections. Solubility of threonine (dashed line) calculated with Eq. (4-1) corresponding to the simulated elution profile of water (dotted line, right axis).
a) at *y*$_{H2O}$=0.4 vol.-fr. in the mobile phase
b) at *y*$_{H2O}$=0.1 vol.-fr. in the mobile phase

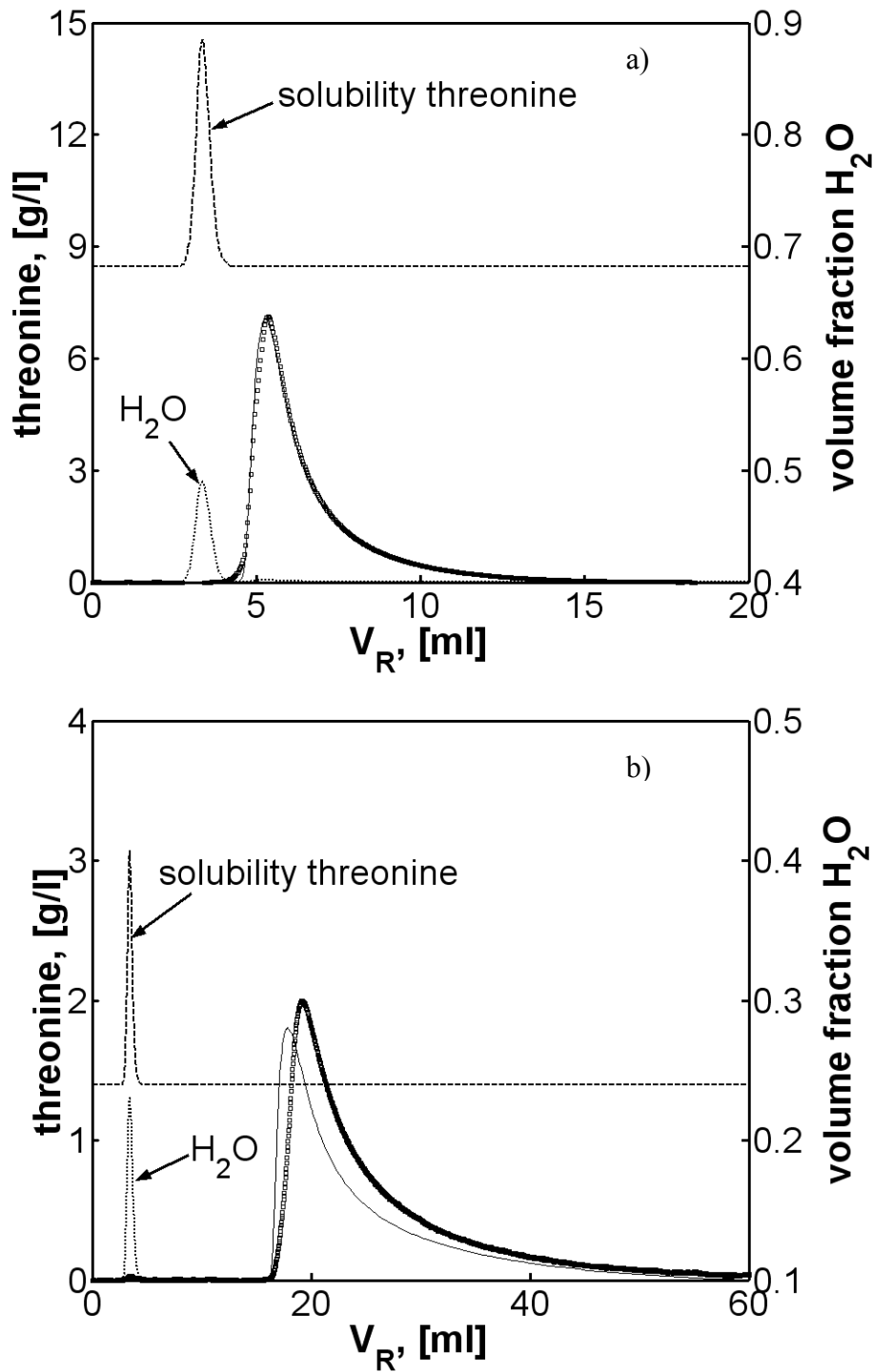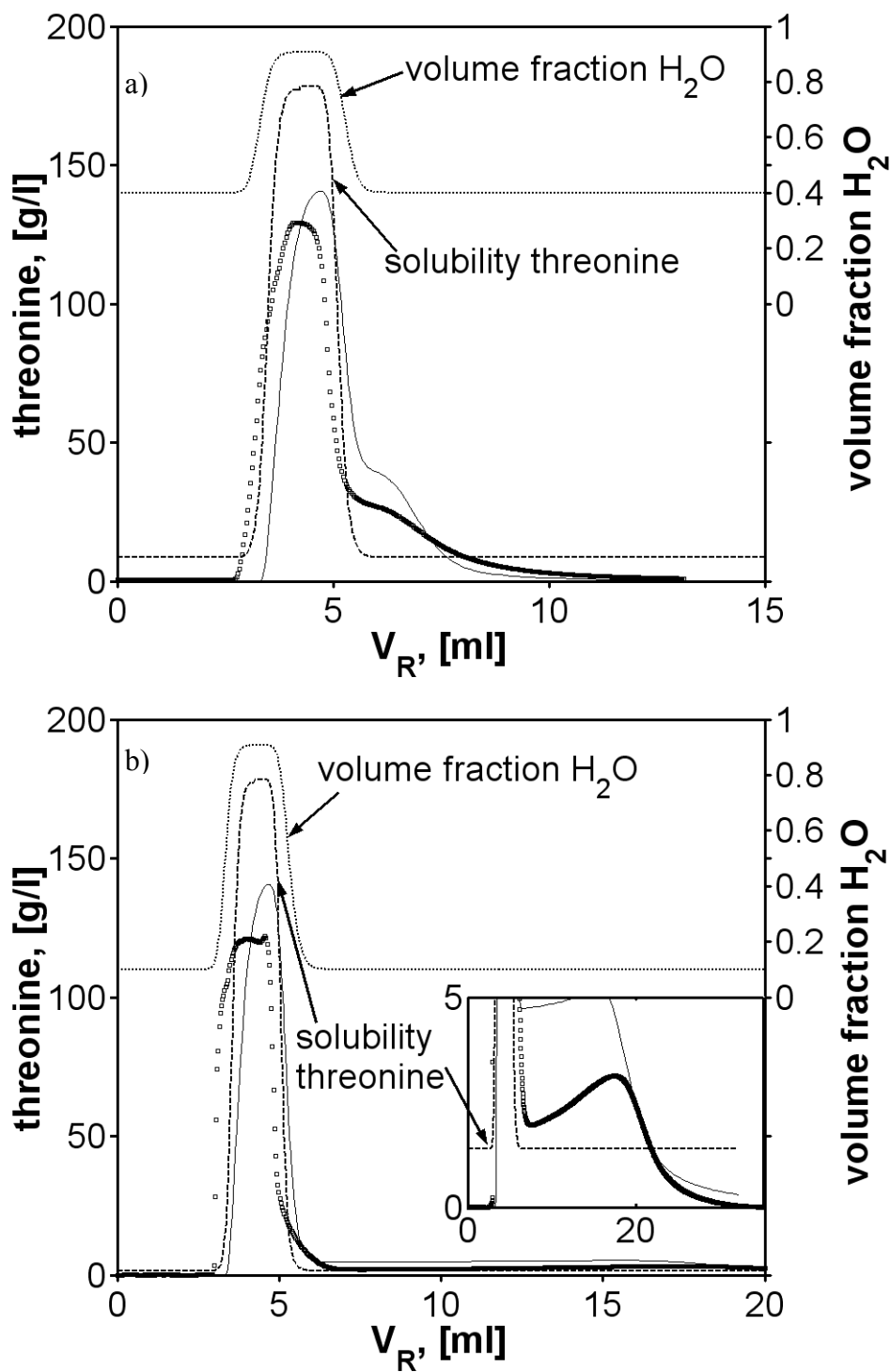**Figure 4.6: Experimental (symbols) and simulated (solid line) elution profile of threonine at the column outlet for 2000 *μl* injections. Solubility of threonine (dashed line) calculated with Eq. (4-1) corresponding to the simulated elution profile of water (dotted line, right axis).**
a) at y_{H2O}=0.4 vol.-fr. of water in the mobile phase
b) at y_{H2O}=0.1 vol.-fr. of water in the mobile phase

Figure 4.5 and Figure 4.6 show, besides a comparison of the experimental and the simulated elution profiles of threonine, also the water content simulated at the column outlet and the corresponding solubility of threonine (calculated with Eq. (4-1)). The solubility limit is not exceeded at the column outlet only for the 100 μl injection with a mobile phase composition g_{H2O}=0.4 (Figure 4.5a). However, the concentrations of DL-threonine exceeded to a large extent the solubility of DL-threonine for all other experiments (Figure 4.5b and Figure 4.6).

Figure 4.7 depicts an example of concentration profiles calculated within the column and the local solubility (related to the local water concentration) for two different times after injection. The development of the band splitting is clearly visible, as well as the spreading of the sample over almost the entire length of the column. Concentrations of threonine above the local solubility limit indicate the danger of precipitation in the column (Figure 4.7) and at the column outlet (Figure 4.5b and Figure 4.6a, b). Even though we observed no blocking of the column, threonine precipitated during one experiment (y_{H2O}=0.1, V_{inj}=2000 μl) in the tubing after the detector (which actually caused a damage of the detector cell). A reason could be, that even if crystals form in the column due to local super saturation (as it seemed to be the case in [6, 9]), these would be too small to result in local reduction of permeability of the column. On the other hand, the cross sectional area of the tubing is much smaller than that of the column. Precipitation in the tubing will therefore more likely result in blocking of the flow path.

In order to predict crystallisation phenomena properly, one needs to determine in detail kinetics of nucleation, growth and dissolution in presence of the heterogeneous surface provided by the stationary phase. Macro-kinetic isothermal growth/dissolution experiments in the presence of stationary phase may be possible, but the determination of heterogeneous nucleation rates remains a challenging future task, since the nuclei will contain just a few molecules [120]. Although different theories exist to predict heterogeneous nucleation rates [120, 126, 157], the author did not feel confident enough to apply these methods here without experimental proof.
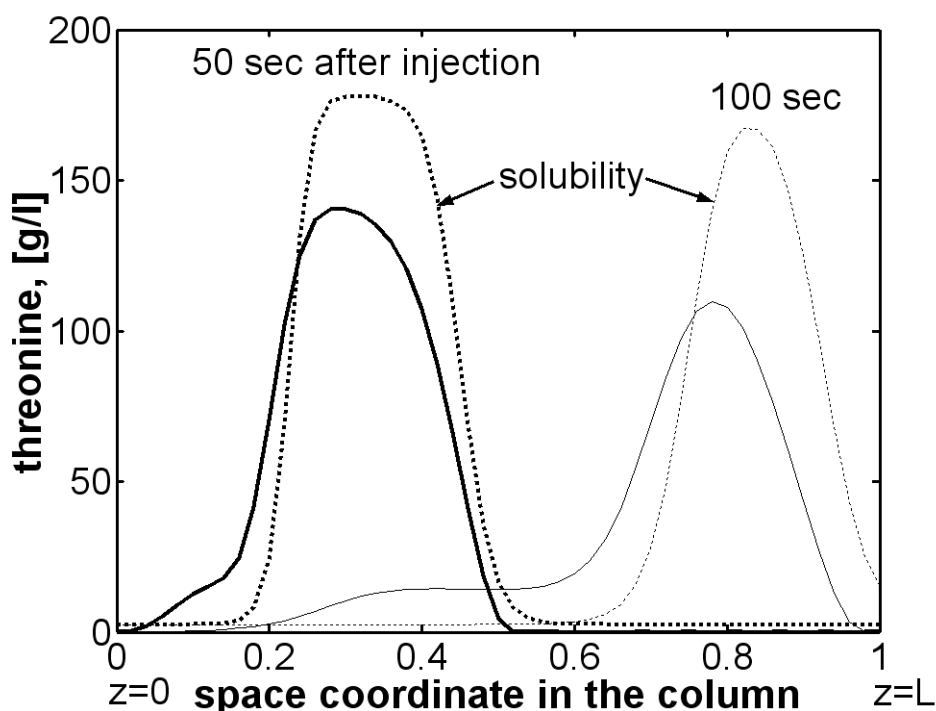
Figure 4.7: Simulated concentration (solid lines) and solubility (dotted lines) distribution of threonine in the column 50 sec (thick lines) and 100 sec (thin lines) after injection (g_{H2O}=0.2 and V_{inj}=1000 μl).

The 1000 and 2000 μl injections represent rather unrealistic large sample volumes for such a small column. Note, that by applying water as a feed solvent rather than the mobile phase, the amount injected was increased by factors of about 17, 31, 57 and 95 compared to the amount applicable in the mobile phase (using the same injection volume). This states the potential of applying a different solvent for the injection. Of course some other aspects have to be accounted for. The injection solvent must separate quickly from the sample, such that band splitting is suppressed and to exploit better the separation properties of the mobile phase. For "safety" reasons the concentration of band profiles at the column outlet should exceed the solubility limits only slightly.

4.4.   Summary

The evolution of significantly overloaded elution profiles of threonine, injected in water on a NH$_2$-column at a much higher concentration than the solubility limit in the mobile phase, has been illustrated for mobile phase compositions containing 0.1-0.4 vol.-fr. of water. Significant band splitting was observed for larger sample amounts. A simplified mathematical model as it is often used to predict gradient elu-

tion was applied. Measurements of the adsorption equilibria and solubility measurements for mobile phases containing varying concentration of the feed solvent have been performed. The resulting adsorption data have been used for correlating the isotherm coefficients of the equilibrium function of the sample with the local concentration of the strong solvent within the column. The solubility measurements have been exploited for calculation of the local solubility limits related to the corresponding local mobile phase compositions. These relationships have been included as model parameters into the model of the column dynamics, which allowed calculating concentration profiles for the sample as well as for the strong solvent water. The model qualitatively reproduced the change of peak shapes as an effect of the differences in the adsorption of the sample in the feed solvent and in the solution.

This experimental study exemplifies the potential of gradient injection as a method to overcome solubility limitations in the mobile phase. Given the injection solvent travels ahead of the solutes to be separated, an on-column dilution of the solutes will happen due to the adsorption equilibria. This on-column dilution already decreases the risk of undesired crystallization within the column, which would diminish separation of the solutes to be separated. Secondly, comparison of the internal concentration and solubility profiles have shown, that supersaturation of the solutes within the column will be spread over the column length. This decreases further the danger of blocking the flow path within the column, even if crystallization would happen, since the forming crystals would be simply too small.

5. Effect of Gradient Injection on Separation – 2nd Case Study

The separation of compounds possessing low solubility in the mobile phase could be improved by applying stronger solvents for dissolving the feed. In this chapter, we discuss quantitatively the effect of gradient injection on the separation of a binary mixture. That is the injection of the solutes to be separated in a different solvent than used for the elution. We will compare on an experimental example the performance of the gradient injection with the performance of the isocratic injection. Special attention will be turned toward to the maximal applicable injection concentration of the isocratic injection based on the corresponding solubility in the mobile phase considered. The results of this work were published in detail in [42].

As a sample system, we considered the separation of the enantiomers of threonine on a Chirobiotic-T column in ethanol-water mixtures, where water and ethanol represent the strong and the weak solvents, respectively. For this solvent-solute system it was already shown in the previous chapter and in [41], that crystallisation in the column is unlikely to happen.

We will present a methodology allowing to specify optimal separation conditions with a low amount of experimental effort. In particular, we will determine the adsorption isotherms of the solutes as function of the modifier concentration by means of a peak fitting method [25, 78]. The adsorption isotherm of the modifier will be estimated applying a perturbation method [64, 160]. Using a suitable column model

we will find optimal conditions for the separation by a limited number of numerical simulations. Finally, the optimal conditions predicted for this case study are experimentally verified.

5.1. *Theoretical Methods Applied*

Here we list the models and assumptions used in this chapter. We apply only standard methods and numerical tools that were derived in detail elsewhere (see section 2.3 as an introduction). It is attempted to yield a flexible mathematical description of the processes, suitable for process prediction and optimization. Although these models capture the main features of the experimental observation and the physical phenomena, they do not necessarily reflect completely the real chemical-physical interactions.

5.1.1.   Process model

The modelling of elution chromatography, where the solvent composition is changing during the process is the main objective in modelling gradient elution. Concepts and models can be found e.g. in [26, 52, 166]. Hereby, reliable models need to account for the elution of both the mobile phase constituents and the solutes. The lumped kinetic model Eqs. (2-19), (2-24) and the numerical solution as proposed in [91] is used here.

The initial and boundary conditions for a mixture of two enantiomers (L and D) and aqueous injection solutions and mobile phases are:

$$
\begin{aligned}
t < 0; z = 0, L: \quad & c_{L,D} = 0; \quad & x_{H2O} = x^0_{H2O} \\
0 < t < t_{inj}; z = 0: \quad & c_{L,D} = c^{inj}_{L,D}; \quad & x_{H2O} = x^{inj}_{H2O} \\
t_{inj} < t; z = 0: \quad & c_{L,D} = 0; \quad & x_{H2O} = x^0_{H2O}
\end{aligned}
\tag{5-1}
$$

with x^0_{H2O} and x^{inj}_{H2O} being the molar fraction of the strong solvent water in the mobile phase and the injection solvent, respectively. Since the solvent constituents, here water ($H2O$) and ethanol ($EtOH$) are present at large concentrations it is expedient to express Eq. (2-19) for these two components in terms of molar fractions x_i and excess loadings Γ_i (Eq. (2-26), e.g. [153]). The differential mass balance, Eq. (2-19), then becomes:

$$\frac{\partial}{\partial t}\left(\frac{\rho}{M}x_i\right) + \frac{1-\varepsilon}{\varepsilon}\frac{\partial \Gamma_i}{\partial t} + u\frac{\partial}{\partial z}\left(\frac{\rho}{M}x_i\right) = D_{app,i}\frac{\partial^2}{\partial z^2}\left(\frac{\rho}{M}x_i\right)$$

(5-2)

$$\text{for } i = EtOH, H2O$$

In the above $M = M(x)$ is the molecular weight of the mobile phase and $\rho = \rho(x)$ is the density of the mobile phase. For a binary mixture holds:

$$x_{EtOH} = 1 - x_{H2O}$$

(5-3)

Eqs. (2-19) and (5-2) alone can be solved efficiently with the backward-in-space–forward-in-time finite difference scheme, Eq. (2-22) initially applied by Rouchon *et al.* [144]. However, the Rouchon algorithm fails for gradient elution, where the retention behavior varies throughout the elution process [5]. Therefore, the transport term of Eq. (2-24) was implemented mainly for numerical reasons, since the combined application of Eq. (2-24) with Eq. (2-19) stabilizes finite difference schemes [3, 5]. In the calculations discussed below the transport coefficient k was set to a value so large that local equilibrium was established and Eq. (2-24) did not contribute to the band broadening. Details on the numerical the solution of the equations are given in [3, 5]. This process model was coupled with the corresponding isotherm functions of the mobile phase constituents $(\Gamma_i^*(x))$ and the solutes $(q_i^*(c,x))^7$.

5.1.2. Adsorption Isotherm of the Solvent

For the example discussed here, the mobile phases consist of ethanol-water mixtures while pure water - the strong solvent - is used as the injection solvent for the gradient injections. Excess isotherms instead of loading isotherms should be used if large concentration ranges are covered [64], as it is the case for the mobile phase constituents considered. Here the definition of the excess according to Everett [28] was used (with reference to the volume rather than the surface of the solid phase). The individual loadings q_i in Eqs. (2-19) and (2-24) can be related to excess concentrations Γ_i,

---

[7] The equilibrium loading and the actual loading have to be distinguished, due to usage of the mass transfer term Eq. (2-24). Thus, the equilibrium loading will be denoted by * in this chapter.

Eq. (2-26), as shown in detail by Oscik [129]. For the binary mixture considered Eq. (2-26) becomes:

$$\Gamma_i^* = q_i^* - (q_{EtOH}^* + q_{H2O}^*)x_i \qquad i = EtOH, H2O \qquad \text{(5-4)}$$

A displacement-adsorption mechanism incorporating activity coefficients γ_i to take real phase behavior into account (e.g. [129, 134]) was used in this work to describe the equilibrium loadings of the mobile phase components:

$$q_i^* = q_i^\infty \frac{K_{d,i}\gamma_i x_i}{\gamma_j \gamma_i^s (1-x_i) + K_{d,i}\gamma_i \gamma_j^s x_i} \qquad \text{(5-5)}$$

with: $\quad i, j = EtOH, H2O \qquad and \qquad K_{d,i} = 1/K_{d,j}$

For the equation above the following simplifying assumptions are used below:

- $q_{H2O}^\infty = q_{EtOH}^\infty = q^\infty$,[8]

- surface activity coefficients are unity ($\gamma_i^S = 1$)

These assumptions provide for Eq. (5-5) the following expression of the equilibrium loadings:

$$q_i^* = q^\infty \frac{K_{d,i}\gamma_i x_i}{\gamma_j(1-x_i) + K_{d,i}\gamma_i x_i} \qquad \text{(5-6)}$$

with $i, j = EtOH, H2O$ *and* $K_{d,i} = 1/K_{d,j}$

5.1.3.   Adsorption Isotherm of the Solutes

Adsorption isotherms of the solutes can be described in a simplified manner taking in the adsorption isotherm model only the competition between the solutes into account [52]. The parameters of the adsorption isotherm are functions of the mobile phase composition. Here, the Langmuir equation, Eq. (2-10), was used to model the competitive adsorption isotherms of the two solutes considered (D- and L-threonine):

---

[8] Although physically improbable, this assumption was found in the course of the work to be sufficient for the description of the experimental observations. See discussion in section 5.3.2.

$$q_i^* = q_S \frac{b_i(x_{H2O})c_i}{1 + \sum_{j=1}^{2} b_j(x_{H2O})c_j} = \frac{a_i(x_{H2O})c_i}{1 + \sum_{j=1}^{2} \frac{a_j(x_{H2O})}{q_S} c_j}$$

(5-7)

$$i = L, D$$

In the above b_i, q_S and $a_i = q_S b_i$ are the equilibrium constants, the saturation capacity and the Henry coefficients, respectively. It is assumed in Eq. (5-7) that the mobile phase composition only influences the equilibrium constants and does not influence the saturation capacity. The equilibrium constants (b_i) are difficult to measure, contrary to the Henry coefficients (a_i), which can be directly obtained from simple pulse experiments with the chromatographic column. Although the model presented is quite simple considering the manifold of interactions occurring on a chiral stationary phase, it captures essential features of the distribution equilibria. We will introduce observed dependencies of the Henry coefficients on the mobile phase composition in section 5.3.3 on page 115.

5.2. Chemicals and Experimental Procedures

5.2.1. Chemicals and Apparatus

A Chirobiotic-T stationary phase (Astec, USA) with a mean particle diameter of 16 μm was used. It was packed into 15x1 cm columns by Muder&Wochele (VDS-Optilab, Berlin, Germany). The mobile phase consisted of HPLC-grade ethanol (Merck, Darmstadt, Germany) and deionized water further purified with a Milli-Q-system (Millipore, Molsheim, France). The binary mobile phases were prepared volumetrically and the mixture compositions were checked with density measurements. D- (*2R,3S*), L- (*2S,3R*) and DL-threonine (Sigma-Aldrich, Steinheim, Germany) were used as the solutes and were of reagent grade (>98%).

Chromatograms were recorded at 20°C on analytical and preparative Dionex HPLC systems (Dionex, Idstein, Germany). These systems consisted of quaternary low-pressure gradient and binary high-pressure gradient pumps, an autosampler (up to 2 ml injections) and a column oven. Detection of threonine was done with an UV-spectrometer at appropriate wavelengths (205, 220, 230 and 240 *nm*, depending on the outlet concentrations). The linearity of the detector signals was verified by plot-

ting the peak areas vs. the amounts injected. A third HPLC system was utilized for additional measurements of the excess isotherms of the mobile phase constituents. Here, a LaChrom system (Merck, Darmstadt, Germany) with a refractive index detector was used.

5.2.2.   Experimental Procedures

Chromatograms of DL-threonine were recorded at eight different mobile phase compositions. The water content in the mobile phase was varied between g_{H2O}=0.2-1 v/v (corresponding molar fraction $x_{H2O} = $ 44-100 $mol\%$). For each mobile phase composition, a solution was prepared with a concentration close to the corresponding solubility limit in the mobile phase. The injection concentrations were kept at a value of about 90 % of the measured/interpolated solubility in the mobile phase. The solubility data were taken from [151]. Injections of 1 up to 240 μl were performed. Details of the experimental conditions are given in Table 5.1. Of the experiments carried out, those belonging to the largest injections in each mobile phase composition were selected for the peak fitting.

Excess loadings of the two mobile phase constituents were determined by means of a perturbation method [13]. The equilibrated column was perturbed at various mobile phase compositions by 20 µl injections of pure water or pure ethanol.

Table 5.1: Experimental conditions (mobile phase compositions g_{H2O} resp. x_{H2O}, injection concentrations $c_D^{inj} = c_L^{inj} = 0.5\,c_{total}^{inj}$, injection volumes V_{inj} and wave lengths used for detection) of the data used for peak fitting and the corresponding solubility of the racemate of DL-threonine $c_{S,DL}$ in the respective solvent composition (recalculated from [151]).

g_{H2O}, v/v	x_{H2O}, mol%	c_{total}^{inj}, g/l	$c_{S,DL}$, g/l	V_{inj}, µl	wavelength, nm
1.0	100.0	150	165.7	80	230
0.8	92.8	70	78.2	240	230
0.7	88.3	45		200	230
0.6	82.9	28	29.3	240	230
0.5	76.4	16		200	220
0.4	68.3	9	10.3	200	220
0.3	58.1	4		200	220
0.2	44.7	2	2.4	200	215

5.3. Results and Discussion

5.3.1. Analysis of the Experimental Data

In order to optimize conditions for the separation of the two threonine enantiomers the mathematical model described above was used. This mathematical model consists of a process model (Eqs. (2-19) resp. (5-2) and (2-24)) in combination with descriptions of the adsorption isotherms of the components present in the system, i.e. the mobile phase constituents (Eqs. (5-4) and (5-6)) and the solutes to be separated (Eq. (5-7)). At first, with the a peak fitting method (or inverse method e.g. [25, 78]) was applied to estimate the adsorption isotherms of the enantiomers for different mobile phase compositions.

5.3.2. Adsorption Isotherm of the Solvent

For the mean retention volume of a small perturbation holds for small deviations from the equilibrium state x^*_{H2O} (quasi constant density and molecular weight of the mobile phase):

$$V^*_R\bigg|_{x^*_{H2O}} = V_0\left(1 + F'\frac{M}{\rho}\bigg|_{x^*_{H2O}}\frac{d\Gamma^*_{H2O}}{dx_{H2O}}\bigg|_{x^*_{H2O}}\right) \tag{5-8}$$

An integration of Eq. (5-8) yields the excess equilibrium loading of water (using for the binary mixture considered $\Gamma_{H2O} = -\Gamma_{EtOH}$):

$$\Gamma^*_{H2O}(x^*_{H2O}) = \int_0^{x^*_{H2O}}\left(\frac{V^*_R(x_{H2O})}{V_0} - 1\right)\frac{\varepsilon}{1-\varepsilon}\frac{\rho(x_{H2O})}{M(x_{H2O})}dx_{H2O}$$
$$\approx \sum_{n=1}^{ndata}\left(\frac{V^*_{R,n}}{V_0} - 1\right)\frac{\varepsilon}{1-\varepsilon}\frac{\rho_n}{M_n}\Delta x_{H2O,n} \tag{5-9}$$

Eq. (5-9) can be also used to calculate the total porosity of the column, since excess loadings are zero for pure components [145]. However, integration of Eq. (5-9) can be inaccurate due to the approximation of the integral by a sum and its sensitivity to small deviations of the retention volumes. In this work, we attempted to reproduce correctly the retention of the solutes, thus the parameters of the equilibrium excess

loading (Eq. (5-5)) were fitted directly to the retention volumes (Eq. (5-8)) using the following objective function.

$$OF = \min \left\langle \sum_{n=1}^{ndata} \left[V_{R,\exp,k}^* - V_{R,calc,k}^* (K_{d,H_2O}, q^\infty) \right]^2 \right\rangle \tag{5-10}$$

For the fitting the built-in "Microsoft Excel Solver" was applied. Initially, different saturation capacities were applied for ethanol and water. This fitting (results omitted here) did not result in significantly reduced error residuals (OF), compared to a fitting with the same saturation capacity for both ethanol and water ($q_{EtOH}^\infty = q_{H_2O}^\infty = q^\infty$). Although physically questionable, this simplification was found to be sufficient for the description of the experimental observations.

Table 5.2: Comparison of the experimentally determined and theoretically predicted retention volumes of small pulses of pure water (or pure ethanol) on a Chirobiotic T column in equilibrium with the mobile phase compositions depicted in the first column. The measured retention volumes were corrected by the dead volume of the connecting capillaries.

x_{H2O}, mol%	$V_{R,\exp}^*$, ml	$V_{R,calc}^*$, ml
100.0	10.58	9.83
99.7	10.03	9.78
99.4	9.82	9.73
99.1	9.68	9.68
98.7	9.56	9.64
98.4	9.46	9.60
97.7	9.35	9.52
96.7	9.23	9.41
92.8	9.09	9.12
88.3	8.88	8.91
82.9	8.51	8.76
*76.4	**8.25**	**8.64**
*68.3	**8.26**	**8.55**
*58.1	**8.43**	**8.50**
*44.7	**8.93**	**8.54**
*26.5	**9.47**	**8.90**
22.0	9.58	9.08
14.6	9.75	9.51
6.2	10.01	10.24
0.0	9.58	10.99

*mobile phase compositions given in bold are suitable for separation (see text)

To apply Eq. (5-5) the dependence of the liquid phase activity coefficients γ_i, the densities ρ and the molecular weights M on the mobile phase composition must be known. These values can be extracted from literature information and are listed in appendix A 5.

Table 5.2 shows the experimentally determined and the calculated retention volumes (Eq. (5-8) with the parameters given in Table 5.3). A reasonable separation of the solutes (D,L-threonine) is achieved for solvent compositions between $x_{H2O} = 26 - 76$ mol%. The agreement between predicted and determined retention times as results of mobile phase perturbations is quite good in that range and appears to be sufficient to carry out useful predictions of gradient elution. For a simplified description one could roughly set the adsorption of the mobile phase components to zero.

Table 5.3: Parameters determined with the experimental data given in Table 5.2.

ε	$K_{d,H2O}, \dfrac{mol_{H2O}}{mol_{MP}}$ (Eq. (5-6))	$q^{\infty}, \dfrac{mol}{ml}$ (Eq. (5-6))
0.758	1.328	0.0064

5.3.3. Adsorption isotherms of D- and L-threonine

Based on overloaded chromatograms of D- and L-threonine a peak fitting method was used to approximate isotherm parameters to model the elution of D- and L-threonine as a function of the mobile phase composition in the range $x_{H2O} = 44.7 - 100\,mol\%$. From analytical injections for a certain mobile phase compositions the initial slopes (Henry coefficients) of the isotherms can be obtained from the measured retention volumes using the well-known relation (rearranged Eq. (2-17)):

$$a_i = \left.\frac{dq_i}{dc_i}\right|_{c_i \to 0} = \frac{\varepsilon}{1-\varepsilon}\left(\frac{V_{R,i}^{*}}{V_0} - 1\right)$$

$$i = D, L$$

(5-11)

The experimentally determined apparent Henry coefficients of D,L-threonine in ethanol water mixtures are shown in Figure 5.1. The L-enantiomer is the less retained

component. Figure 5.2 depicts the solubility of the racemate ($c_{S,DL}$) [151] and the separation factor ($\alpha = a_D / a_L$) as a function of the solvent composition. The solubility is increasing with increasing amount of the strong solvent water from 2.4 g/l at $x_{H2O} = 44.7$ $mol\%$ to 165.7 g/l at $x_{H2O} = 100$ $mol\%$. The separation factor α decreases from 1.7 to 1.1 between $x_{H2O} = 44.7$ $mol\%$ and pure water ($x_{H2O} = 100$ $mol\%$). The retention (and a_i) decreases continuously with increasing water content between $x_{H2O} = 44.7\text{-}92.8$ $mol\%$ ($g_{H2O} = 0.2 - 0.8$ v/v). Afterwards a small increase of the retention is found in the direction to pure water. In this range of mobile phase compositions $x_{H2O} = 92.8\text{-}100$ $mol\%$, no separation is obtained. For the modelling of the retention as a function of the mobile phase composition, this small increase of the retention was neglected. The dependence of the isotherm parameters a_i was approximated using the following empirical function, which is an empirical extension of the Snyder-Soczewinski relation developed for normal phase chromatography (e.g. [79]).
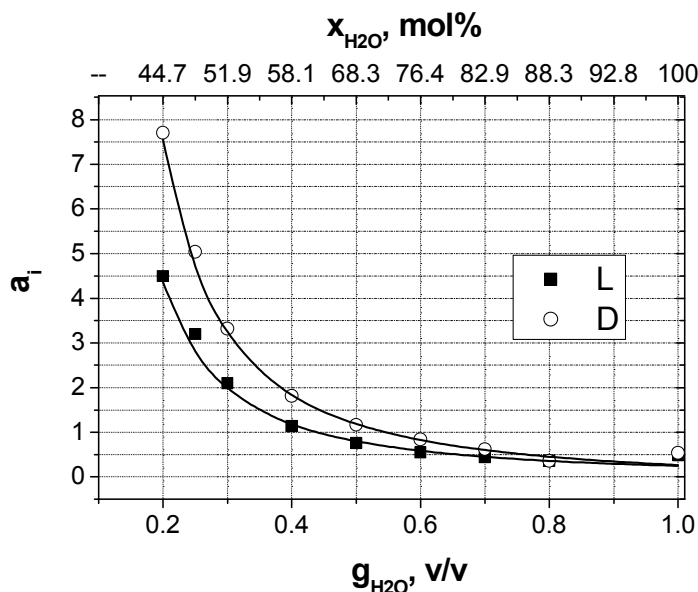

Figure 5.1: Henry coefficients (H_i) of D- and L-threonine isotherms on a Chirobiotic T column as a function of the water content in the mobile phase (in *mol%*, upper axis and as *v/v*, bottom axis). The symbols correspond to the initial slopes of the isotherms as obtained from experimental data. The lines are calculated with Eq. (5-12) and the parameters shown in Table 5.4.
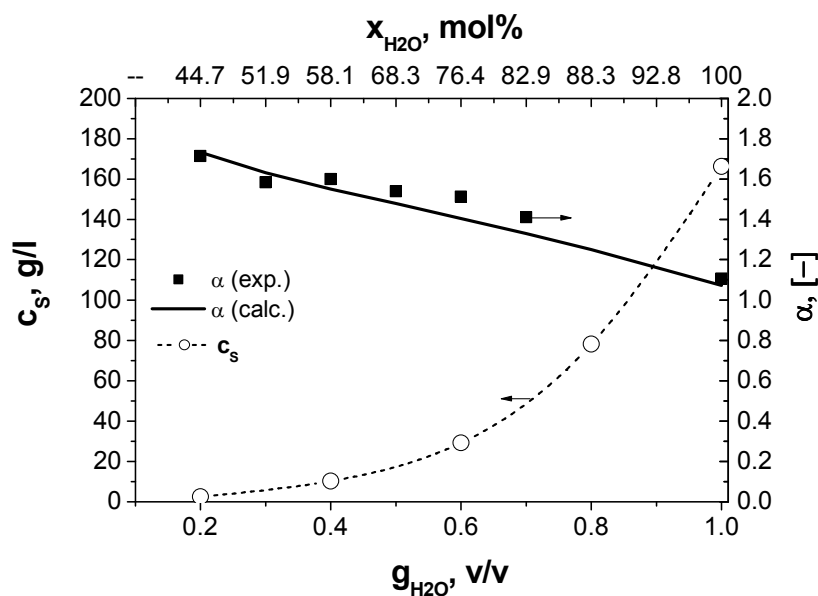
Figure 5.2: Solubility ($c_{S,DL}$, **left axis) and separation factor** (α, **right axis) of D,L-threonine as a function of the water content of the solvent. Solubility data (open circles, the dotted line is guide to the eye) were taken from [151]. Separation factors were calculated with the experimental Henry coefficients shown in Figure 5.1 (solid squares) and with the calculated Henry coefficients (solid line) using Eq. (5-12) and the parameters in Table 5.4.**

$$a_i = p_{1i} x_{H2O}^{p2i} + p_{3i} \qquad i = L, D \qquad \text{(5-12)}$$

Hereby, the classical logarithmic-linear dependence did not apply over the broad scale range of mobile phase compositions considered, as pointed out also in [64]. The mean plate numbers ($NTP = Lu/2/D_{app}$) were extracted from analytical injections and were found to vary between 1400-2100 (for $x_{H2O} = 100\text{-}44.7$ *mol%*) at a flow rate of 1 *ml/min*.

The seven parameters of Eq. (5-7) (q_s) and Eq. (5-12) (p_{1i}, p_{2i}, p_{3i}, $i = L, D$) were obtained by simultaneously fitting one chromatogram per mobile phase composition, corresponding to the largest injection of D- and L-threonine. The best-fit parameters of Eq. (5-12) to the experimentally and independently determined initial slopes of the isotherms (Figure 5.1) were used as initial values for a Nelder-Mead-simplex algorithm applied to minimize the objective function given by Eq. (5-13) below. All chromatograms were normalized with respect to the maximal peak heights, since, depending on the mobile phase composition the applied amount, re-

tention and dilution, thus, the outlet concentrations were very different. In particular, the same amount injected would yield much larger outlet concentrations for those mobile phase compositions with little retention compared to those mobile phase compositions, where the retention is much stronger. Any other normalization, such as amount injected would yield an over pronunciation of the mobile phases with little retention. Due to the normalization, all experimental data had similar importance for the parameter estimation. Also, small outlet concentrations which specify the initial slope of the isotherm contribute in this regard significantly to the parameter estimation.

$$OF = f(q_S, p_{1i}, p_{2i}, p_{3i}) = \min \left\langle \sum_{k=1}^{8} \sum_{n=1}^{n_{data}} \frac{(c_{exp,n}^k - c_{calc,n}^k)^2}{\max(c_{exp,n}^k)} \right\rangle \qquad (5\text{-}13)$$

$$i = D, L$$

In the equation above k is the index of the mobile phase composition and n_{data} denotes the number of data points in an experimental chromatogram. Further, c is the total concentration $(c_D + c_L)$ as obtained from the nonselective UV-detection. To avoid pronunciation of one experiment on the fitting, the same number of data points was used for each mobile phase composition. The simulated concentrations, typically not obtained at the exact same time as the experiment, were linearly approximated to the time of the experiment. The resulting parameters of the fitting are summarized in Table 5.4. The chromatograms in Figure 5.3 show simulated and experimentally determined elution profiles for the isocratic conditions given in Table 5.1. The agreement between simulated and experimentally determined chromatograms is satisfactory, considering the simplicity of the model applied. Apparently, the nonlinearity of the isotherm of the later eluting D-enantiomer is underestimated for small water contents by the simple Langmuir isotherm model. Improvements could be obtained by using more sophisticated column and isotherm models (accounting e.g. for surface heterogeneity). However, the general agreement is acceptable and a mathematical description of the elution of D- and L-threonine on a Chirobiotic-T column is possible in a broad range of mobile phase compositions.

Table 5.4: Parameters of Eqs. (5-7) and (5-12) as obtained from the peak fitting method by simultaneously fitting one chromatogram per mobile phase composition.

	L	D
P_{1i}, [-]	0.3796	0.5819
P_{2i}, [-]	-3.0031	-3.1618
P_{3i}, [-]	-0.0082	-0.1866
q_s, [g/l]	14.2	

$g_{H2O}=0.2v/v \equiv x_{H2O}=44.7mol\%; V_{inj}=0.2ml; c_L^{inj}=1g/l; c_D^{inj}=1g/l$

$g_{H2O}=0.3v/v \equiv x_{H2O}=58.1mol\%; V_{inj}=0.2ml; c_L^{inj}=2g/l; c_D^{inj}=2g/l$

$g_{H2O}=0.4v/v \equiv x_{H2O}=68.3mol\%; V_{inj}=0.2ml; c_L^{inj}=4.5g/l; c_D^{inj}=4.5g/l$

$g_{H2O}=0.5v/v \equiv x_{H2O}=76.4mol\%; V_{inj}=0.2ml; c_L^{inj}=8g/l; c_D^{inj}=8g/l$

$g_{H2O}=0.6v/v \equiv x_{H2O}=82.9mol\%; V_{inj}=0.24ml; c_L^{inj}=14g/l; c_D^{inj}=14g/l$

$g_{H2O}=0.7v/v \equiv x_{H2O}=88.3mol\%; V_{inj}=0.2ml; c_L^{inj}=22.5g/l; c_D^{inj}=22.5g/l$

$g_{H2O}=0.8v/v \equiv x_{H2O}=92.8mol\%; V_{inj}=0.24ml; c_L^{inj}=35g/l; c_D^{inj}=35g/l$

$g_{H2O}=1v/v \equiv x_{H2O}=100mol\%; V_{inj}=0.08ml; c_L^{inj}=75g/l; c_D^{inj}=75g/l$
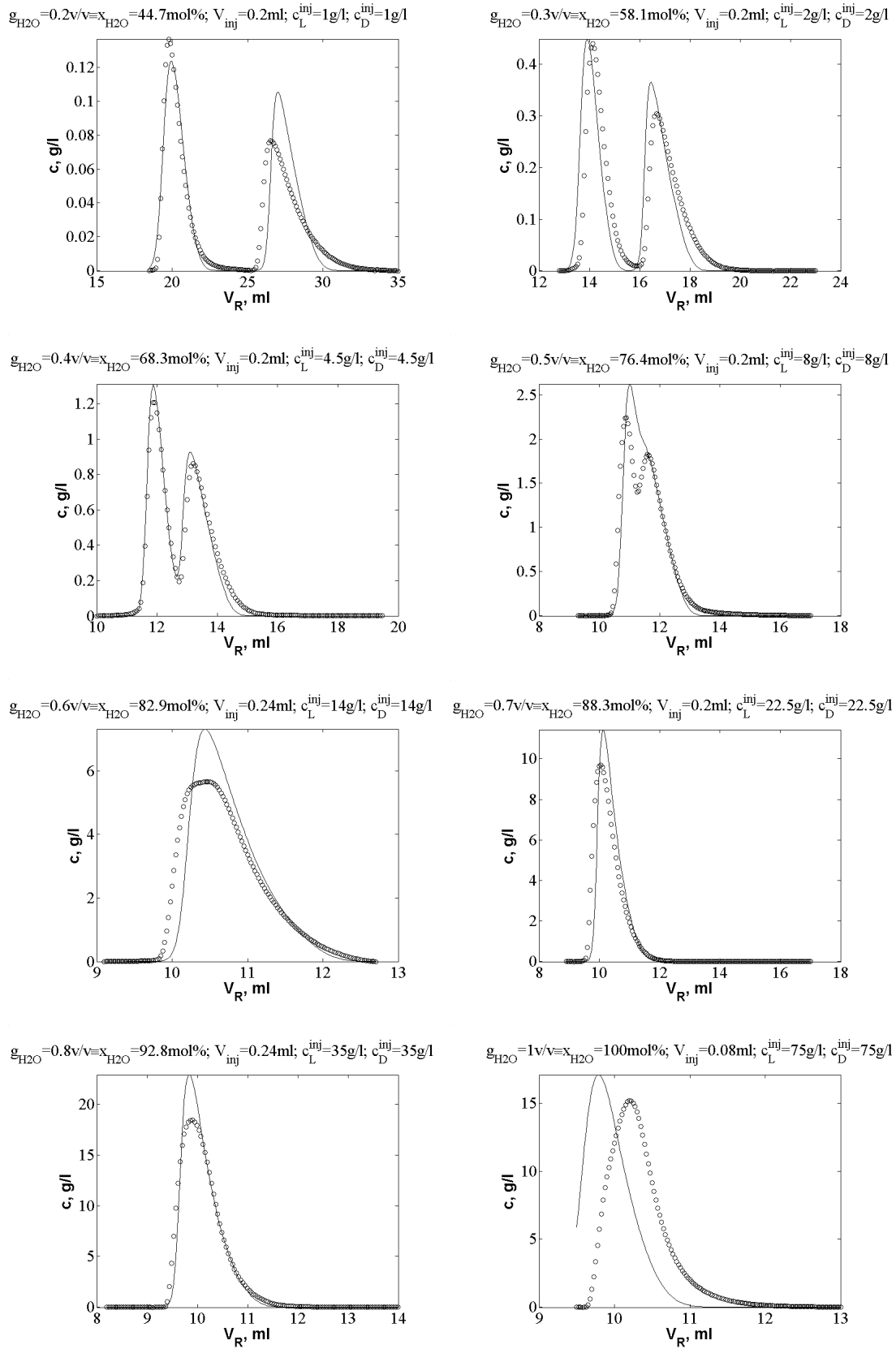
Figure 5.3: Comparison of experimentally determined and simulated chromatograms using Eqs. (2-19),(2-24), (2-25), (5-7), (5-12) and the parameters in Table 5.4. The experimental and simulation conditions are depicted above the chromatograms.

5.3.4. Reproducibility

An observation made during the experiments should be mentioned here. For the columns used, a change of the pressure drop was observed with lifetime. The investigation of the reason for this increase is beyond the scope of this work. It might be due to some fine particles traveling through the column and blocking gradually the outlet frit. Changing the flow direction decreased the pressure drop. However, this flow reversal affected negatively column efficiency.
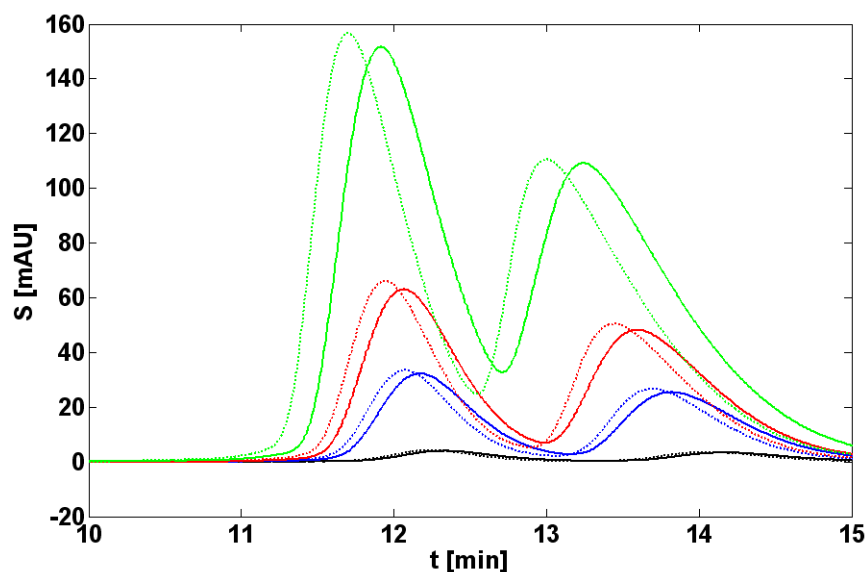
Figure 5.4: Experiments @ x_{H2O} =44.7 mol%: all dotted lines first experiments (05.08.2005); all solid lines repetition (02.09.2005); in between experiments were performed @ x_{H2O} = 68.4, 76.4, 82.9, 88.3, 100, 51.9, 44.7 mol%, consuming approx. 8 l of mobile phases. Injection conditions: 200; 80; 40; 5 µl; c_{inj}=9 g/l; flow rate 1 ml/min

Besides the increase of the pressure drop, also slight changes of the retention times were observed (see Figure 5.4), which cannot be described by the model applied. Note, that the quality of the separation remained relatively constant during the whole period. Bechtold *et al*. [10] made similar observations for a Chirobiotic TAG stationary phase. Such changes in the retention times can be counterbalanced in preparative elution chromatography by detector-signal controlled fractionations of the peaks.

5.3.5. Estimation of Optimal Conditions

Extended Systematic calculations were performed to discuss the effect of injecting a sample in a different solvent. For the sake of clarity, the influence of flow rate and

column length was not considered in this study. There is enough insight regarding these effects (e.g. [64]). We rather concentrated on a given configuration, i.e. a constant column length and a constant flow rate. The flow rate through columns of the size used for the experiments is set to 5 ml/min, resulting in column efficiencies between $NTP = 600 - 900$, depending on the mobile phase composition.

Below *isocratic injection* denotes the case were the composition of the injection solvent is equal to the one used for the mobile phase, while *gradient injection* shall denote the case, where the injection is performed in the strong solvent, i.e. in water. Values close to the solubility limit of threonine in the injection solvent were used for the injection concentrations (see Table 5.1).
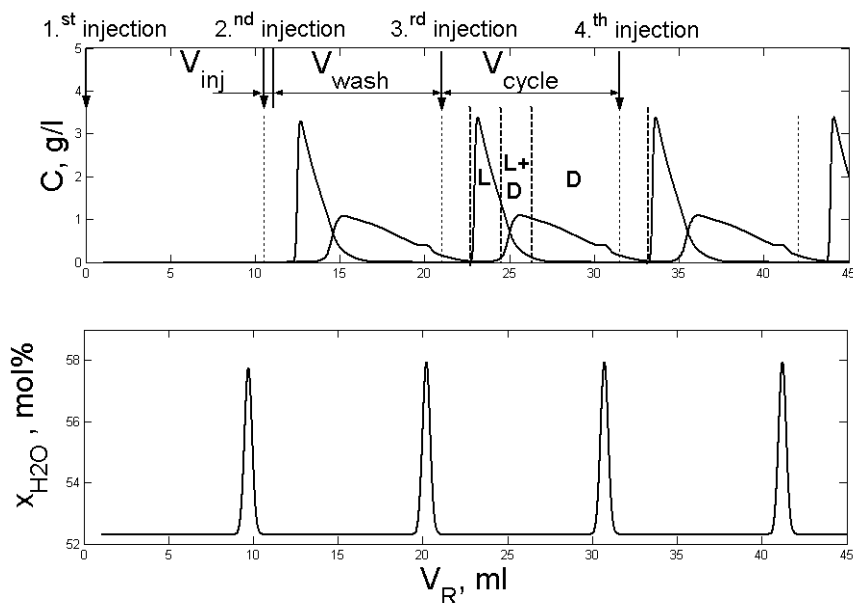
Figure 5.5: Determination of cut times taking into account interactions between consecutive injections. The transient of the predicted solvent composition is shown in the bottom chromatogram. Injections were performed every 10.5 *ml* of elution volume with $V_{inj} = 65$ *µl* and $c_{inj} = 150$ *g/l*. Adsorption isotherm parameters as in Table 5.3 and Table 5.4.

In order to evaluate the performance of the separation always three consecutive injections were simulated. An example of a gradient injection is given in Figure 5.5. The chromatogram in the middle was used to determine the optimal cut times/volumes for a specific purity, based on an algorithm presented by Shan and Seidel-Morgenstern [163]. This algorithm finds the optimal cut points to collect the maximal amount of a substance from a N_c-component mixture for a given purity. Interactions between consecutive injections are regarded for. The upper diagram of

Figure 5.5 depicts the concentration profile of the two solutes D- and L-threonine. The solvent composition is shown in the bottom chromatogram. The pulse of the strong solvent water from the second injection elutes together with the retained solutes of the first injection, causing the additional bump in the concentration profile of the second eluting component (D-threonine). The cycle volume (V_{cycle}) is the important adjustable parameter of the simulation and the free parameter for process optimization. A cycle consists of an injection step (V_{inj}), during which the solutes to be separated are introduced, and a wash step (V_{wash}), lasting until the next injection is performed. Therefore, injection volumes and wash volumes need to be determined for a process optimization. The cycle time is:

$$t_{cycle} = \frac{(V_{inj} + V_{wash})}{Q} \qquad \textbf{(5-14)}$$

Besides the injection and the wash volume also the two relevant mobile phase compositions (x^{0}_{H2O} and x^{inj}_{H2O}) of the corresponding steps are parameters to be optimized. The mobile phase composition of the injection is either equal to the mobile phase composition of the wash step (isocratic injection, $x^{inj}_{H2O} = x^{0}_{H2O}$), or the injection solvent consists completely of the strong solvent water (gradient injection, $x^{inj}_{H2O} = 1$). The injection concentration of the racemic 1:1 mixture of DL-threonine corresponds to a value close to the solubility limit of the respective injection solvent composition (see Table 5.1). A large number of forward simulations at different injection volumes were performed systematically for each mobile phase composition, to estimate optimal operating conditions (injection volume, cycle volume) for a purity of 99% of both individual enantiomers.

Of course, an optimization routine could have been used rather than systematic forward calculations to determine for a given objective function the optimal process conditions. These optimized conditions would have been somewhat anonymous and hard to interpret. Another advantage of systematic forward calculation is the independence of a given objective function, since any objective function can be extracted from the results obtained.

5.3.6.   Objective Functions

Several objective functions are possible to evaluate the separation process, depending on the goal of the separation. Each optimization goal can be formulated with respect to one target component (indicated by the subscript i) or with respect to both enantiomers (no index). An often-used objective function evaluates the productivity:

$$PR_i = \frac{m_{i,col}}{t_{cycle}} \qquad i = L,D \qquad \text{or}$$

$$PR = \frac{m_{L,col^-} + m_{D,col^-}}{t_{cycle}}$$

$$(5\text{-}15)$$

without index denotes the combined collection of both components to be separated

The recovery of the individual components is defined as:

$$REC_i = \frac{m_{i,col}}{m_{i,inj}} \cdot 100\% \qquad i = L,D$$

$$(5\text{-}16)$$

Combined objective functions [30] yield a trade-off between recovery and productivity:

$$PR \times REC_i = PR_i \bullet REC_i \qquad i = L,D$$

$$(5\text{-}17)$$

$$\text{or} \qquad PR \times REC = PR_{L^-} \bullet REC_{L^-} + PR_{D^-} \bullet REC_{D^-}$$

Optimal values for combined collection are typically not optimal for the production of a specific single enantiomer. For the same chromatogram different cut times may need to be applied depending on the desired component.

5.3.7.   Results of Systematic Calculations

Selected results obtained for the gradient injection in water and the isocratic injection in the mobile phase are given in Table 5.5 and Table 5.6, respectively. For both injection methods (gradient and isocratic) the same optimal mobile phase composition of $x_{H_2O} = 52.4 \, mol\%$ was found, regardless of the desired objective function. This optimal mobile phase composition depends of course on the column length. A longer column possessing a higher efficiency would result in a different optimal mobile phase composition, i.e. one with a larger water content causing smaller retention and

resolution. In turn, a less efficient column would require a smaller water content in the mobile phase causing larger retention and resolution.

Table 5.5: Best injection conditions of the <u>gradient injection</u> with water as the injection solvent as found with the systematic forward calculations for a variety of objective functions. The injection concentrations were $c_L^{inj} = c_D^{inj} = 75$ g/l. The optimal conditions for a specific objective function are bold faced.

x_{H2O}^0 mol%	m_{inj} mg	V_{inj} μL	V_{wash} ml	PR mg/min	PRxREC mg/min	PR_L mg/min	PR_D mg/min	PR_LxREC_L mg/min	PR_DxREC_D mg/min	REC_L %	REC_D %
						optimal PR					
68.3	4.2	28	4.8	1.4	0.5	0.6	0.8	0.2	0.3	29	38
63.1	5.6	37	5.9	2.3	1.1	1.1	1.2	0.5	0.6	47	51
58.1	6.6	44	7.3	2.7	1.7	1.4	1.4	0.9	0.8	62	61
52.3	**8.1**	**54**	**10.1**	**2.8**	**2.0**	**1.5**	**1.3**	**1.1**	**0.9**	**74**	**67**
44.7	11.4	76	17.1	2.4	1.7	1.3	1.1	1.0	0.7	78	65
						optimal PRxREC					
68.3	2.7	18	4.7	1.3	0.6	0.6	0.7	0.2	0.4	42	49
63.1	3.2	21	5.7	2.0	1.4	1.0	1.0	0.7	0.7	68	71
58.1	4.4	29	7.0	2.5	2.0	1.2	1.3	1.0	1.0	80	80
52.3	**5.7**	**38**	**9.7**	**2.6**	**2.3**	**1.3**	**1.3**	**1.2**	**1.1**	**89**	**89**
44.7	7.4	49	16.5	2.1	2.0	1.1	1.1	1.0	1.0	96	94
						optimal PR_L					
68.3	4.2	28	4.9	1.4	0.5	0.6	0.8	0.2	0.3	31	37
63.1	5.5	37	6.1	2.3	1.1	1.1	1.1	0.5	0.6	49	51
58.1	7.3	49	7.6	2.7	1.6	1.4	1.3	0.8	0.7	59	55
*52.3	**9.8**	**65**	**10.9**	**2.8**	**1.7**	**1.5**	**1.3**	**1.0**	**0.7**	**68**	**57**
44.7	12.3	82	17.8	2.3	1.6	1.3	1.0	1.0	0.6	76	60
						optimal PR_D					
68.3	7.2	48	4.5	0.0	0.0	0.0	0.9	0.0	0.2	0	23
63.1	6.0	40	5.1	0.0	0.0	0.0	1.3	0.0	0.6	0	43
58.1	6.6	44	5.9	0.0	0.0	0.0	1.5	0.0	0.8	0	54
*52.3	**6.5**	**43**	**7.5**	**0.0**	**0.0**	**0.0**	**1.5**	**0.0**	**1.1**	**0**	**71**
44.7	7.4	49	11.9	0.0	0.0	0.0	1.3	0.0	1.0	0	82
						optimal PR_LxREC_L					
68.3	2.3	15	4.8	1.2	0.6	0.5	0.6	0.3	0.3	47	54
63.1	3.8	25	6.1	2.0	1.3	1.0	1.0	0.7	0.7	65	66
58.1	5.1	34	7.3	2.6	2.0	1.3	1.3	1.0	1.0	76	74
52.3	**6.5**	**43**	**10.1**	**2.7**	**2.2**	**1.4**	**1.3**	**1.2**	**1.1**	**86**	**82**
44.7	9.3	62	17.1	2.3	1.9	1.2	1.1	1.1	0.8	90	78
						optimal PR_DxREC_D					
68.3	2.7	18	4.3	1.3	0.6	0.6	0.7	0.2	0.4	36	48
63.1	3.2	21	5.1	1.9	1.2	0.9	1.1	0.5	0.7	54	69
58.1	4.4	29	6.2	2.1	1.4	0.8	1.4	0.3	1.0	44	77
52.3	**5.7**	**38**	**8.4**	**1.8**	**1.3**	**0.4**	**1.4**	**0.1**	**1.2**	**23**	**85**
44.7	7.4	49	13.9	1.7	1.3	0.5	1.2	0.2	1.1	38	90

*commented in text

Gradient injections in the stronger solvent yield about 15-30% larger objective function values compared to isocratic injections in the mobile phase. This will be illustrated below for two examples, focusing on the optimal productivities PR_L and PR_D. The largest optimal injection volume of the gradient injection is about 65 μl (Table 5.5, optimal PR_L, x_{H2O}=52.3 mol%), i.e. a loading of 9.8 mg (results in

$PR_{L,max}$ =1.5 *mg/min*). For the same objective function and mobile phase composition the corresponding injection volume of isocratic elution (see Table 5.6) is much larger (2776 *μl*), while the amount injected is smaller (8.3 *mg*), resulting in a 19% reduced productivity of the first eluting L-enantiomer ($PR_{L,max}$ =1.3 *mg/min*).

Table 5.6: Best injection conditions of the <u>isocratic injection</u> as found with the systematic forward calculations for a variety of objective functions. The injection concentrations of DL-threonine were c_{tot}^F =9, 7, 4, 3, 2 g/l for $x_{H_2O}^F$ = 68.3, 63.1, 58.1, 52.3, 44.7 mol%, respectively. The optimal conditions for a specific objective function are bold faced.

x_{H2O}^0 mol%	m_{inj} mg	V_{inj} μL	V_{wash} ml	PR mg/min	PRxREC mg/min	PR_L mg/min	PR_D mg/min	PR_LxREC_L mg/min	PR_DxREC_D mg/min	REC_L %	REC_D %
					optimal PR						
68.3	4.3	476	4.5	1.4	0.5	0.6	0.8	0.2	0.3	30	35
63.1	5.3	759	5.3	2.1	1.0	1.1	1.0	0.6	0.5	50	47
58.1	5.6	1407	6.1	2.3	1.5	1.3	1.1	0.8	0.6	67	57
52.3	**7.2**	**2397**	**8.1**	**2.3**	**1.6**	**1.3**	**1.0**	**0.9**	**0.6**	**74**	**60**
44.7	8.2	4079	12.6	1.8	1.4	1.0	0.8	0.8	0.6	82	69
					optimal PRxREC						
68.3	2.4	269	4.5	1.2	0.6	0.6	0.7	0.3	0.3	45	52
63.1	3.1	448	5.3	1.9	1.3	0.9	1.0	0.6	0.7	68	70
58.1	3.6	912	6.1	2.1	1.7	1.1	1.1	0.9	0.9	82	81
52.3	**4.9**	**1638**	**8.1**	**2.2**	**1.9**	**1.1**	**1.1**	**1.0**	**0.9**	**88**	**85**
44.7	5.8	2924	13.2	1.7	1.6	0.9	0.9	0.8	0.8	96	94
					optimal PR_L						
68.3	4.0	441	4.5	1.4	0.5	0.7	0.8	0.2	0.3	33	37
63.1	5.7	821	5.5	2.1	1.0	1.1	1.0	0.5	0.4	49	44
58.1	6.9	1736	6.4	2.3	1.2	1.3	1.0	0.8	0.5	60	47
***52.3**	**8.3**	**2776**	**8.1**	**2.3**	**1.4**	**1.3**	**1.0**	**0.9**	**0.5**	**67**	**52**
44.7	10.0	5003	13.2	1.8	1.2	1.0	0.8	0.8	0.4	75	56
					optimal PR_D						
68.3	4.3	476	3.9	0.0	0.0	0.0	0.8	0.0	0.3	0	33
63.1	4.4	634	4.3	0.0	0.0	0.0	1.1	0.0	0.6	0	51
58.1	4.3	1077	4.9	0.0	0.0	0.0	1.2	0.0	0.8	0	65
***52.3**	**4.9**	**1638**	**6.3**	**0.0**	**0.0**	**0.0**	**1.2**	**0.0**	**0.9**	**0**	**76**
44.7	5.8	2924	10.0	0.0	0.0	0.0	1.0	0.0	0.8	0	85
					optimal PR_LxREC_L						
68.3	2.4	269	4.7	1.2	0.6	0.6	0.6	0.3	0.3	46	52
63.1	3.6	510	5.5	2.0	1.3	1.0	1.0	0.7	0.6	66	66
58.1	4.6	1159	6.4	2.2	1.6	1.2	1.1	0.9	0.7	77	69
52.3	**6.1**	**2017**	**8.6**	**2.2**	**1.7**	**1.2**	**1.0**	**1.0**	**0.7**	**84**	**71**
44.7	7.2	3617	13.2	1.8	1.5	1.0	0.8	0.9	0.7	90	78
					optimal PR_DxREC_D						
68.3	2.4	269	4.1	1.2	0.5	0.5	0.7	0.2	0.3	37	50
63.1	3.1	448	4.6	1.7	1.0	0.7	1.0	0.3	0.7	45	67
58.1	3.3	830	5.5	1.9	1.4	0.9	1.1	0.6	0.9	65	82
52.3	**4.3**	**1448**	**7.2**	**1.9**	**1.4**	**0.8**	**1.1**	**0.5**	**1.0**	**61**	**88**
44.7	5.4	2693	11.3	1.4	1.1	0.5	0.9	0.3	0.8	54	94

*commented in text

About the same amounts of mobile phase are used with $V_{inj} + V_{wash}$=11.0 and

10.9 *ml* for the gradient and the isocratic injections, respectively.

If the later eluting D-threonine would be the sole product (PR_D), then we would

find significantly reduced injection and wash volumes for both injection methods.

Here only 43 or 1638 μl should be applied for the gradient or the isocratic injection.

The mobile phase cycle volumes are 7.5 ml and 7.9 ml compared to 11.0 and 10.9 ml

(for optimal PR_L), resulting in almost the same productivity (PR_D=1.5 resp.

1.2 *mg/min*) as for the first eluting L-enantiomer. Here the productivity could be im-

proved using the gradient injection by 25%. This is the order of magnitude (15-30%)

achievable for all objective functions at the best mobile phase composition for the

studied examples (see also Figure 5.6). The achievable recoveries are about the same

for both injection methods.
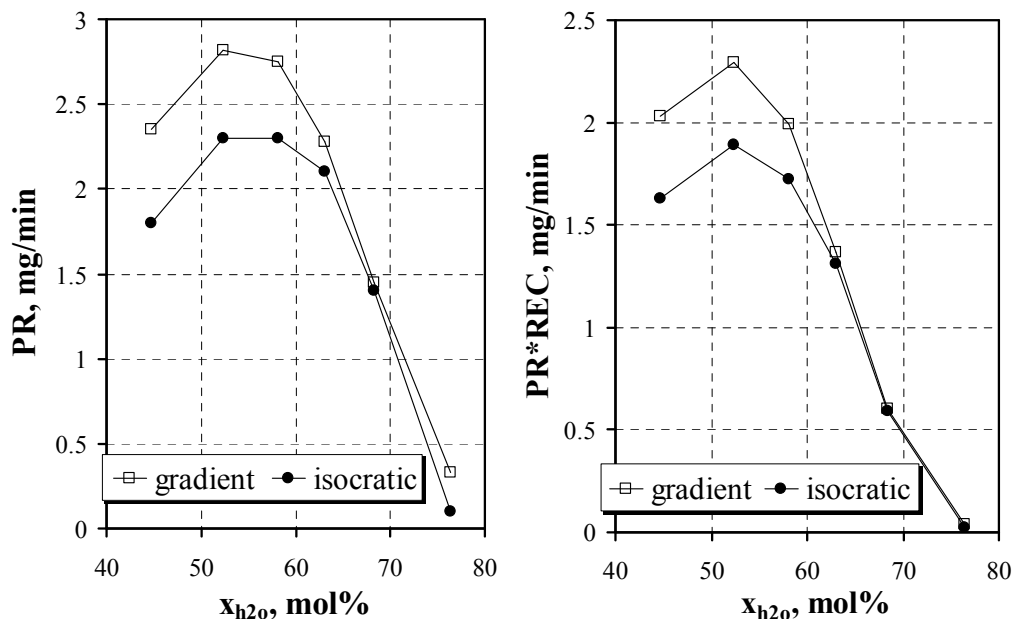
Figure 5.6: Comparison of the optimal productivity PR (Eq. (5-15)) and of the optimal product PRxREC (Eq. (5-17)) for both threonine enantiomers using gradient and isocratic injection for different mobile phase compositions. The injection concentration of DL-threonine was 150 g/L for the injection in pure water while the injection concentrations were 2, 3, 4, 7, 9, 16 *g/l* for $x_{H2O}^{inj} = x_{H2O}^{0}$ =44.7, 52.3, 58.1, 63.1, 68.3, 76.4 *mol%* (bold numbers represent the optimum).

The main reason for the better performance of the gradient injection is the fact that

considerably smaller injection volumes can be applied for injections in the stronger

solvent compared to the injections in the mobile phase. Of course, the method is only

applicable when the samples have a retention in the strong solvent (here, the enanti-

omers of threonine, $a_{D,L} \approx 0.3$), which is different from the retention of the strong solvent itself (here water ≈ 0). More precisely, the solutes to be separated need to have a different retention than the solvent used for injection. The larger these differences the earlier leave the solutes within the column the pulse of the strong solvent and enter a region where the weak solvent with its better separation potential is present. Thus, this difference should be large, in order to exploit the separation potential of the mobile phase.

5.3.8.   Experimental Verification

In order to verify the results obtained, the optimal conditions predicted for $PR \times REC$ were experimentally realized for both injection methods (see Table 5.7 for details of the performed experiments). Three consecutive injections were performed. depicts both, the observed experimental chromatograms and the simulation results. Note, that for the mobile phase composition of $x_{H2O} = 52.3$ *mol%* no preliminary experiments were performed in order to determine model parameters. The simulated and the experimental elution profiles show a relatively good qualitative agreement. However, the elution volumes observed are slightly shifted compared to the predictions. This could be essentially attributed to the aforementioned shift of the retention times with increasing use of the chiral stationary phase and inaccuracies in the description of the adsorption equilibria.

Table 5.7: Experimental and simulation conditions for the verification of the simulation results. Optimal conditions for PRxREC (Table 5.5 and Table 5.6).

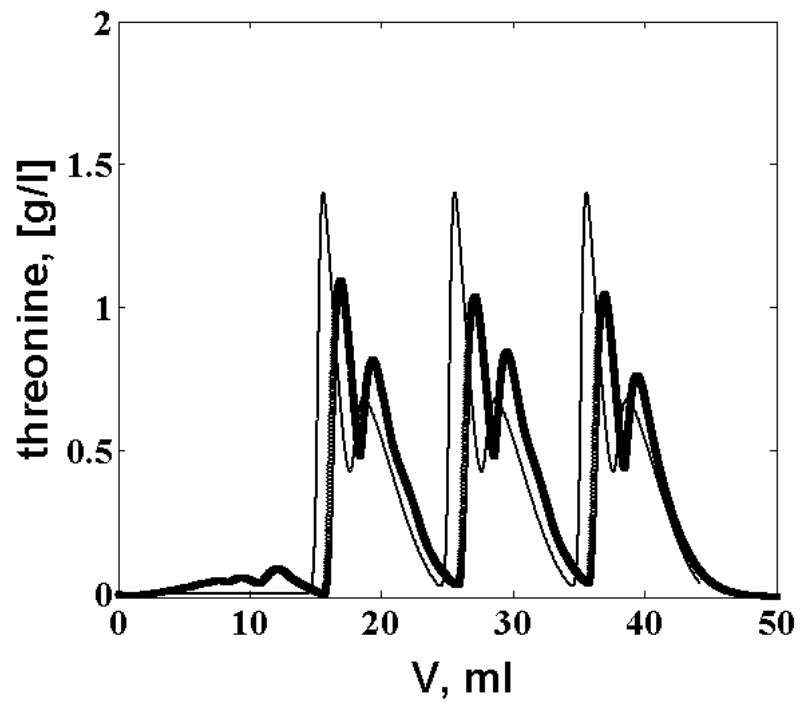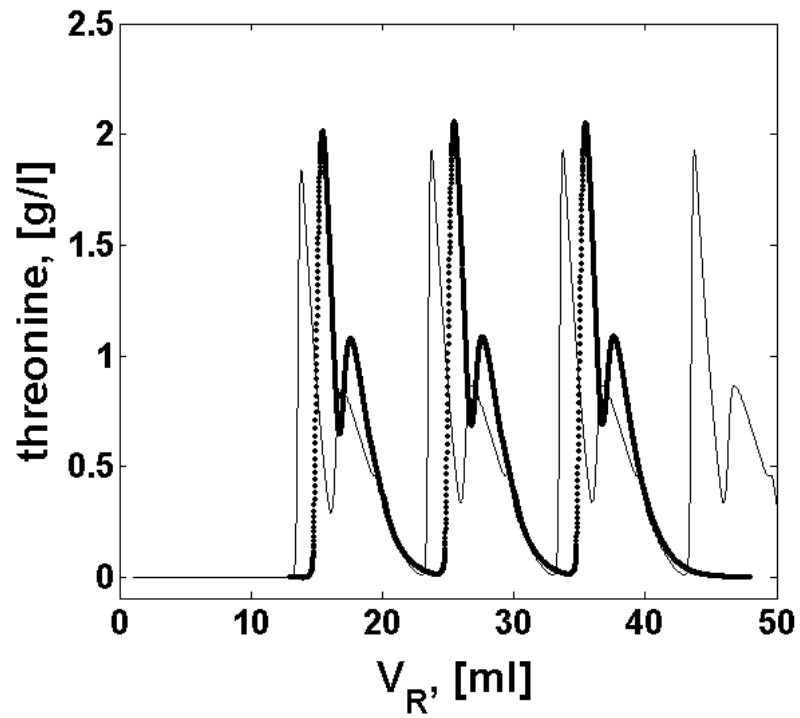|	gradient injection (in water)	isocratic injection (in mobile phase)
mobile phase composition	x_{H2O}=52.3 *mol%* (g_{H2O}=0.25 *v/v*)	
c_{total}^{inj} [g/l]	150	3
V_{inj} [ml]	0.038	1.638
m_{inj} [mg]	5.7	4.9
V_{wash} [ml]	9.7	8.1
V_{cycle} [ml]	9.7	9.7

Figure 5.7: Experimental verification of the optimization results. Experimental (symbols) and simulation (lines) conditions for the gradient injection (left) and the isocratic injection (right) are listed in Table 5.7.

5.4.   Summary

Based on a case study we have presented a relatively simple and fast method to evaluate the application of injecting the sample in a different solvent than used for the elution (gradient injection). The method is based on an estimation of the adsorption isotherms as a function of mobile phase composition using the inverse or peak fitting method. To determine optimal separation conditions optimization calculations can be performed with standard column models using the estimated adsorption isotherms, including the dependence of the solubility on the mobile phase composition.

For the example studied, the separation of the racemic mixture of DL-threonine on a Chirobiotic-T column using ethanol water mixtures as the mobile phase, optimal separation conditions were identified. The gradient injections in a stronger solvent (here pure water) resulted in 15-30% larger objective function values compared to the corresponding isocratic injections. This improvement is due to the fact, that significantly smaller injection volumes can be used to load the column, confirming again the well-known rule that concentration overloading is better than volume overloading. It should be noted that the method of injecting the sample in a different solvent is only applicable if the solutes possess a different migration velocity in the injection solvent than the injection solvent itself.

6. Summary and Conclusions

In preparative chromatography, it is the goal to obtain the products at a desired purity in an efficient manner. One of the concepts for batch chromatography to reach this goal is the use of a different solvent for the injection than for the elution – gradient injection. The concept of using a stronger solvent for the injection than for the elution is often applied in pharmaceutical industry to overcome solubility limitations of the solutes in the mobile phase. The current work attempts to contribute to the understanding, applicability and limitations of gradient injections. It has been shown both theoretically and experimentally, that the application of gradient injections has potential to increase efficiency of a separation. Methods and rules for process design and evaluation are given.

The equilibrium theory was applied to extract general effects for gradient injections. It was performed exemplary for different isotherm combinations of the solvent and the solute, linear-linear and linear-Langmuir. Both isotherm combinations result in the same general effects for the elution profiles. It can be deducted, just based on the variation of the adsorption isotherms with the mobile phase composition, that on-column dilution, on-column concentration and split / distorted peaks of the solutes can be expected for such an injection method. On-column concentration and on-column dilution depend on the elution strength of the injection solvent and its relative retention compared to the solutes. The theoretically extracted general effects could be verified in an experimental study.

Based on these results it has been deducted that the injection in a strong solvent is only applicable to overcome solubility issues of the mobile phase, if the modifier is the least retained component. The general assumption behind this finding is that with increasing modifier concentration, both, the solubility of the solutes as well as the elution strength increase. In this case, an on-column dilution of the solutes occurs as soon as they leave the modifier plug, thus minimizing supersaturation in the mobile

phase and reducing the danger of undesired crystallisation of the solutes in the chromatographic system. If the modifier would be stronger retained compared to the solutes, than the concentration of the solutes would increase even above the injection concentration and may trigger undesired precipitation. Such a combination of a stronger injection eluent and a stronger retention of the former are applicable, if the desired solute is much diluted and needs to be concentrated. The injection in a weaker solvent may be only desirable if the solubility of the components to be separated is not an issue and the solutes to be separated posses markedly different elution times (large separation coefficients). This injection method corresponds then to a typical gradient operation, where the elution strength of the mobile phase is immediately increased after the injection.

A limitation of gradient injections is that it is only applicable if the solutes possess a different migration velocity in the injection solvent than the injection solvent itself.

In another experimental study, a relatively simple and fast method to evaluate the application of injecting the sample in a different solvent than used for the elution has been proposed and experimentally verified. It is based on an estimation of the adsorption isotherms as a function of mobile phase composition using the inverse method. To determine optimal separation conditions optimization calculations can be performed with standard column models using the estimated adsorption isotherms, including the dependence of the solubility on the mobile phase composition.

The potential of improved efficiency of the separation process of gradient injections compared to the optimized isocratic elution has been the order of magnitude of 15-50% for a parametric study (linear isotherms) and an experimental study (non-linear isotherms). This improvement is due to the fact, that significantly smaller injection volumes can be used to load the column, confirming again the well-known rule that concentration overloading is better than volume overloading. The dependence of the solubility on the modifier concentration is of the uttermost importance for the productivity. The most productive injection method depends on the solubility dependence of the solutes on the modifier concentration. A positive effect for a gradient injection can be expected for strong nonlinear dependence of the solubility on the modifier concentration. The isocratic injection is the better choice if this strong nonlinear increase is not observed.

Appendix A   Data

A 1   Data Used for the Example Shown in Section 3.1.2

Jandera used the logarithmic-linear relation to describe the dependence of the Henry coefficients of phenol and o-cresol on the methanol concentration (expressed in volume-fractions) [85].

$$\ln(H_i) = p_{1i} - p_{2i}c_1 \tag{A-1}$$

Table A.1: Parameters of Eq. (A-1) for phenol and o-cresol for methanol-water mixtures on a reversed phase column (methanol=modifier, corresponds to component 1). Data taken from [85].

	p_1	p_2
phenol (index 2)	1.404	1.899
o-cresol (index 3)	-2.326	-2.739

The dependence of the Henry coefficients on the modifier concentration is shown in Figure A.1. To be more flexible for a parametric study I use a fictive system where I only apply the data of Jandera *et al.* for the Henry coefficient of one of the solutes. The Henry coefficient of the other solute is calculated with a fictive separation factor. The separation factor is assumed as linearly dependent on the modifier concentration:

$$\alpha = \alpha\left(c_1^{\min}\right) - \frac{\alpha\left(c_1^{\min}\right) - \alpha\left(c_1^{\max}\right)}{c_1^{\min} - c_1^{\max}}\left(c_1^{\min} - c_1\right) \tag{A-2}$$

The Henry coefficient of the modifier is set to zero. This is not a special case, it is just an example where the modifier is always the least retained component.

The solubility of the feed mixture of the solutes is increasing with increasing modifier concentration. I apply two dependencies here, once a typical exponential dependency

$$\ln[c_s] = \ln\left[c_s\left(c_1^{\min}\right)\right] - \frac{\ln\left[c_s\left(c_1^{\min}\right)\right] - \ln\left[c_s\left(c_1^{\max}\right)\right]}{c_1^{\min} - c_1^{\max}}\left(c_1^{\min} - c_1\right) \quad \text{(A-3)}$$

and a linearly dependent solubility on the modifier concentration

$$c_s = c_s\left(c_1^{\min}\right) - \frac{c_s\left(c_1^{\min}\right) - c_s\left(c_1^{\max}\right)}{c_1^{\min} - c_1^{\max}}\left(c_1^{\min} - c_1\right). \quad \text{(A-4)}$$

In the above, c_s is the solubility of the feed mixture of the solutes. $c_1^{\min}$ and $c_1^{\max}$ are the minimal and the maximal modifier concentration applicable. An injection with a weak solvent corresponds to the minimal modifier concentration and an injection with a strong solvent corresponds to the maximum modifier concentration.
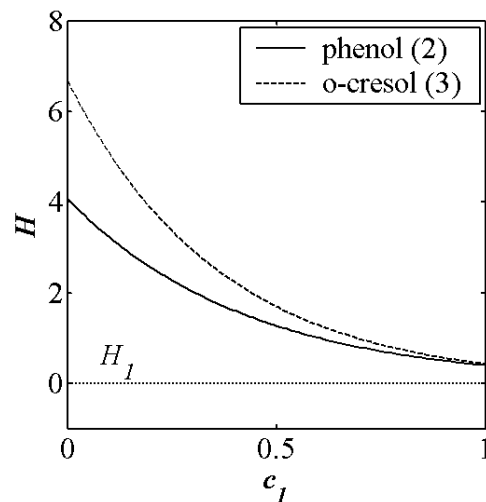
Figure A.1: Dependence of the Henry coefficients of phenol and o-cresol on the methanol concentration. Henry coefficients calculated with Eq. (A-1) and the parameters given in Table A.1. Data taken from [85].

A 2   Cycle Time for Interactions between Consecutive Injections

The optimal injection and cycle time were determined for two scenarios: a) no interaction between consecutive injections as described in section 3.1.2 on page 65, and

b) interactions between consecutive injections are allowed. For the latter scenario the same goal of the separation should be assured, i.e. touching band separation of the solutes with 100% purity and recovery. Thus, only interactions of the modifier with the solute plug of previous and ensuing injections were allowed. This yields the following 2 necessary conditions:

$$\tau_2^{des}\Big|_k = \tau_3^{ads}\Big|_k$$
$$\tau_2^{ads}\Big|_k \geq \tau_3^{des}\Big|_{k-1}$$

(A-5)

as well as 1 limiting condition:

$$\tau_3^{des}\Big|_k \leq \tau_1^{ads}\Big|_{k+2}$$

(A-6)

k is the count of the injection. This results for the productivity in a set of 2 lengthy equations which was maximized by varying injection and cycle time for a given modifier concentration in the feed and in the mobile phase. The optimization was performed with the non-linear solver implemented in Microsoft Excel 2002. The spreadsheets are available on a CD upon request. For the isocratic injection the same results as for scenario a) are obtained. Typical profiles in the physical plane and in the concentration time domain are shown for the injection of a modifier absence (Figure A.2, left) and for the injection of a modifier plus (Figure A.2, right). Notice the severe interactions of the solutes with modifier plugs of consecutive injections. The solutes are overtaken on their course through the column by the modifier of the next injection. In the example presented they elute in the modifier plug and in the mobile phase, thus the peak shape of the solutes is distorted. For the injection of a modifier absence we observe the concentration of the effluent above the feed concentration (Figure A.2, bottom left). The cycle time is dominated by the injection time (in principle the grey modifier plugs). The injection in the strong solvent results again in the diluted peaks, which are also distorted (Figure A.2, bottom right). Here the injection time is still much smaller compared to the cycle time. The touching band separation is now also achieved between the solutes of consecutive injections. We still achieve touching band separation, however, the cycle times are much shorter than the cycle times for the injection method without interactions of consecutive injections. So the productivity for the former injection method is larger. The additional

degree of freedom results in increases by 20-300% for the examples covered in the parametric study below.
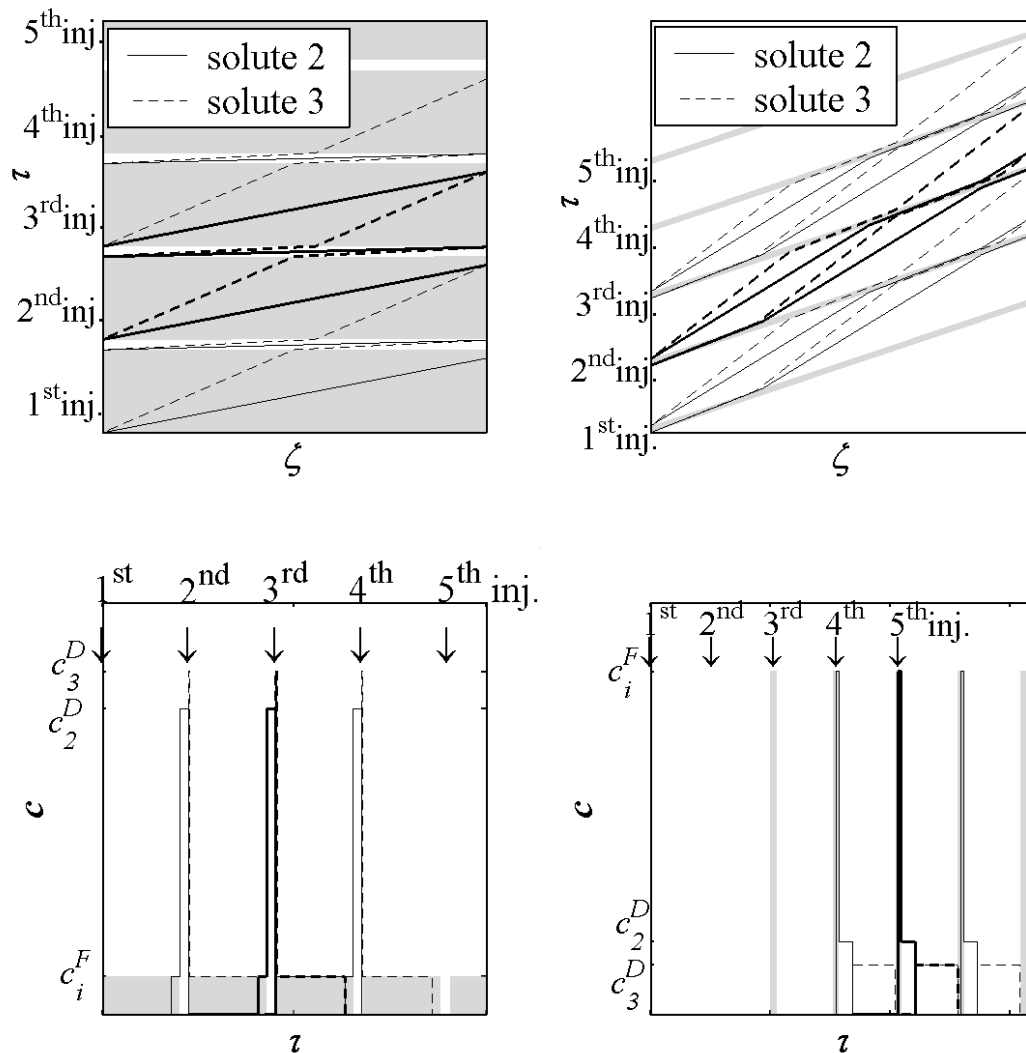

Figure A.2: Separation of two solutes (2, 3) with interactions of consecutive injections when the modifier is always the strongest retained component. left for the injection in a weak solvent and right for the injection in a strong solvent. Upper diagrams show characteristics of the solutes in the physical plane $\tau(\zeta)$. The modifier of the injection plug is depicted in grey. The bottom diagram show the corresponding $c(\tau)$ diagrams at the column outlet. The lines corresponding to the solutes of the second injection are bold faced.

A 3   Results of the Productivity for Several Examples

This section is a continuation of the results presented for one example in section 3.1.2. In this section I list a number of theoretical results obtained for the separation of two solutes with linear isotherms. The modifier also adsorbs linearly. I start with a small parametric study based on the dependence of the Henry coefficients of phenol and o-cresol on the methanol concentration. Here I apply both, an increasing and a decreasing separation factor with increasing modifier concentration. The increasing separation factor (case 1) is rather exotic case and is only treated once. For the more realistically decreasing separation factor of the solutes I span two ranges: once it decreases from 2 to 1 (case 2) and once it decreases from 10 to 1 (case 3) over the range of modifier concentrations applicable. Using once the less adsorbed solute and once the stronger adsorbed solute as the reference component accounts for another two scenarios. In the first scenario span the Henry coefficients a rather large window, thus resulting in larger cycle times. In the latter case the opposite is true. This is visualized in Figure A.3.
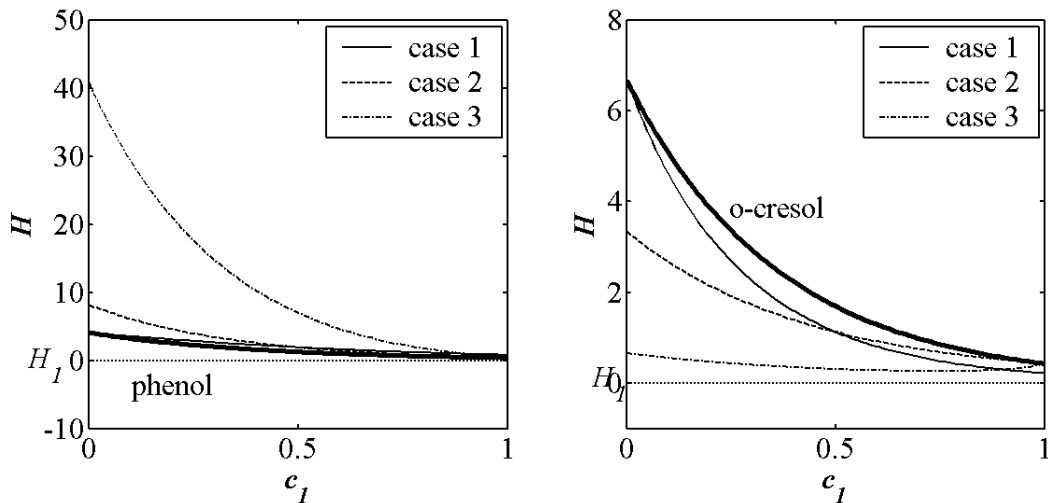

Figure A.3: Henry coefficients for the parametric study presented below. The separation factor is increasing from 1 to 2 (case 1) and decreasing from 2 to 1 (case 2) and decreasing from 10 to 1 (case 3).
**left: The less adsorbed phenol is the reference component (bold line).**
right: The stronger adsorbed o-cresol is the reference component (bold line).

In the following figures are the separation factors and the corresponding Henry coefficients shown above the ratio of the injection time over the cycle time and the corre-

sponding productivity. All results were produced with and without interactions of consecutive injections.

The productivity of the isocratic injection depends on the form of the solubility function of the solutes to be separated. In neither case outperforms the injection in a weak solvent the isocratic injection. Note that the injection in a weak solvent corresponds to typical gradient elution, where the gradient starts some time after the injection. The injection in a strong solvent has the potential to outperform the isocratic injection only if the solubility function is strongly nonlinear.

A 3.1   Phenol as the Reference Component
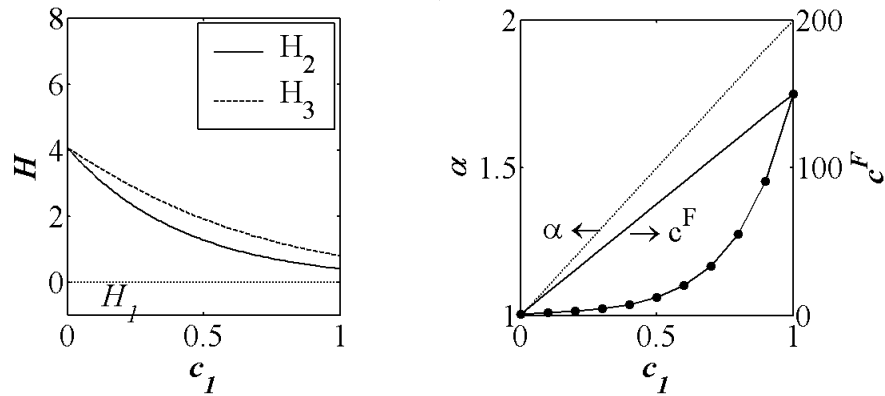
without interactions of consecutive injections
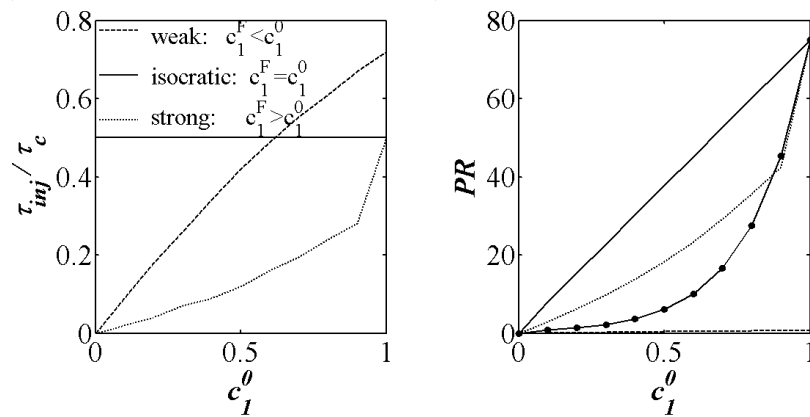
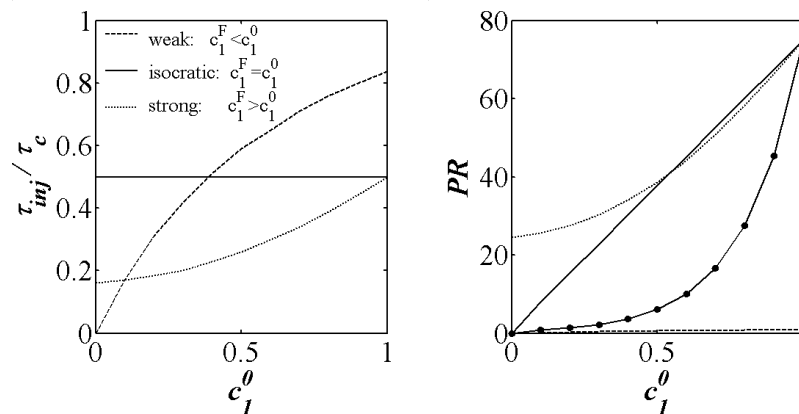with interactions of consecutive injections

Figure A.4: Case 1 with Phenol as reference component. Separation factor increases from 1 to 2. Henry coefficients of the solutes (upper left) and the corresponding separation factor and solubility (upper right) for a linear dependence (solid line, no symbols) and an exponential dependence on the modifier concentration (solid line, circles). Ratio of injection time over cycle time (bottom left) and the corresponding productivity (bottom right) for the three injection methods. The productivity of the isocratic injection is shown for a linear dependence on the modifier concentration (solid lines, no symbols) and for an exponential dependence (solid lines, circles).
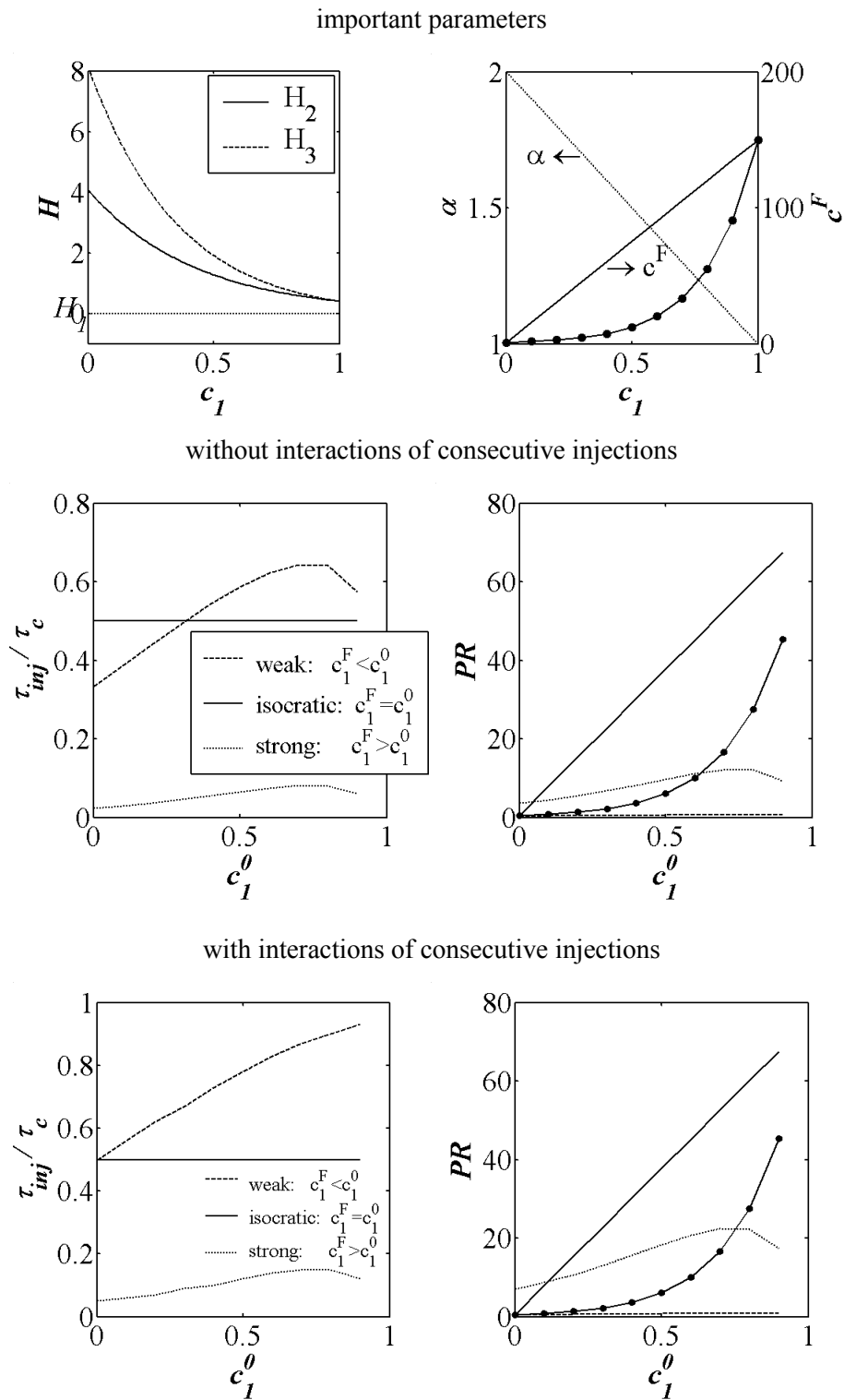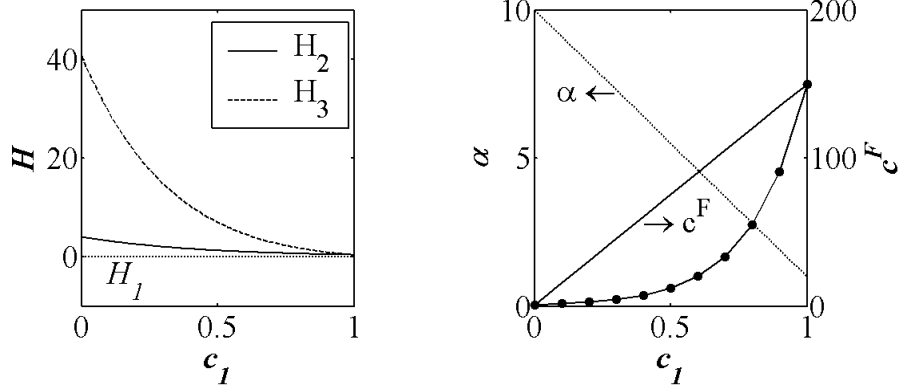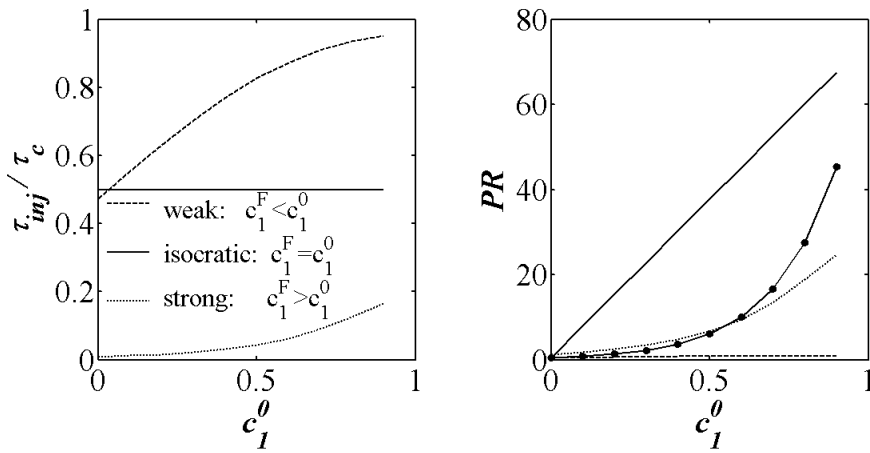
important parameters

without interactions of consecutive injections

with interactions of consecutive injections

Figure A.5: Case 2 with Phenol as reference component. Separation factor decreases from 2 to 1. Description see Figure A.4.

important parameters

without interactions of consecutive injections
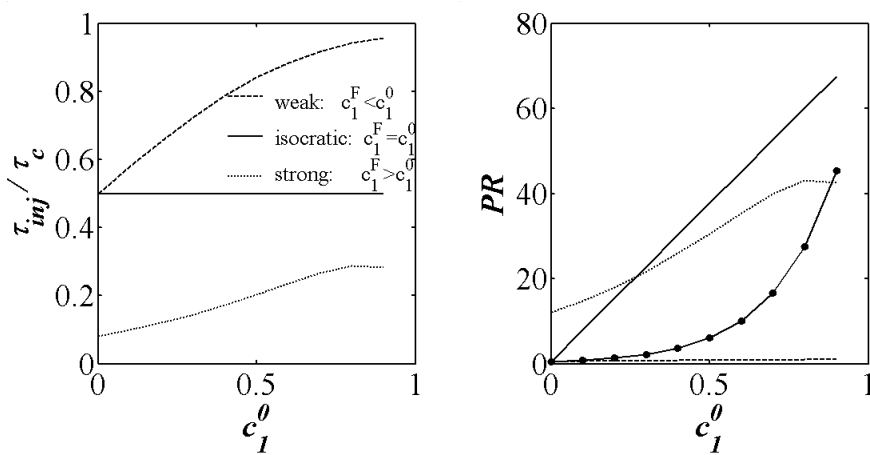

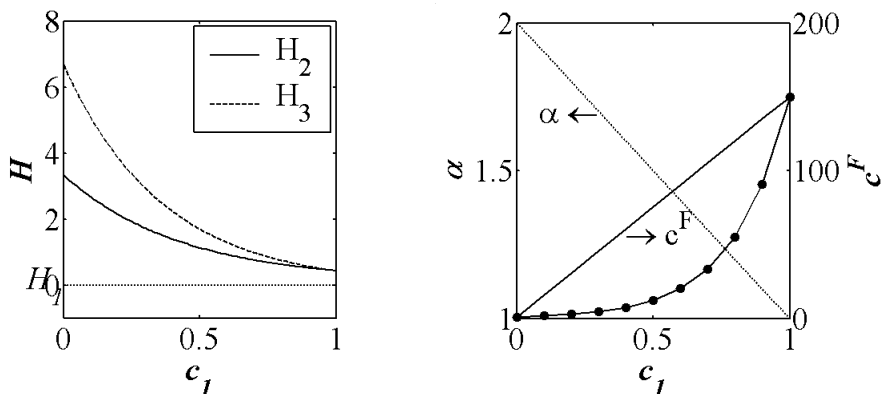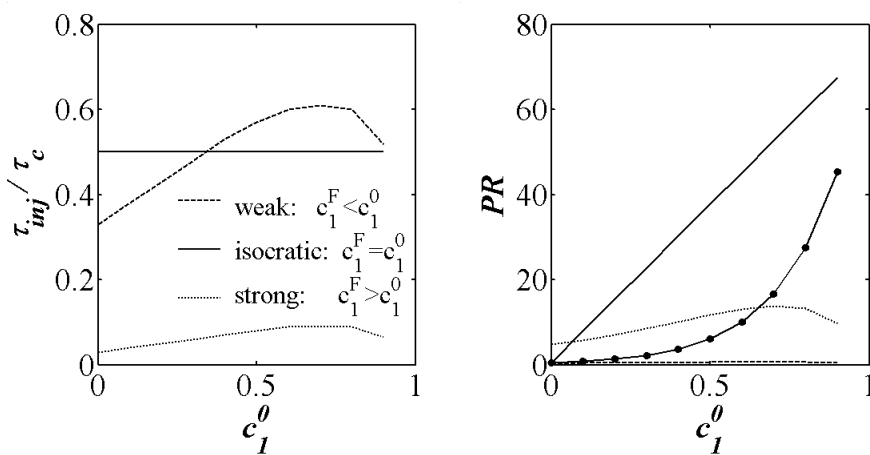with interactions of consecutive injections

Figure A.6: Case 3 with Phenol as reference component. Separation factor decreases from 10 to1. Description see Figure A.4.

A 3.2   o-Cresol as the Reference Component

without interactions of consecutive injections
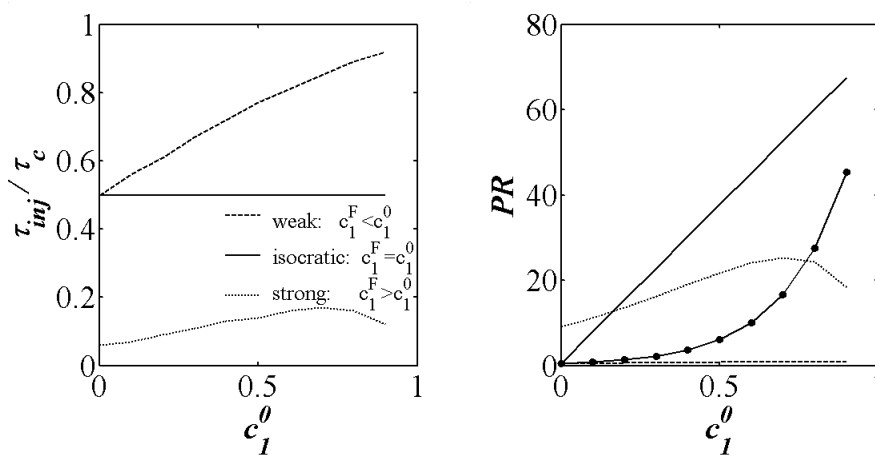

with interactions of consecutive injections

Figure A.7: Case 2 with o-Cresol (3) as reference component. Separation factor decreases from 2 to 1. Description see Figure A.4.

without interactions of consecutive injections
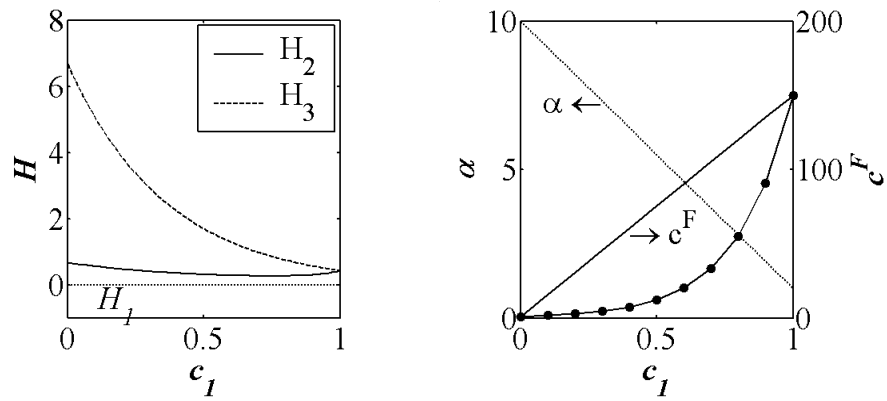

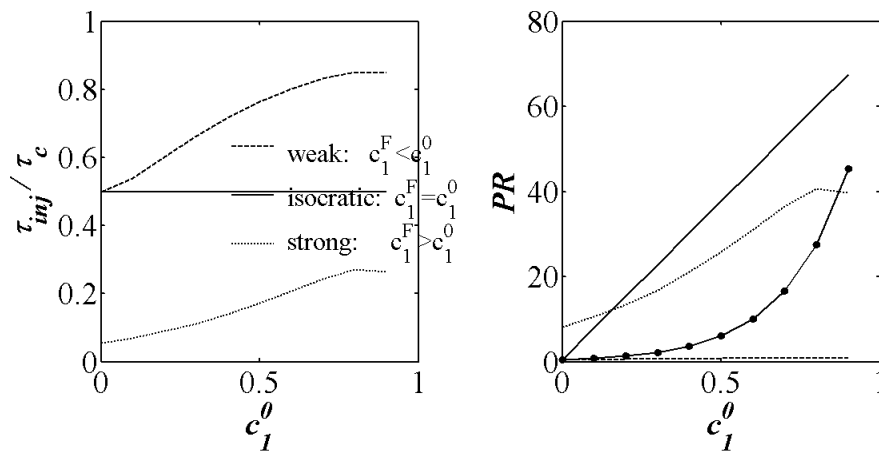with interactions of consecutive injections
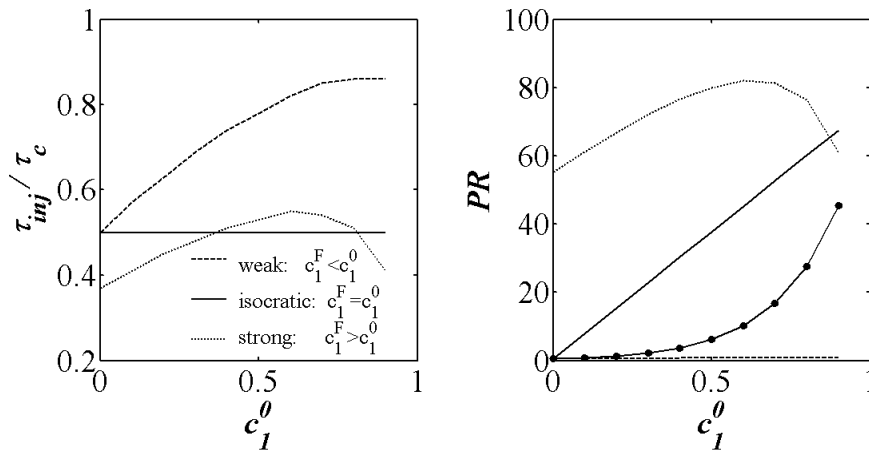
Figure A.8: Case 3 with o-Cresol (3) as reference component. Separation factor decreases from 10 to 1. Description see Figure A.4.
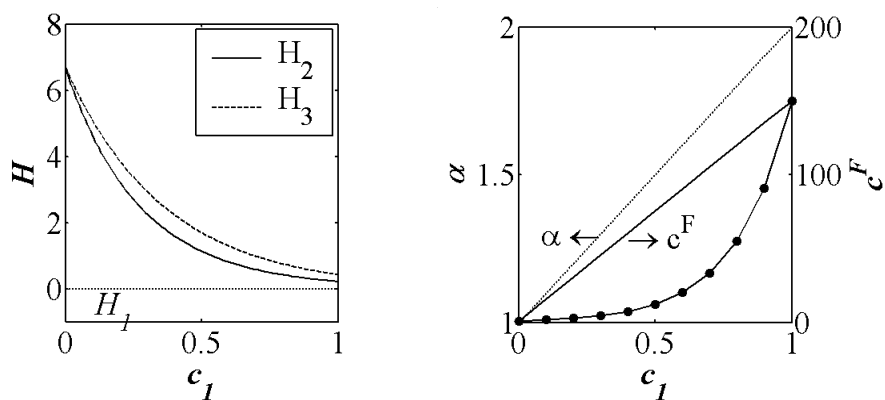
without interactions of consecutive injections
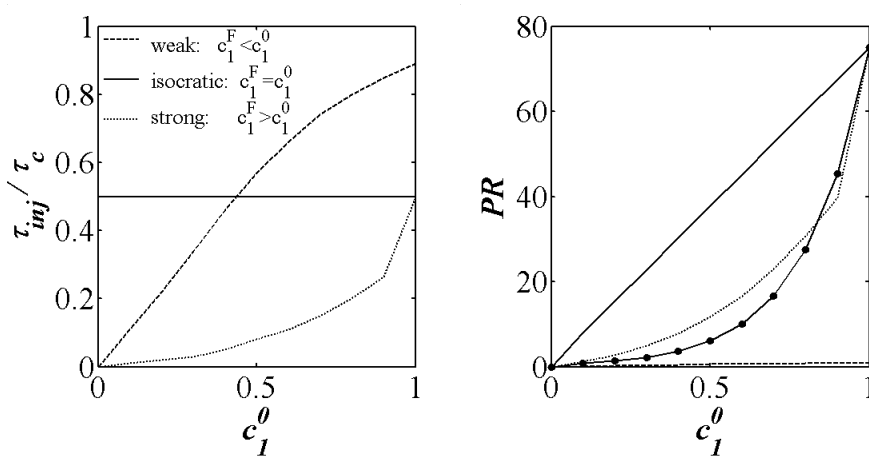
with interactions of consecutive injections
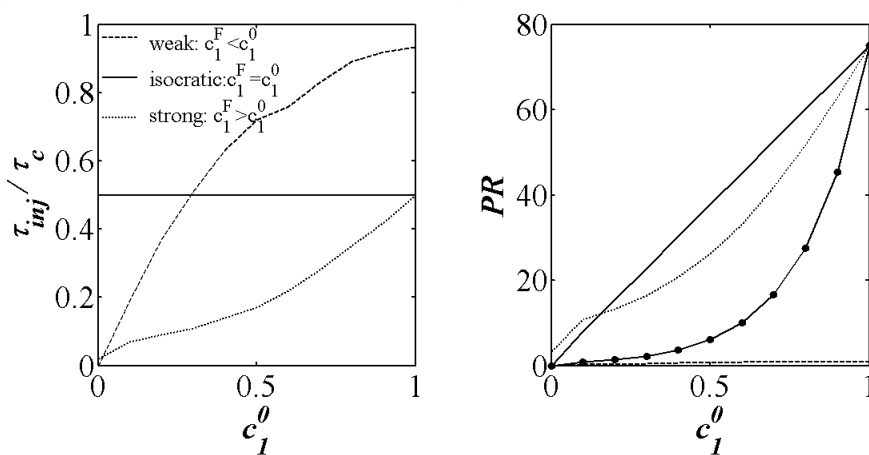
Figure A.9: o-Cresol (3) as reference component. Separation factor increases from 1 to 2. Description see Figure A.4.

A 3.3 Threonine

Here the parameters of threonine were used.
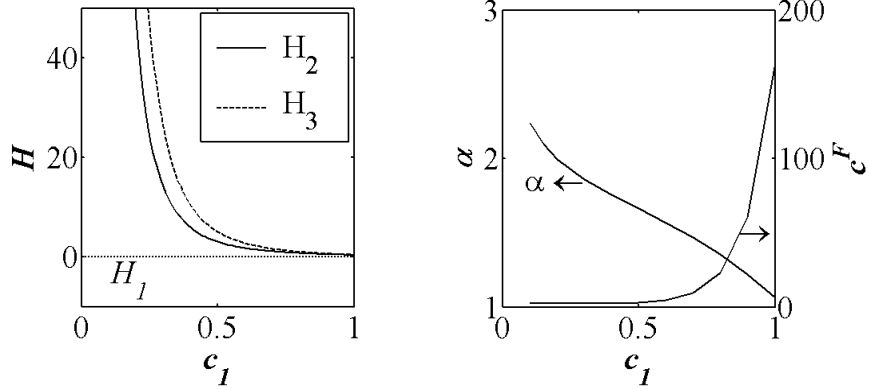
without interactions of consecutive injections
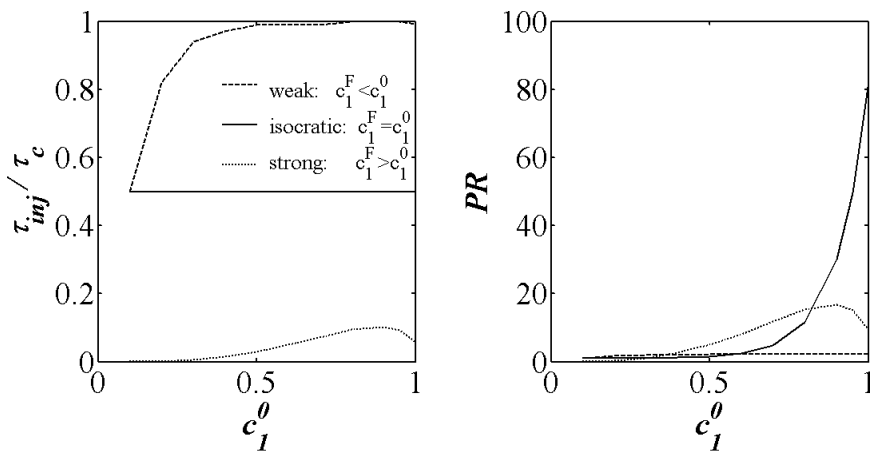
with interactions of consecutive injections
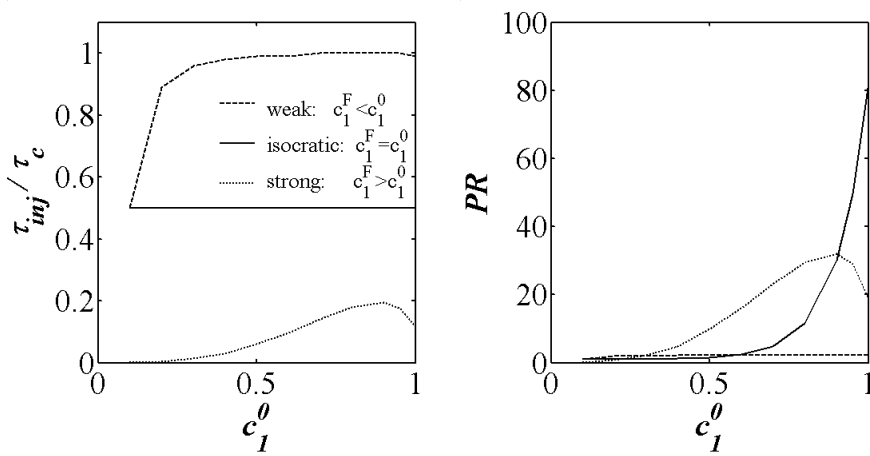
A 4   Data of the Experimental System Used in Chapter 4

The deactiviation of the LiChoprep-NH4 stationary phase is visualized below.
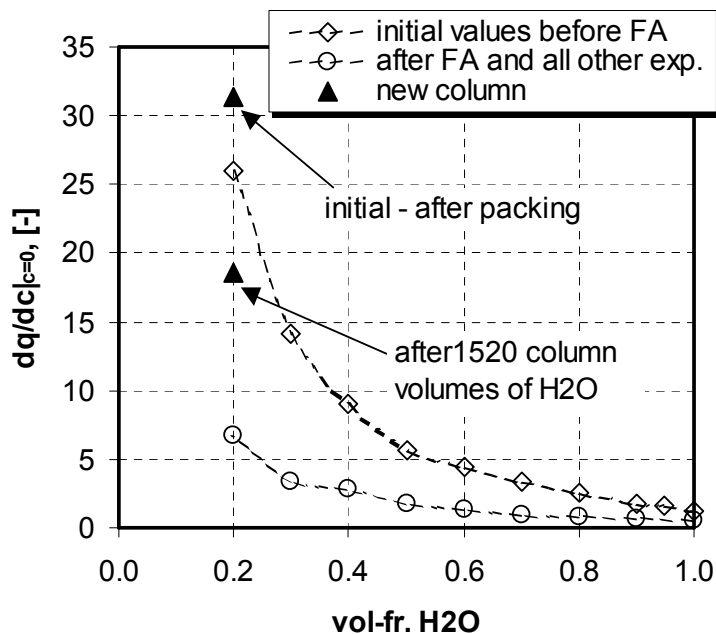
Figure A.10: Initial slope of the isotherms of DL-threonine. Development with experiments and its dependence on the applied amount of water.
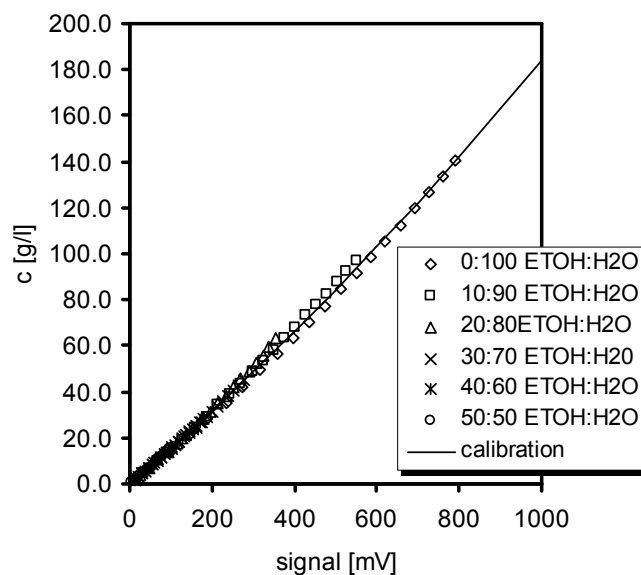
Figure A.11: Independence of the DL-threonine concentration on the water content in the mobile phase

A 5 Data for Ethanol Water Mixtures

The dependence of the liquid phase activity coefficients γ_i, the density ρ and the molecular weight M on the mobile phase composition must be known for the use of Eq. (5-5). The liquid phase activity coefficients were calculated using Margules equation [130]. The interaction parameters are listed in Table A.2.

Table A.2: Interaction parameters of the Margules equation (A-7) of the ethanol/water system at 20°C (1=ethanol, 2=water) [130].

	Λ_{12}	Λ_{21}
Margules	1.6022	0.7947

$$\ln \gamma_1 = \left[\Lambda_{12} + 2(\Lambda_{21} - \Lambda_{12})x_1 \right] x_2^2$$
$$\ln \gamma_2 = \left[\Lambda_{21} + 2(\Lambda_{12} - \Lambda_{21})x_2 \right] x_1^2$$

with 1=ethanol, 2=water   **(A-7)**

The density of the mobile phase at 20°C was approximated using the following forth order polynomial fitted through the data given in [130] page 2-113.

$$\rho = -0.0559\, x_{H2O}^4 \;+\; 0.1292\, x_{H2O}^3 \;+\ldots$$
$$0.0164\, x_{H2O}^2 \;+\; 0.1177\, x_{H2O} \;+\; 0.7894 \tag{A-8}$$

ρ in g/ml;   x in mol$_{H2O}$/mol$_{MP}$;

The molecular weight of the mobile phase was calculated with:

$$M_{MP} = (1 - x_{H2O})M_{EtOH} + x_{H2O}M_{H2O} \tag{A-9}$$

Appendix B   Special Solutions of the Equilibrium Theory

B 1   *Solution for Linear-Linear-Linear Interactions*

Inserting the expressions of Table 3.4 in the process matrix **A** result in:

$$\mathbf{A} = \begin{bmatrix} 1+FH_1 & 0 & 0 \\ F\dfrac{dH_2(c_1)}{dc_1}c_2 & 1+FH_2(c_1) & 0 \\ F\dfrac{dH_3(c_1)}{dc_1} & 0 & 1+FH_3(c_1) \end{bmatrix} \tag{B-1}$$

The corresponding eigenvalues of **A** are:

$$\boldsymbol{\lambda} = \begin{bmatrix} \lambda_1 \\ \lambda_2 \\ \lambda_3 \end{bmatrix} = 1+F\begin{bmatrix} H_1 \\ H_2(c_1) \\ H_3(c_1) \end{bmatrix} \tag{B-2}$$

While the eigenvectors become:

$$
\mathbf{r}(\lambda_1) = \begin{bmatrix} dc_1 \\ dc_2 \\ dc_3 \end{bmatrix} = \begin{bmatrix} \left(H_1 - H_2(c_1)\right)\left(H_1 - H_3(c_1)\right) \\[2mm] \left(H_1 - H_3(c_1)\right)c_2 \dfrac{dH_2(c_1)}{dc_1} \\[2mm] \left(H_1 - H_2(c_1)\right)c_3 \dfrac{dH_3(c_1)}{dc_1} \end{bmatrix}
$$

$$
\mathbf{r}^*(\lambda_1) = \begin{bmatrix} \dfrac{dc_1}{dc_1} \\[2mm] \dfrac{dc_2}{dc_1} \\[2mm] \dfrac{dc_3}{dc_1} \end{bmatrix} = \begin{bmatrix} 1 \\[2mm] \dfrac{c_2}{\left(H_1 - H_2(c_1)\right)} \dfrac{dH_2(c_1)}{dc_1} \\[2mm] \dfrac{c_3}{\left(H_1 - H_3(c_1)\right)} \dfrac{dH_3(c_1)}{dc_1} \end{bmatrix}
$$

(B-3)

$$
\mathbf{r}(\lambda_2) = \begin{bmatrix} dc_1 \\ dc_2 \\ dc_3 \end{bmatrix} = \begin{bmatrix} 0 \\ 1 \\ 0 \end{bmatrix} = \begin{bmatrix} \dfrac{dc_1}{dc_2} \\[2mm] \dfrac{dc_2}{dc_2} \\[2mm] \dfrac{dc_3}{dc_2} \end{bmatrix}
$$

(B-4)

$$
\mathbf{r}(\lambda_3) = \begin{bmatrix} dc_1 \\ dc_2 \\ dc_3 \end{bmatrix} = \begin{bmatrix} 0 \\ 0 \\ 1 \end{bmatrix} = \begin{bmatrix} \dfrac{dc_1}{dc_3} \\[2mm] \dfrac{dc_2}{dc_3} \\[2mm] \dfrac{dc_3}{dc_3} \end{bmatrix}
$$

(B-5)

To obtain the trajectories in the hodograph space, we have to integrate Eqs. (B-2)-(B-5). Due to the nonzero denominator it is appropriate to integrate the trajectories $R(\lambda_1)$ along c_1, $R(\lambda_2)$ along c_2 and $R(\lambda_3)$ along c_3:

$$R(\lambda_1): \qquad \int_{c_1} \mathbf{r}^*(\lambda_1)dc_1$$

$$R(\lambda_2): \qquad \int_{c_2} \mathbf{r}(\lambda_2)dc_2 \qquad \qquad \textbf{(B-6)}$$

$$R(\lambda_2): \qquad \int_{c_3} \mathbf{r}(\lambda_3)dc_3$$

B 2   *Solution of the Shockpath for Linear-Langmuir Interactions, Case b)*

The slope of the shock is:

$$\frac{d\tau}{d\zeta} = \tilde{\lambda}\Big|_{0 \to c_2^{out}} \qquad \qquad \textbf{(B-7)}$$

with c_2^{out} as the actual concentration of the shock outside the injection media. The slope of the shock is:

$$\tilde{\lambda}\Big|_{0 \to c_2^{out}} = 1 + F\frac{q_2(c_1^0, c_2^{out}) - q_2(c_1^0, c_2^0)}{c_2^{out} - c_2^0} \qquad \qquad \textbf{(B-8)}$$

The actual retention time of a certain concentration on the disperse end of the shock is obtained from:

$$\tau = \lambda_1 \zeta^*\Big|_{c_2^{in}} + \left[\zeta - \zeta^*\Big|_{c_2^{in}}\right]\lambda_2(c_1^0, c_2^{out}) \qquad \qquad \textbf{(B-9)}$$

Differentiating Eq. (B-9) with respect to c_2^{out} yields:

$$
\frac{d\tau}{dc_2^{out}} = \left[\lambda_1 - \lambda_2(c_1^0, c_2^{out}) \right] \frac{d\zeta^*\big|_{c_2^{in}}}{dc_2^{out}} + \ldots
$$

$$
\left[\zeta - \zeta^*\big|_{c_2^{in}} \right] \frac{d\lambda_2(c_1^0, c_2^{out})}{dc_2^{out}} + \lambda_2(c_1^0, c_2^{out}) \frac{d\zeta}{dc_2^{out}}
$$

(B-10)

In the above $\dfrac{d\tau}{dc_2^{out}}$ is replaced by $\dfrac{d\tau}{d\zeta}\dfrac{d\zeta}{dc_2^{out}}$ and combined with Eq. (B-7). This

yields the ODE:

$$
\frac{d\zeta}{dc_2^{out}} = \frac{1}{\underset{0 \to c_2^{out}}{\tilde{\lambda}} - \lambda_2(c_1^0, c_2^{out})} \left[\left(\lambda_1 - \lambda_2(c_1^0, c_2^{out}) \right) \frac{d\zeta^*\big|_{c_2^{in}}}{dc_2^{out}} + \ldots \right.
$$

$$
\left. \left(\zeta - \zeta^*\big|_{c_2^{in}} \right) \frac{d\lambda_2(c_1^0, c_2^{out})}{dc_2^{out}} \right]
$$

(B-11)

$\zeta^*\big|_{c_2^{in}}$ denotes the position, where a concentration of the solute c_2^{in}, with its origin at

the column entrance ($\zeta = 0$) and the end of the injection ($\tau = \tau_{inj}$), leaves the injec-

tion media. Each solute concentration leaves the modifier at a different space posi-

tion. This position is obtained in a similar manner like Eq. (3-45) on page 85.

$$
\zeta^*\big|_{c_2^{in}} = \frac{\tau_{inj}}{\lambda_1 - \lambda_2(c_1^F, c_2^{in})}
$$

(B-12)

At this position, i.e. the boundary between the injection media and the initial solvent,

the concentration c_2^{in} jumps with a contact discontinuity to c_2^{out} (see enlarged region

in Figure 3.21 on page 86). Both concentrations are connected via Eq. (3-37) (shown

again here for the sake of readability).

$$
c_2^{end} = \frac{1}{2 H_1 H_2(c_1^{end})} \times
$$

$$
\left\{ -H_1 q_s + \frac{\left(c_2^{start}\right)^2 H_1 H_2(c_1^{start}) + \left(q_s\right)^2 + H_1 q_s c_2^{start}}{\left[q_s + c_2^{start} H_2(c_1^{start})\right] H_2(c_1^{end})} + \right.
$$

$$
\left. \sqrt{\begin{array}{c} \left(H_1 q_s\right)^2 - 4\left(q_s\right)^2 H_1 H_2(c_1^{end}) + \dots \\[2mm] \dfrac{2 q_s H_1 H_2(c_1^{end}) \left[\left(q_s\right)^2 + q_s H_1 c_2^{start} + \left(c_2^{start}\right)^2 H_1 H_2(c_1^{start})\right]}{q_s + c_2^{start} H_2(c_1^{start})} + \\[4mm] \dfrac{\left[\left(q_s\right)^2 + q_s H_1 c_2^{start} + \left(c_2^{start}\right)^2 H_1 H_2(c_1^{start})\right]^2 \left[H_2(c_1^{end})\right]^2}{\left[q_s + c_2^{start} H_2(c_1^{start})\right]^2} \end{array}} + \right\}
\qquad \textbf{(3-37)}
$$

c_2^{in} in Eq. (B-12) is replaced by Eq. (3-37), with $c_2^{start} = c_2^{out}$, $c_1^{start} = c_1^{0}$, $c_1^{end} = c_1^{F}$ and $c_2^{end} = c_2^{in}$. The resulting expression for $\zeta^*\big|_{c_c^{in}}$ (omitted here) is differentiated with respect to c_2^{out} and inserted into the ODE Eq. (B-11). This ODE can now be integrated (by a numerical solver) between c_2^{I1} and c_2^{out}, with the corresponding initial condition of ζ^* (according to Eq. (3-45), since c_2^{I1} and c_2^{F} are the coupled concentrations of the solute outside and inside the injection media). The result of this routine is the shockpath $\widetilde{\zeta} = f(c_2^{out})$. The ODE in Eq. (B-11) could be rearranged to obtain the concentration of the shock as a function of the space position. However, this is even more exhausting, compared to the method presented here. I rather recommend using this solution with the shockpath as a function of the solute concentration and scanning for the concentration at a desired space position.

Nomenclature

Matrices and vectors are printed in bold face (e.g. $\mathbf{A}$), while its elements are defined as A_{ij} resp. A_i.

A_c, (cm^2)	cross sectional area of a column, Eqs. (2-2), (2-5)
$\mathbf{A}$, (-)	process matrix or process function, Eqs. (2-33), (2-34)
a or H, (-)	Henry coefficient, Eqs. (2-8), (2-9), (2-12), (5-7), (5-12)
a_{cou}, (-)	courant number / numerical stability criteria, Eq. (2-23)
b, ml/mg or ml/mol	equilibrium constant of an isotherm, Eqs. (2-8), (2-10), (2-12), (5-7)
c, mg/ml or mol/ml	concentration in the fluid phase, Eqs. (2-13), (2-19)
c_S, mg/ml	solubility, Eqs. (4-1), (A-3), (A-4)
d, cm	inner diameter of a cylindrical column, Eq. (2-2)
D_{app}, cm^2/s	apparent axial dispersion coefficient, Eqs. (2-19), (2-20), (2-23)
F, (-)	phase ratio between volume of solid and liquid phase in a column, Eq. (2-4)
g, v/v	modifier based solvent composition, defined as $g = \dfrac{V_{mod}}{V_{mod} + V_{inert}}$
$\mathbf{I}$, (-)	Unit matrix, Eq. (2-36)
K, (-)	equilibrium constant of displacement adsorption isotherm, Eq. (5-5)
k, 1/s	apparent mass transfer coefficient, Eqs. (2-1), (2-25)
k', (-)	retention factor, $k' = F \times H$, Eqs. (2-27), (2-28)
L, cm	length of the column, Eq. (2-2)

m, g	mass
M, g/mol	molecular weight
n, mol	amount of substance
N_C, *(-)*	number of adsorbable components in the system, Eq. (2-13)
NTP, (-)	number of theoretical stages, Eqs. (2-6), (2-7)
OF	objective function, Eqs. (5-10), (5-13)
p, (-)	parameters in Eq. (5-12)
PR, mg/min	productivity, Eq. (5-15)
Q, ml/min	volumetric flow rate, Eq. (2-3)
q, mg/ml or mol/ml	concentration on the surface of the solid phase, Eqs. (2-8)-(2-12), (2-13), (2-19), (2-29)
q^{∞}, *mol/ml*	saturation constant of displacement adsorption isotherm, Eq. (5-6)
q_S, *mg/ml*	saturation constant of the Langmuir isotherm, Eqs. (2-8), (2-11), (5-7)
REC, (-)	recovery, Eq. (5-16)
t, s or min	time, Eqs. (2-13), (2-19)
t_R, *s or min*	retention time Eqs. (2-7)(2-17)
t_0, *s or min*	dead time, Eq. (2-3)
u, cm/s	linear velocity of the mobile phase, Eq. (2-5)
u_c, *cm/s*	propagation / wave velocity of a certain concentration, Eq. (2-17)
u_z, *cm/s*	propagation velocity of a shock, Eq. (2-18)
V_c, *ml*	volume of an empty column, Eq. (2-2)
V_S, *ml*	volume of the solid phase within a column, Eq. (2-4)
V_0, *ml*	volume of the liquid phase within a column / dead volume, Eqs. (2-1), (2-3)

x, mol%	concentration / solvent composition defined as $x_{mod} = \dfrac{n_{mod}}{n_{mod} + n_{inert}}$, Eqs. (2-26), (5-2), (5-3), (5-7)
y,	volume fraction in the solution defined as $y_i = \dfrac{V_i}{V_{solution}}$
z, cm	axial space coordinate, Eqs. (2-13), (2-19)

Sub- and superscripts

*	equilibrium, Eq. (2-24), (5-7)
0	initial condition / initial state
calc	calculated
EtOH	ethanol
exp	experimental
F	feed condition / feed state
H2O	water
I1	intermediate state on the transition from the initial to the feed state
I2	intermediate state on the transition from the feed to the initial state
inert	inert component of the mobile phase
inj	injection
k	index of time increment, (2-22)
MeOH	Methanol
mod	modifier component of the mobile phase
n	index of space increment, Eq. (2-22)

Greek

α, (–)	separation factor defined as $\alpha = \dfrac{H_2}{H_1}, H_2 > H_1$, Eq. (A-2)
Γ, mol/ml	excess loading, Eqs. (2-26), (5-4), (5-9)
ε, (–)	overall column porosity, Eq. (2-1)
γ, (–)	activity coefficient, Eqs. (5-5), (A-7)
ρ, g/ml	density, Eqs. (5-2), (A-8)
ζ, (–)	dimensionless space variable, Eqs. (2-32), (2-33)
λ, (–)	vector of Eigenvalues of the process matrix A, Eq. (2-36)
Λ, (–)	interaction parameters of the Margules equation, Eq. (A-7)
μ, (–)	first absolute moment, Eq. (2-6)
σ, (–)	second relative moment, Eq. (2-6)
τ, (–)	dimensionless time variable, Eqs. (2-32), (2-33)

References

1.   Ahmad, T. and G. Guiochon, *Numerical determination of the adsorption isotherms of tryptophan at different temperatures and mobile phase compositions.* Journal of Chromatography A **1142** 2007: p. 148-163.

2.   Antos, D., W. Piatkowski and K. Kaczmarski, *Determination of mobile phase effect on single-component adsorption isotherm by use of numerical estimation.* Journal of Chromatography A **874** 2000: p. 1-12.

3.   Antos, D. and A. Seidel-Morgenstern, *Application of gradients in the simulated moving bed process.* Chemical Engineering Science **56** 2001: p. 6667-6682.

4.   Antos, D. and A. Seidel-Morgenstern, *Continuous step gradient elution for preparative separations.* Separation Science and Technology **37** 2002: p. 1469-1487.

5.   Antos, D., *Gradient techniques in preparative chromatography*, Habilitation, Universität Magdeburg, Fakultät für Verfahrens- und Systemtechnik & Oficyna Wyd. Politechn. Rzeszowskiej: 2003.

6.   Antos, D., K. Kaczmarski, W. Piatkowski and A. Seidel-Morgenstern, *Concentration dependence of lumped mass transfer coefficients - Linear versus non-linear chromatography and isocratic versus gradient operation.* Journal of Chromatography A **1006** 2003: p. 61-76.

7.   Araújo, J.M.M., R.C.R. Rodrigues and J.P.B. Mota, *Determination of competitive isotherms of enantiomers by a hybrid inverse method using overloaded band profiles and the periodic state of the simulated moving-bed process.* Journal of Chromatography A **1189** 2008: p. 302-313.

8.   Arnell, R., P. Forssén and T. Fornstedt, *Accurate and rapid estimation of adsorption isotherms in liquid chromatography using the inverse method on plateaus.* Journal of Chromatography A **1099** 2005: p. 167-174.

9.   Ayrton, J., G.J. Dear, W.J. Leavens, D.N. Mallett and R.S. Plumb, *Use of generic fast gradient liquid chromatography tandem mass spectroscopy in quantitative bioanalysis.* Journal of Chromatography B **709** 1998: p. 243-254.

10.   Bechtold, M., M. Heinemann and S. Panke, *Suitability of teicoplaninaglycone bonded stationary phase for simulated moving bed enantioseparation of racemic amino acids employing composition-constrained eluents.* Journal of Chromatography A **1113** 2006: p. 167-176.

11.   Berninger, J.A., R.D. Whitley, X. Zhang and N.-H.L. Wang, *A versatile model for simulation of reaction and nonequilibrium dynamics in multicom-*

ponent fixed-bed adsorption processes. Computers & Chemical Engineering **15** 1991: p. 749-768.

12. Blehaut, J. and R.M. Nicoud, *Recent aspects in simulated moving bed.* Analusis **26** 1998: p. M60-M70.

13. Blümel, C., P. Hugo and A. Seidel-Morgenstern, *Quantification of single solute and competitive adsorption isotherms using a closed-loop perturbation method.* Journal of Chromatography A **865** 1999: p. 51-71.

14. Broughton, D.B. and C.G. Gerold, *Continuous sorption process employing fixed bed of sorbent and moving inlets and outlets*, US patent 2.985.589, 1961

15. Broughton, D.B., *Production-Scale Adsorptive Separations of Liquid Mixtures by Simulated Moving-Bed Technology.* Separation Science and Technology **19** 1984: p. 723 - 736.

16. Brunnauer, S., P.H. Emmet and E. Teller, *Adsorption of Gases in Multimolecular Layers.* Journal of the American Chemical Society **60** 1938: p. 309-319.

17. Camin, D.L. and A.J. Raymond, *Chromatography in Petroleum-Industry.* Journal of Chromatographic Science **11** 1973: p. 625-638.

18. Cavazzini, A., A. Felinger and G. Guiochon, *Comparison between adsorption isotherm determination techniques and overloaded band profiles on four batches of monolithic columns.* Journal of Chromatography A **1012** 2003: p. 139-149.

19. Coates, J.I. and E. Glueckauf, *Theory of Chromatography .3. Experimental Separation of 2 Solutes and Comparison with Theory.* Journal of the Chemical Society 1947: p. 1308-1314.

20. Cretier, G., M. El Khabchi and J.L. Rocca, *Preparative liquid chromatography : II. Existence of optimum injection conditions for overloaded gradient elution separations.* Journal of Chromatography A **596** 1992: p. 15-25.

21. Czok, M. and G. Guiochon, *Comparison of the results obtained with different models for the simulation of preparative chromatography.* Computers & Chemical Engineering **14** 1990: p. 1435-1443.

22. Denet, F., W. Hauck, R.M. Nicoud, O. Di Giovanni, M. Mazzotti, J.N. Jaubert and M. Morbidelli, *Enantioseparation through supercritical fluid simulated moving bed (SF-SMB) chromatography.* Industrial & Engineering Chemistry Research **40** 2001: p. 4603-4609.

23. DeVault, D., *The theory of chromatography.* Journal of the American Chemical Society **65** 1943: p. 532-540.

24. Dolan, J.W., J.R. Gant and L.R. Snyder, *Gradient elution in high-performance liquid chromatography: II. Practical application to reversed-phase systems.* Journal of Chromatography **165** 1979: p. 31-58.

25. Dose, E.V., S. Jacobson and G. Guiochon, *Determination of Isotherms from Chromatographic Peak Shapes.* Analytical Chemistry **63** 1991: p. 833-839.

26. Elfallah, M.Z. and G. Guiochon, *Comparison of Experimental and Calculated Results in Overloaded Gradient Elution Chromatography for a Single-Component Band.* Analytical Chemistry **63** 1991: p. 859-867.

27. Everett, D.H., *Manual of Symbols and Terminology for Physico-chemical Quantities and Units, Appendix II, Part 1: Definitions,Terminology and Symbols in Colloid and Surface Chemistry.* Pure and Applied Chemistry **31** 1972: p. 579-638.

28. Everett, D.H., *Thermodynamics of Interfacial Phenomena.* Pure and Applied Chemistry **53** 1981: p. 2181-2198.

29. Everett, D.H., *Reporting Data on Adsorption from Solution at the Solid/Solution Interface.* Pure and Applied Chemistry **58** 1986: p. 9976-984.

30. Felinger, A. and G. Guiochon, *Optimizing preparative separations at high recovery yield.* Journal of Chromatography A **752** 1996: p. 31-40.

31. Felinger, A., A. Cavazzini and G. Guiochon, *Numerical determination of the competitive isotherm of enantiomers.* Journal of Chromatography A **986** 2003: p. 207-225.

32. Felinger, A., D. Zhou and G. Guiochon, *Determination of the single component and competitive adsorption isotherms of the 1-indanol enantiomers by the inverse method.* Journal of Chromatography A **1005** 2003: p. 35-49.

33. Feng, W., X. Zhu, L. Zhang and X. Geng, *Retention behaviour of proteins under conditions of column overload in hydrophobic interaction chromatography.* Journal of Chromatography A **729** 1996: p. 43-47.

34. Forssén, P., J. Lindholm and T. Fornstedt, *Theoretical and experimental study of binary perturbation peaks with focus on peculiar retention behaviour and vanishing peaks in chiral liquid chromatography.* Journal of Chromatography A **991** 2003: p. 31-45.

35. Forssén, P., R. Arnell and T. Fornstedt, *An improved algorithm for solving inverse problems in liquid chromatography.* Computers & Chemical Engineering **30** 2006: p. 1381-1391.

36. Francotte, E. and A. Junkerbuchheit, *Preparative Chromatographic-Separation of Enantiomers.* Journal of Chromatography B **576** 1992: p. 1-45.

37. Francotte, E., *Contribution of Preparative Chromatographic Resolution to the Investigation of Chiral Phenomena.* Journal of Chromatography A **666** 1994: p. 565-601.

38. Francotte, E.R., *Enantioselective chromatography as a powerful alternative for the preparation of drug enantiomers.* Journal of Chromatography A **906** 2001: p. 379-397.

39. Fung, K.Y., K.M. Ng and C. Wibowo, *Synthesis of chromatography and crystallization hybrid separation processes.* Industrial & Engineering Chemistry Research **44** 2005: p. 910-921.

40. Gedicke, K., W. Beckmann, A. Brandt, D. Sapoundjiev, H. Lorenz, U. Budde and A. Seidel-Morgenstern, *Coupling chromatography and crystallization for efficient separations of isomers.* Adsorption **11** 2005: p. 591-596.

41. Gedicke, K., M. Tomusiak, D. Antos and A. Seidel-Morgenstern, *Analysis of applying different solvents for the mobile phase and for sample injection.* Journal of Chromatography A **1092** 2005: p. 142-148.

42.   Gedicke, K., D. Antos and A. Seidel-Morgenstern, *Effect on Separation of Injecting Samples in a Solvent Different from the Mobile Phase.* Journal of Chromatography A **1162** 2007: p. 62-73.

43.   Gedicke, K., M. Kaspereit, W. Beckmann, U. Budde, H. Lorenz and A. Seidel-Morgenstern, *Conceptual Design & Feasibility Study of Combining Continuous Chromatography and Crystallisation for Stereoisomer Separations.* Chemical Engineering Research and Design **85** 2007: p. 928-936.

44.   Gibbs, J.W., *The Collected Works Of J. Willard Gibbs.* Vol. 1. 1948, Yale University Press: New Haven.

45.   Giddings, J.C., *Unified separation science.* 1991, Wiley: New York.

46.   Glueckauf, E., *Chromatography of 2 Solutes.* Nature **156** 1945: p. 205-206.

47.   Glueckauf, E., *Contributions to the Theory of Chromatography.* Proceedings of the Royal Society of London Series a-Mathematical and Physical Sciences **186** 1946: p. 35-57.

48.   Glueckauf, E., *Theory of Chromatography .2. Chromatograms of a Single Solute.* Journal of the Chemical Society 1947: p. 1302-1308.

49.   Glueckauf, E., *Theory of Chromatography .5. Separation of 2 Solutes Following a Freundlich Isotherm.* Journal of the Chemical Society 1947: p. 1321-1329.

50.   Glueckauf, E., *Theory of Chromatography .7. The General Theory of 2 Solutes Following Non-Linear Isotherms.* Discussions of the Faraday Society 1949: p. 12-25.

51.   Golshan-Shirazi, S., S. Ghodbane and G. Guiochon, *Comparison between Experimental and Theoretical Band Profiles in Nonlinear Liquid-Chromatography with a Pure Mobile Phase.* Analytical Chemistry **60** 1988: p. 2630-2634.

52.   Golshan-Shirazi, S. and G. Guiochon, *Comparison between Experimental and Theoretical Band Profiles in Nonlinear Liquid-Chromatography with a Binary Mobile Phase.* Analytical Chemistry **60** 1988: p. 2634-2641.

53.   Golshan-Shirazi, S. and G. Guiochon, *Analytical solution of the ideal model of elution chromatography in the case of a binary mixture with competitive Langmuir isotherms : II. Solution using the h-transform.* Journal of Chromatography A **484** 1989: p. 125-151.

54.   Golshan-Shirazi, S. and G. Guiochon, *Analytical solution for the ideal model of chromatography in the case of a pulse of a binary mixture with competitive Langmuir isotherm.* Journal of Physical Chemistry **93** 1989: p. 4143-4157.

55.   Golshan-Shirazi, S. and G. Guiochon, *Modeling of preparative liquid chromatography.* Journal of Chromatography A **658** 1994: p. 149-171.

56.   Grill, C.M., *Closed-loop recycling with periodic intra-profile injection: a new binary preparative chromatographic technique.* Journal of Chromatography A **796** 1998: p. 101-113.

57.   Grill, C.M. and L. Miller, *Separation of a racemic pharmaceutical intermediate using closed-loop steady state recycling.* Journal of Chromatography A **827** 1998: p. 359-371.

58.   Grill, C.M., L. Miller and T.Q. Yan, *Resolution of a racemic pharmaceutical intermediate: A comparison of preparative HPLC, steady state recycling, and simulated moving bed.* Journal of Chromatography A **1026** 2004: p. 101-108.

59.   Gritti, F., A. Felinger and G. Guiochon, *Overloaded gradient elution chromatography on heterogeneous adsorbents in reversed-phase liquid chromatography.* Journal of Chromatography A **1017** 2003: p. 45–61.

60.   Gritti, F. and G. Guiochon, *Bandsplitting in overloaded isocratic elution chromatography II. New competitive adsorption isotherms.* Journal of Chromatography A **1008** 2003: p. 23–41.

61.   Grüner, S. and A. Kienle, *Equilibrium theory and nonlinear waves for reactive distillation columns and chromatographic reactors.* Chemical Engineering Science **59** 2004: p. 901-918.

62.   Grüner, S., M. Mangold and A. Kienle, *Dynamics of reaction separation processes in the limit of chemical equilibrium.* AIChE Journal **52** 2006: p. 1010-1026.

63.   Guiochon, G. and S. Golshan-Shirazi, *A retrospective on the solution of the ideal model of chromatography.* Journal of Chromatography A **658** 1994: p. 173-177.

64.   Guiochon, G., S. Golshan-Shirazi and A.M. Katti, *Fundamentals of Preparative and Nonlinear Chromatography.* 1994, Academic Press: Boston.

65.   Guiochon, G., *Preparative liquid chromatography.* Journal of Chromatography A **965** 2002: p. 129-161.

66.   Guiochon, G., A. Felinger, S.G. Shirazi and A.M. Katti, *Fundamentals of Preparative and Nonlinear Chromatography.* 2.nd ed. 2006, Elsevier: Amsterdam.

67.   Heikkila, H., G. Hyöky and J. Kuisma, *Method for the recovery of betaine from molasses*, US patent 5.127.957, 1992

68.   Helfferich, F. and D.B. James, *An equilibrium theory for rare-earth separation by displacement development.* Journal of Chromatography A **46** 1970: p. 1-28.

69.   Helfferich, F.G., *Multicomponent Ion Exchange in Fixed Beds - Generalized Equilibrium Theory for Systems with Constant Separation Factors.* Industrial & Engineering Chemistry Fundamentals **6** 1967: p. 362-&.

70.   Helfferich, F.G., *Theory of multicomponent chromatography a state-of-the-art report.* Journal of Chromatography A **373** 1986: p. 45-60.

71.   Helfferich, F.G. and P.W. Carr, *Non-linear waves in chromatography: 1. Waves, shocks, and shapes.* Journal of Chromatography A **629** 1993: p. 97-122.

72.   Helfferich, F.G. and R.D. Whitley, *Non-linear waves in chromatography: 2. Wave interference and coherence in multicomponent systems.* Journal of Chromatography A **734** 1996: p. 7-47.

73.   Helfferich, F.G., *Non-linear waves in chromatography: 3. Multicomponent Langmuir and Langmuir-like systems.* Journal of Chromatography A **768** 1997: p. 169-205.

74.   Hesse, G. and H. Weil, *Michael Tswett's erste chromatographische Schrift.* 1954, Woelm: Eschwege.

75.   Heuer, C., H. Kniep, T. Falk and A. Seidel-Morgenstern, *Comparison of Various Process Engineering Concepts of Preparative Chromatography.* Chemical Engineering & Technology **21** 1998: p. 469-477.

76.   Hoffman, N.E., S.-L. Pan and A.M. Rustum, *Injection of eluites in solvents stronger than the mobile phase in reversed-phase liquid chromatography.* Journal of Chromatography A **465** 1989: p. 189-200.

77.   Howard, A.J., G. Carta and C.H. Byers, *Separation of Sugars by Continuous Annular Chromatography.* Industrial & Engineering Chemistry Research **27** 1988: p. 1873-1882.

78.   James, F., M. Sepulveda, F. Charton, I. Quinones and G. Guiochon, *Determination of binary competitive equilibrium isotherms from the individual chromatographic band profiles.* Chemical Engineering Science **54** 1999: p. 1677-1696.

79.   Jandera, P. and J. Churácek, *Gradient elution in liquid chromatography: I. The influence of the composition of the mobile phase on the capacity ratio (retention volume, band width, and resolution) in isocratic elution -- theoretical considerations.* Journal of Chromatography A **91** 1974: p. 207-221.

80.   Jandera, P. and G. Guiochon, *Effect of the sample solvent on band profiles in preparative liquid chromatography using non-aqueous reversed-phase high-performance liquid chromatography.* Journal of Chromatography **588** 1991: p. 1-14.

81.   Jandera, P. and G. Guiochon, *Adsorption isotherms of cholesterol and related compounds in non-aqueous reversed-phase chromatographic systems.* Journal of Chromatography A **605** 1992: p. 1-17.

82.   Jandera, P., Z. Posvec and P. Vraspir, *Mobile phase effects on single-component and competitive adsorption isotherms in reversed-phase systems.* Journal of Chromatography A **734** 1996: p. 125-136.

83.   Jandera, P., D. Komers and G. Guiochon, *Effects of the gradient profile on the production rate in reversed-phase gradient elution overloaded chromatography.* Journal of Chromatography A **760** 1997: p. 25-39.

84.   Jandera, P. and M. Kucerova, *Prediction of retention in gradient-elution normal-phase high-performance liquid chromatography with binary solvent gradients.* Journal of Chromatography A **759** 1997: p. 13-25.

85.   Jandera, P., D. Komers and G. Guiochon, *Optimization of the recovery yield and of the production rate in overloaded gradient-elution reversed-phase chromatography.* Journal of Chromatography A **796** 1998: p. 115-127.

86.   Jandera, P., M. Skavrada, L. Andel, D. Komers and G. Guiochon, *Description of adsorption equilibria in liquid chromatography systems with binary mobile phases.* Journal of Chromatography A **908** 2001: p. 3–17.

87.   Jüneman, S., W. Wewers and H. Schmidt-Traub, *Combination of Chromatography and crystallization in biotechnological downstream processes.* 2002: Heidelberg.

88. Kaczmarski, K. and D. Antos, *Modified Rouchon and Rouchon-like algorithms for solving different models of multicomponent preparative chromatography.* Journal of Chromatography A **756** 1996: p. 73-87.

89. Kaczmarski, K. and D. Antos, *Erratum to "Modified Rouchon and Rouchon-like algorithms for solving different models of multicomponent preparative chromatography": [J. Chromatogr. A, 756 (1996) 73-87].* Journal of Chromatography A **777** 1997: p. 383.

90. Kaczmarski, K., M. Mazzotti, G. Storti and M. Morbidelli, *Modeling fixed-bed adsorption columns through orthogonal collocations on moving finite elements.* Computers & Chemical Engineering **21** 1997: p. 641-660.

91. Kaczmarski, K. and D. Antos, *Calculation of chromatographic band profiles with an implicit isotherm.* Journal of Chromatography A **862** 1999: p. 1-16.

92. Kaczmarski, K., *Estimation of adsorption isotherm parameters with inverse method—Possible problems.* Journal of Chromatography A **1176** 2007: p. 57–68.

93. Kaspereit, M., P. Jandera, M. Skavrada and A. Seidel-Morgenstern, *Impact of adsorption isotherm parameters on the performance of enantioseparation using simulated moving bed chromatography.* Journal of Chromatography A **944** 2002: p. 249-262.

94. Kaspereit, M., H. Lorenz and A. Seidel-Morgenstern, *Coupling of simulated moving bed technology and crystallization to separate enantiomers*, in *Fundamentals of Adsorption 7*, K. Kaneko, H. Kanoh, and Y. Hanzawa, Editors. 2002, IK International Ltd.: Shinjuko (Japan). p. 101-108.

95. Kaspereit, M., K. Gedicke, V. Zahn, A.W. Mahoney and A. Seidel-Morgenstern, *Shortcut method for evaluation and design of a hybrid process for enantioseparations.* Journal of Chromatography A **1092** 2005: p. 43-54.

96. Kaspereit, M., *Separation of Enantiomers by a Process Combination of Chromatography and Crystallisation.* 2006, Shaker Verlag: Aachen.

97. Kaspereit, M., A. Seidel-Morgenstern and A. Kienle, *Design of simulated moving bed processes under reduced purity requirements.* Journal of Chromatography A **1162** 2007: p. 2–13.

98. Katti, A. and G. Guiochon, *Optimization of sample size and sample volume in preparative liquid chromatography.* Analytical Chemistry **61** 1989: p. 982-990.

99. Kennedy, J.H., M.D. Belvo, V.S. Sharp and J.D. Williams, *Comparison of separation efficiency of early phase active pharmaceutical intermediates by steady state recycle and batch chromatographic techniques.* Journal of Chromatography A **1046** 2004: p. 55-60.

100. Khachik, F., G. Beecher, J. Vanderslice and G. Furrow, *Liquid chromatographic artifacts and peak distortion: sample-solvent interactions in the separation of carotenoids.* Analytical Chemistry **60** 1988: p. 807 - 811.

101. Kishihara, S., S. Fuji, H. Tamaki, K.B. Kim, N. Wakiuchi and T. Yamamoto, *Continuous chromatographic separation of sucrose, glucose and fructose us-*

ing a simulated moving bed adsorber. International Sugar Journal **94** 1992: p. 305–308.

102. Kniep, H., *Vergleich verschiedener verfahrenstechnischer Konzepte zur Durchführung der präparativen Flüssigkeitschromatographie*, Dissertation, Fakultät für Verfahrens- und Systemtechnik, Otto-von-Guericke-Universität, Magdeburg, Germany: 1998.

103. Langmuir, I., *Constitution of Solids and Liquids.* Journal of the American Chemical Society **38** 1916: p. 2221-2295.

104. Layne, J., T. Farcas, I. Rustamov and F. Ahmed, *Volume-load capacity in fast-gradient liquid chromatography: Effect of sample solvent composition and injection volume on chromatographic performance.* Journal of Chromatography A **913** 2001: p. 233-242.

105. Lisec, O., P. Hugo and A. Seidel-Morgenstern, *Frontal analysis method to determine competitive adsorption isotherms.* Journal of Chromatography A **908** 2001: p. 19-34.

106. Lorenz, H., P. Sheehan and A. Seidel-Morgenstern, *Coupling of simulated moving bed chromatography and fractional crystallisation for efficient enantioseparation.* Journal of Chromatography A **908** 2001: p. 201-214.

107. Lorenz, H., D. Sapoundjiev and A. Seidel-Morgenstern, *Solubility Equilibria in Chiral Systems and Their Importance for Enantioseparation.* Engineering in Life Sciences **3** 2003: p. 132-136.

108. Ludemann-Hombourger, O., R.M. Nicoud and M. Bailly, *The "VARICOL" process: A new multicolumn continuous chromatographic process.* Separation Science and Technology **35** 2000: p. 1829-1862.

109. Ma, Z. and G. Guiochon, *Application of orthogonal collocation on finite elements in the simulation of non-linear chromatography.* Computers & Chemical Engineering **15** 1991: p. 415-426.

110. Mair, B.J., A.L. Gaboriault and F.D. Rossini, *Assembly and Testing of 52-Foot Laboratory Adsorption Column - Separation of Hydrocarbons by Adsorption.* Industrial and Engineering Chemistry **39** 1947: p. 1072-1081.

111. Mair, B.J., A.J. Sweetman and F.D. Rossini, *Separation of Gas-Oil and Wax Fractions of Petroleum by Adsorption.* Industrial and Engineering Chemistry **41** 1949: p. 2224-2230.

112. Mair, B.J., J.W. Westhaver and F.D. Rossini, *Theoretical Analysis of Fractionating Process of Adsorption.* Industrial and Engineering Chemistry **42** 1950: p. 1279-1286.

113. Mair, B.J., M.J. Montjar and F.D. Rossini, *Fractionation of Hydrocarbons by Adsorption with Added Components.* Analytical Chemistry **28** 1956: p. 56-61.

114. Mann, G. personal communication: Schering AG, Berlin.

115. Mazzotti, M., G. Storti and M. Morbidelli, *Robust Design of Countercurrent Adsorption Separation Processes .2. Multicomponent Systems.* AIChE Journal **40** 1994: p. 1825-1842.

116. Mazzotti, M., G. Storti and M. Morbidelli, *Robust design of countercurrent adsorption separation .3. Nonstoichiometric systems.* AIChE Journal **42** 1996: p. 2784-2796.

117. Mazzotti, M., G. Storti and M. Morbidelli, *Optimal operation of simulated moving bed units for nonlinear chromatographic separations.* Journal of Chromatography A **769** 1997: p. 3-24.

118. Mazzotti, M., G. Storti and M. Morbidelli, *Robust design of countercurrent adsorption separation processes .4. Desorbent in the feed.* AIChE Journal **43** 1997: p. 64-72.

119. Mazzotti, M., G. Storti and M. Morbidelli, *Optimal operation of simulated moving bed units for nonlinear chromatographic separations.* Journal of Chromatography A **769** 1997: p. 3-24.

120. Mersmann, A., K. Bartosch, B. Braun, A. Eble and C. Heyer, *Approaches to the predictive estimation of crystallisation kinetics.* Chemie Ingenieur Technik **72** 2000: p. 17-30.

121. Michel, M., A. Epping and A. Jupke, *Modeling and Determination of Model Parameters*, in *Preparative Chromatography of Fine Chemicals and Pharmaceutical Agents*, H. Schmidt-Traub, Editor. 2005, Wiley-VCH: Weinheim. p. 215-313.

122. Migliorini, C., M. Mazzotti and M. Morbidelli, *Continuous chromatographic separation through simulated moving beds under linear and nonlinear conditions.* Journal of Chromatography A **827** 1998: p. 161-173.

123. Migliorini, C., M. Mazzotti and M. Morbidelli, *Robust design of countercurrent adsorption separation processes: 5. Nonconstant selectivity.* AIChE Journal **46** 2000: p. 1384-1399.

124. Ndzié, E., O. Ludemann-Hombourger, J. Bléhaut, S.R. Perrin and W. Hauck, *Coupling chromatography with crystallization: Global purification process*, in *10th International Workshop on Industrial Crystallization (BIWIC 2003)*, G. Coquerel, Editor. 2003: Rouen (France). p. 87-94.

125. Nicoud, R.M., G. Fuchs, P. Adam, M. Bailly, E. Kusters, F.D. Antia, R. Reuille and E. Schmid, *Preparative-Scale Enantioseparation of a Chiral Epoxide - Comparison of Liquid-Chromatography and Simulated Moving-Bed Adsorption Technology.* Chirality **5** 1993: p. 267-271.

126. Nielsen, A.E., *Kinetics of precipitation.* 1964, Pergamon Press [distributed in the Western Hemisphere by Macmillan, New York]: Oxford.

127. Nowak, J., K. Gedicke, D. Antos, W. Piatkowski and A. Seidel-Morgenstern, *Synergistic effects in competitive adsorption of carbohydrates on an ion-exchange resin.* Journal of Chromatography A **1164** 2007: p. 224-234.

128. Nowak, J., I. Poplewska, D. Antos and A. Seidel-Morgenstern, *Adsorption behaviour of sugars versus their activity in single and multicomponent liquid solutions.* Journal of Chromatography A **1216** 2009: p. 8697-8704.

129. Oscik, J., *Adsorption.* 1982, Ellis Horwood Limited: Chichester.

130. Perry, J.H. and D.W. Green, *Perry's Chemical Engineers' Handbook.* 7th ed. 1998, McGraw-Hill: New York.

131.   Piatkowski, W., D. Antos and K. Kaczmarski, *Modeling of preparative chromatography processes with slow intraparticle mass transport kinetics.* Journal of Chromatography A **988** 2003: p. 219-231.

132.   Piatkowski, W., I. Petrushka and D. Antos, *Adsorbed solution model for prediction of normal-phase chromatography process with varying composition of the mobile phase.* Journal of Chromatography A **1092** 2005: p. 65-75.

133.   Piatkowski, W., R. Kramarz, I. Poplewska and D. Antos, *Deformation of gradient shape as a result of preferential adsorption of solvents in mixed mobile phases.* Journal of Chromatography A **1127** 2006: p. 187-199.

134.   Poplewska, I. and D. Antos, *Effect of adsorption of organic solvents on the band profiles in reversed-phase non-linear chromatography.* Chemical Engineering Science **60** 2005: p. 1411-1427.

135.   Poplewska, I., W. Piatkowski and D. Antos, *Effect of temperature on competitive adsorption of the solute and the organic solvent in reversed-phase liquid chromatography.* Journal of Chromatography A **1103** 2006: p. 284-295.

136.   Poplewska, I., R. Kramarz, W. Piatkowski, A. Seidel-Morgenstern and D. Antos, *Behavior of adsorbed and fluid phases versus retention properties of amino acids on the teicoplanin chiral selector.* Journal of Chromatography A **1192** 2008: p. 130-138.

137.   Press, W.H., S.A. Teukolsky, W.T. Vetterling and B.P. Flannery, *Numerical Recipes: The Art of Scientific Computing.* 2.nd ed. 1992, Cambridge University Press

138.   Quinones, I., C.M. Grill, L. Miller and G. Guiochon, *Modeling of separations by closed-loop steady-state recycling chromatography of a racemic pharmaceutical intermediate.* Journal of Chromatography A **867** 2000: p. 1-21.

139.   Radke, C.J. and J.M. Prausnitz, *Thermodynamics of multi-solute adsorption from dilute liquid solutions.* AIChE Journal **18** 1972: p. 761-768.

140.   Rhee, H.K., R. Aris and N.R. Amundson, *Theory of Multicomponent Chromatography.* Philosophical Transactions of the Royal Society of London Series a-Mathematical and Physical Sciences **267** 1970: p. 419-&.

141.   Rhee, H.K., R. Aris and N.R. Amundson, *Multicomponent Adsorption in Continuous Countercurrent Exchangers.* Philosophical Transactions of the Royal Society of London Series a-Mathematical and Physical Sciences **269** 1971: p. 187-&.

142.   Rhee, H.-K., R. Aris and N.R. Amundson, *First -Order Partial Differential Equations: Volume 2 Theory and Application of Hyperbolic Systems of Quasiliniear Equations.* 2001, Dover Publications, Inc.: Mineola.

143.   Rhee, H.-K., R. Aris and N.R. Amundson, *First -Order Partial Differential Equations: Volume 1 Theory and Application of Single Equations.* 2001, Dover Publications, Inc.: Mineola.

144.   Rouchon, P., M. Schonauer, P. Valentin and G. Guiochon, *Numerical-Simulation of Band Propagation in Nonlinear Chromatography.* Separation Science and Technology **22** 1987: p. 1793-1833.

145. Rustamov, I., T. Farcas, F. Ahmed, F. Chan, R. LoBrutto, H.M. McNair and Y.V. Kazakevich, *Geometry of chemically modified silica.* Journal of Chromatography A **913** 2001: p. 49-63.

146. Ruthven, D.M., *Principles of Adsorption and Adsorption Processes.* 1984: Wiley & Sons.

147. Ruthven, D.M. and C.B. Ching, *Counter current and simulated counter current adsorption separation processes.* Chemical Engineering Science **44** 1989: p. 1011-1038.

148. Sainio, T. and M. Kaspereit, *Analysis of steady state recycling chromatography using equilibrium theory.* Separation and Purification Technology **66** 2009: p. 9-18.

149. Samuelsson, J., P. Sajonz and T. Fornstedt, *Impact of an error in the column hold-up time for correct adsorption isotherm determination in chromatography: I. Even a small error can lead to a misunderstanding of the retention mechanism.* Journal of Chromatography A **1189** 2008: p. 19-31.

150. Samuelsson, J., J. Zang, A. Murunga, T. Fornstedt and P. Sajonz, *Impact of an error in the column hold-up time for correct adsorption isotherm determination in chromatography: II. Can a wrong column porosity lead to a correct prediction of overloaded elution profiles?* Journal of Chromatography A **1194** 2008: p. 205-212.

151. Sapoundjiev, D., H. Lorenz and A. Seidel-Morgenstern, *Solubility of chiral threonine species in water/ethanol mixtures.* Journal of Chemical and Engineering Data **51** 2006: p. 1562-1566.

152. Sapoundjiev, D., *Löslichkeitsgleichgewichte von Stereoisomeren-Bedeutung, experimentelle Ermittlung und Anwendung*, Dissertation, Fakultät für Verfahrens- und Systemtechnik, Otto-von-Guericke Universität, Mageburg, Germany: 2007.

153. Schay, G., *Adsorption of Solutions of Nonelectrolytes*, in *Surface and Colloid Science*, E. Matijevic, Editor. 1969, Wiley: London. p. 155-212.

154. Schay, G., *A comprehensive presentation of the thermodynamics of adsorption excess quantities.* Pure & Applied Chemistry **48** 1976: p. 393-400.

155. Schramm, H., M. Kaspereit, A. Kienle and A. Seidel-Morgenstern, *Simulated moving bed process with cyclic modulation of the feed concentration.* Journal of Chromatography A **1006** 2003: p. 77-86.

156. Schramm, H., A. Kienle, M. Kaspereit and A. Seidel-Morgenstern, *Improved operation of simulated moving bed processes through cyclic modulation of feed flow and feed concentration.* Chemical Engineering Science **58** 2003: p. 5217-5227.

157. Schubert, H. and A. Mersmann, *Determination of heterogeneous nucleation rates.* Chemical Engineering Research & Design **74** 1996: p. 821-827.

158. Schulte, M. and J. Strube, *Preparative enantioseparation by simulated moving bed chromatography.* Journal of Chromatography A **906** 2001: p. 399-416.

159.   Seidel-Morgenstern, A., *Mathematische Modellierung der präparativen Flüssigchromatographie.* 1995, DUV: Wiesbaden.

160.   Seidel-Morgenstern, A., *Experimental determination of single solute and competetive adsorption isotherms.* Journal of Chromatography A **1037** 2004: p. 255-272.

161.   Seidel-Morgenstern, A., *Preparative gradient chromatography.* Chemical Engineering & Technology **28** 2005: p. 1265-1273.

162.   Seidel-Morgenstern, A., U. Budde, H. Lorenz, W. Beckmann, A. Brandt, K. Gedicke and D. Sapoundjiev, *Report of Research Project funded by the German Ministry of Education and Research: Stofftrennung durch Kopplung von Chromatographie und Kristallisation.* 2005, FKZ 03C0319: Magdeburg.

163.   Shan, Y. and A. Seidel-Morgenstern, *Analysis of the isolation of a target component using multicomponent isocratic preparative elution chromatography.* Journal of Chromatography A **1041** 2004: p. 53–62.

164.   Snyder, L.R., J.W. Dolan and J.R. Gant, *Gradient elution in high-performance liquid chromatography: I. Theoretical basis for reversed-phase systems.* Journal of Chromatography **165** 1979: p. 3-30.

165.   Snyder, L.R. and H. POPPE, *Mechanism of Solute Retention in Liquid-Solid Chromatography and the Role of the Mobile Phase Affecting Separation - Competion versus "Sorption".* Journal of Chromatography **184** 1980.

166.   Snyder, L.R., G.B. Cox and P.E. Antle, *Preparative separation of peptide and protein samples by high-performance liquid chromatography with gradient elution : I. The craig model as a basis for computer simulations.* Journal of Chromatography **444** 1988: p. 303-324.

167.   Snyder, L.R., J.W. Dolan and G.B. Cox, *Preparative high-performance liquid chromatography based on reversed-phase gradient elution : Optimum experimental conditions for heavily overloaded separation.* Journal of Chromatography **540** 1991: p. 21-40.

168.   Spedding, F.H., E.I. Fulmer, T.A. Butler, E.M. Gladrow, M. Gobush, P.E. Porter, J.E. Powell and J.M. Wright, *The Separation of Rare Earths by Ion Exchange .3. Pilot Plant Scale Separations.* Journal of the American Chemical Society **69** 1947: p. 2812-2818.

169.   Spedding, F.H., A.F. Voigt, E.M. Gladrow and N.R. Sleight, *The Separation of Rare Earths by Ion Exchange .1. Cerium and Yttrium.* Journal of the American Chemical Society **69** 1947: p. 2777-2781.

170.   Spedding, F.H., A.F. Voigt, E.M. Gladrow, N.R. Sleight, J.E. Powell, J.M. Wright, T.A. Butler and P. Figard, *The Separation of Rare Earths by Ion Exchange .2. Neodymium and Praseodymium.* Journal of the American Chemical Society **69** 1947: p. 2786-2792.

171.   Spedding, F.H., E.I. Fulmer, T.A. Butler and J.E. Powell, *The Separation of Rare Earths by Ion Exchange .4. Further Investigations Concerning Variables Involved in the Separation of Samarium, Neodymium and Praseodymium.* Journal of the American Chemical Society **72** 1950: p. 2349-2354.

172. Spedding, F.H., E.I. Fulmer, J.E. Powell and T.A. Butler, *The Separation of Rare Earths by Ion Exchange .5. Investigations with One-10th Per Cent. Citric Acid-Ammonium Citrate Solutions.* Journal of the American Chemical Society **72** 1950: p. 2354-2361.

173. Spedding, F.H., E.I. Fulmer, J.E. Powell, T.A. Butler and I.S. Yaffe, *The Separation of Rare Earths by Ion Exchange .6. Conditions for Effecting Separations with Nalcite Hcr and 1/10-Per Cent - Citric Acid Ammonium Citrate Solutions.* Journal of the American Chemical Society **73** 1951: p. 4840-4847.

174. Spedding, F.H. and J.E. Powell, *Separation of Yttrium-Group Rare Earths from Gadolinite by Ion Exchange.* Chemical Engineering Progress Symposium Series **50** 1954: p. 7-15.

175. Spedding, F.H. and J.E. Powell, *The Separation of Rare Earths by Ion Exchange .8. Quantitative Theory of the Mechanism Involved in Elution by Dilute Citrate Solutions.* Journal of the American Chemical Society **76** 1954: p. 2550-2557.

176. Spedding, F.H. and J.E. Powell, *The Separation of Rare Earths by Ion Exchange .7. Quantitative Data for the Elution of Neodymium.* Journal of the American Chemical Society **76** 1954: p. 2545-2550.

177. Storti, G., M. Mazzotti, M. Morbidelli and S. Carra, *Robust Design of Binary Countercurrent Adsorption Separation Processes.* AIChE Journal **39** 1993: p. 471-492.

178. Ströhlein, G., M. Schulte and J. Strube, *Hybrid Processes: Design Method for optimal coupling of chromatography and crystallization units.* Separation Science and Technology **38** 2003: p. 3353-3383.

179. Ströhlein, G., M. Mazzotti and M. Morbidelli, *Optimal operation of simulated-moving-bed reactors for nonlinear adsorption isotherms and equilibrium reactions.* Chemical Engineering Science **60** 2005: p. 1525-1533.

180. Ströhlein, G., M. Mazzotti and M. Morbidelli, *Analysis of sample-solvent induced modifier-solute peak interactions in biochromatography using equilibrium theory and detailed simulations.* Journal of Chromatography A **1091** 2005: p. 60-71.

181. Ströhlein, G., L. Aumann, L. Melter, K. Buescher, B. Schenkel, M. Mazzotti and M. Morbidelli, *Experimental verification of sample-solvent induced modifier-solute peak interactions in biochromatography.* Journal of Chromatography A **1117** 2006: p. 146-153.

182. Ströhlein, G., M. Morbidelli, H.K. Rhee and M. Mazzotti, *Modeling of modifier-solute peak interactions in chromatography.* AIChE Journal **52** 2006: p. 565-573.

183. Szanya, T., J. Argyelan, S. Kovats and L. Hanak, *Separation of steroid compounds by overloaded preparative chromatography with precipitation in the fluid phase.* Journal of Chromatography A **908** 2001: p. 265-272.

184. Szymura-Oleksiak, J., J. Bojarski and H.Y. Aboul-Enein, *Recent applications of stereoselective chromatography.* Chirality **14** 2002: p. 417-435.

185. Tondeur, D., H. Kabir, L.A. Luo and J. Granger, *Multicomponent Adsorption equilibria from impulse response chromatography.* Chemical Engineering Science **51** 1996: p. 3781-3799.

186. Tseng, P.K. and L.B. Rogers, *Effect of a Change in Solvent on Chromatographic Peak Shapes.* Journal of Chromatographic Science **16** 1978: p. 436-438.

187. Tsimidou, M. and R. Macrae, *Influence of injection solvent on the reversed-phase chromatography of triglycerides.* Journal of Chromatography **285** 1984: p. 178-181.

188. Unger, K.K., *Handbuch der HPLC. Teil 2: Präparative Säulenflüssig-Chromatographie.* 1994, GIT-Verlag: Darmstadt.

189. Vaccari, G., G. Mantovani, G. Sgualdino and W.J. Colonna, *Cooling crystallization of SMB-fractionated molasses.* International Sugar Journal **100** 1998: p. 345–351.

190. Vu, T.D., A. Seidel-Morgenstern, S. Grüner and A. Kienle, *Analysis of ester hydrolysis reactions in a chromatographic reactor using equilibrium theory and a rate model.* Industrial & Engineering Chemistry Research **44** 2005: p. 9565-9574.

191. Vukmanic, D. and M. Chiba, *Effect of Organic-Solvents in Sample Solutions and Injection Volumes on Chromatographic Peak Profiles of Analytes in Reversed-Phase High-Performance Liquid-Chromatography.* Journal of Chromatography **483** 1989: p. 189-196.

192. Wicke, E., *Empirical and theoretic tests on the sorption rate of gases in porous substances I.* Kolloid-Zeitschrift **86** 1939: p. 167-186.

193. Wicke, H., *Empirical and theoretical tests on the rate of sorption of gases in porous materials.* Kolloid-Zeitschrift **86** 1939: p. 295-313.

194. Wilson, J.N., *A theory of chromatography.* Journal of the American Chemical Society **62** 1940: p. 1583-1591.

195. Yan, T.Q. and C. Orihuela, *Rapid and High Throughput Separation Technologies--Steady State Recycling and Supercritical Fluid Chromatography for Chiral Resolution of Pharmaceutical Intermediates.* Journal of Chromatography A **1156** 2007: p. 220-227.

196. Zhang, L., J. Selkera, A. Qub and A. Velayudhana, *Numerical estimation of multicomponent adsorption isotherms in preparative chromatography: implications of experimental error.* Journal of Chromatography A **934** 2001: p. 13–29.

197. Zhang, L., K. Gedicke, M.A. Kuznetsov, S.M. Staroverov and A. Seidel-Morgenstern, *Application of an eremomycin-chiral stationary phase for the separation of DL-methionine using simulated moving bed technology.* Journal of Chromatography A **1162** 2007: p. 90-96.

198. Zhang, W., Y. Shan and A. Seidel-Morgenstern, *Breakthrough curves and elution profiles of single solutes in case of adsorption isotherms with two inflection points.* Journal of Chromatography A **1107** 2006: p. 216-225.

199.   Zhang, Y., K. Hidajat and A.K. Ray, *Determination of competitive adsorption isotherm parameters of pindolol enantiomers on α_1-acid glycoprotein chiral stationary phase.* Journal of Chromatography A **1131** 2006: p. 176–184.

200.   Zhang, Y., S. Rohani and A.K. Ray, *Numerical determination of competitive adsorption isotherm of mandelic acid enantiomers on cellulose-based chiral stationary phase.* Journal of Chromatography A **1202** 2008: p. 34–39.

curriculum vitae

day of birth   25-Feb-1975

1981-1990:   Polytechnische Oberschule Rosa-Luxemburg, Magdeburg

1990-1993:   Geschwister-Scholl-Gymnasium, Magdeburg, high school diploma

1993-994:   Basic Military Service at the 92.nd Panzergrenadierbataillon, Munster

1994-1997:   Otto-von-Guericke-University, Magdeburg

- Summer 1996 Preliminary Diploma Mechanical Engineering

- Summer/winter 1996/97 start of the main course of Chemical Engineering

1997-1998:   Rose-Hulman-Institute of Technology, Terre Haute, U.S.A

- 12/1998: Master of Science in Chemical Engineering GPA 3.641 (4.000), Title of the master thesis: 'Multiple input multiple output systems: Decoupled temperature and level control'

1999-2000:   Otto-von-Guericke University, Magdeburg

- 11/2000: Diplom-Ingenieur Verfahrens- und Energietechnik (very good), Title of the diploma thesis: 'Zur Enantiomerentrennung mittels optisch aktiver Membranen' (On the Separation of Enantiomers Using Optically Active Membranes)

2001-2007:   Otto-von-Guericke University, Magdeburg

- Scientific assistant at the Institute of Process Engineering.

since 05/21/2007: The Dow Chemical Company, Dow Olefinverbund GmbH, Werk Böhlen

- Sr. Improvement Engineer